Fall 2019

The Antimicrobial Activity and Cellular Targets of Plant Derived Aldehydes and Degradable Pro-Antimicrobial Networks in Pseudomonas Aeruginosa

Yetunde Adewunmi
University of Southern Mississippi

THE ANTIMICROBIAL ACTIVITY AND CELLULAR TARGETS OF PLANT DERIVED ALDEHYDES AND DEGRADABLE PRO-ANTIMICROBIAL NETWORKS IN PSEUDOMONAS AERUGINOSA

by

Yetunde Zainab Adewunmi

A Dissertation
Submitted to the Graduate School,
the College of Arts and Sciences
and the School of Biological, Environmental, and Earth Sciences
at The University of Southern Mississippi
in Partial Fulfillment of the Requirements
for the Degree of Doctor of Philosophy

Approved by:

Dr. Dmitri Mavrodi, Committee Chair
Dr. Glenmore Shearer
Dr. Janet Donaldson
Dr. Mohammed Elasri
Dr. Kevin Kuehn

Dr. Dmitri Mavrodi Committee Chair	Dr. Jake Schaefer Director of School	Dr. Karen S. Coats Dean of the Graduate School

December 2019

ABSTRACT

Essential oils (EOs) are plant-derived products that have been long exploited for their antimicrobial activities in medicine, agriculture, and food preservation. EOs represent a promising alternative to conventional antibiotics due to the broad-range antimicrobial activity, low toxicity to human commensal bacteria, and the capacity to kill microorganisms without promoting resistance. Despite the progress in the understanding of the biological activity of EOs, many aspects of their mode of action remain inconclusive. The overarching aim of this work was to address these gaps by studying molecular interactions between antimicrobial plant aldehydes and the opportunistic human pathogen *Pseudomonas aeruginosa*. We initiated my project by identifying synergistically acting combinations of phytoaldehydes and using thiol-ene chemistry to incorporate the synergistic pairs into pro-antimicrobial polymers. Such polymers released phytoaldehydes upon a change in pH and humidity and controlled growth of *P. aeruginosa*. Next, we used a combination of transposon mutagenesis, and RNA-seq to elucidate cellular pathways targeted by *p*-anisaldehyde (an EO constituent from star anise) and the polyphenol from green tea epigallocatechin gallate (EGCG). The results of these experiments identified key microbial genes and associated pathways involved in response to antimicrobial plant-derived phenylpropanoids and revealed molecular mechanisms governing the synergistic effects of individual constituents within essential oils. Finally, we broadened the antimicrobial potential of the thiol-ene polymer platform by incorporating a combination of *p*-anisaldehyde and furaneol, which is a natural plant-derived inhibitor of quorum sensing. The treatment with furaneol/*p*-anisaldehyde-containing polymeric discs strongly repressed the production of pyocyanin, reduced the

exoprotease activity, and effectively eradicated established *P. aeruginosa* biofilms. Our results will facilitate the development of polymeric systems capable of dual phytochemical delivery and controlling microbial growth without promoting antibiotic resistance. Such materials enable the high loading, efficient encapsulation, and sustained release of hydrophobic and volatile phytochemicals and could be used as antimicrobial wound dressings, sprays, surface coatings, and packaging materials.

ACKNOWLEDGMENTS

My deepest and sincerest appreciation goes to my advisor and mentor, Dr. Dmitri V. Mavrodi and Dr. Olga V. Mavrodi without whom I never would have been able to grow, learn and flourish as a scientific researcher. Their dedication to me, trust, honest concern, limitless availability, and constructive criticisms have been invaluable to my personal and professional life. I thank them for teaching and directing me to numerous rewarding opportunities. Without a doubt, choosing the Mavrodi lab was one of the best decisions of my life that has positively impacted my future. I will forever be grateful to Dr. Mavrodi and Olga for always pushing me to do my best, I never would have been able to make it this far without their support.

I also want to say a big thank you to my committee members, Dr. Janet Donaldson, Dr. Mohamed Elasri, Dr. Glenmore Shearer, and Dr. Kevin Kuehn for their support, open door policy and encouragement. Their jobs' as active research faculty is very busy, hence, I am very grateful for the all the time they set out for me. I am also sincerely thankful to Dr. Derek L. Patton, his past and present research group, specifically Dr. Dahlia Amato, Dr. Douglas Amato and William D. Walker for their collaboration– which contributed to a significant portion of my project. Through the NSF/NRT INTERFACE program, Dr. Patton also played a big role in my professional development and for that I am grateful.

My gratitude also goes out to Dr. Jonathan Lindner of MS-INBRE for teaching me how to use numerous instruments, and Dr. Gyan Sahukhal of Elasri lab for giving me their computer to analyze my RNA seq data. Additionally, I would like to thank the director of the school of BEES, Dr. Jake Schaefer and the entire administrative staff for

working behind the scenes to ensure a smoothly run program. My sincere thanks also go to Ms. Cynthia Littlejohn, my teaching lab coordinator for making it smooth and easy to teach General and Nursing Microbiology labs. Special thanks also go to Dr. Rebecca Fillmore for giving me the chance to come study at USM. I had a good education here, and it would not have been possible without her help. I would also like to thank Dr. Jennifer Walker and all faculty members at the USM Gulf-Park campus including Dr. Shiao Wang for helping me tremendously when I first arrived at USM. Many thanks to my undergraduate mentees, Dana Jones, Sarah Jamison, and especially Sanchirmaa Namjilsuren who also worked tirelessly with me on this project.

My ability to start and push through my degree would not have been possible without the motivation, love, support, prayers and encouragement provided by my beloved family including Temitope Ilori, Adeyemi Adewunmi and Omotayo Adewunmi. I am especially grateful to my parents, Mr. and Mrs. O.A Adewunmi, for paving the way for me and giving me a good life. Lastly, I want to thank the past and present Mavrodi lab members, Janiece, Sam, Clint, and Ankita as well as my wonderful friends Samantha, Moyo, Evi, Halimah, Kehinde, Chidinma, Francis, Promise, Grace, Doyin, Emmanuel, Mr. Nosa (of blessed memory), and the Atawodis'. I thank them for being there with me and supporting me through the pleasantness and woes of graduate school.

The funding for this project was provided through NSF Gulf Coast Advance Fellowship, the NSF National Research Trainee award 1449999, and the NSF SusCheM award 1710589. I also acknowledge the Mississippi INBRE, funded by an Institutional Development Award (IDeA) from the National Institute of General Medical Sciences of NIH under grant P20GM103476.

DEDICATION

To God Almighty, the One who shines a light unto my path and never leaves my side.

TABLE OF CONTENTS

LIST OF TABLES

LIST OF ILLUSTRATIONS

LIST OF SCHEMES

LIST OF ABBREVIATIONS

EO	Essential Oil
MOA	Mode of Action
EPI	Efflux Pump Inhibitor
QS	Quorum Sensing
QSI	Quorum Sensing Inhibitor

CHAPTER I - INTRODUCTION

1.1 Infectious diseases and antibiotic resistance

Pathogenic microorganisms are a continuous threat to humans regardless of age, sex, ethnic background, and socioeconomic status. Infectious diseases represent the 3rd leading cause of death in the US and infect almost a billion people across the globe causing 15 million deaths annually.[12] These diseases also impose a significant financial burden on affected people and the society at large, and their incidence is exacerbated by the rise in the number of people with organ transplants, cancer, and genetic diseases, such as cystic fibrosis.[3] Although most infections can be readily treated with antibiotics, the global spread of resistance driven by the misuse and overuse of antibiotics in medicine and agriculture threatens the sustainability of public health.[4,5] The antibiotic-resistant pathogens persist longer, inflict more damage to the host via the tissue inflammation, sepsis, and, in some cases, death.[1] The World Health Organization (WHO) estimates that antibiotic-resistant infections cause up to 700,000 deaths globally.[6] The United States alone spends an extra $35 billion annually on health care associated with the rise in antibiotic resistance.[7]

The WHO recognizes *Acinetobacter baumannii*, *Pseudomonas aeruginosa*, and carbapenem-resistant Enterobacteriaceae, such as *Klebsiella*, *Escherichia coli*, *Serratia*, and *Proteus* as the greatest threat to hospitals, nursing facilities, and patients on ventilators or with blood catheters.[8] Other important multidrug (MDR) species include the vancomycin-resistant *Enterococcus faecium*, methicillin- and vancomycin-resistant *Staphylococcus aureus*, clarithromycin-resistant *Helicobacter pylori*, and fluoroquinolone-resistant *Campylobacter*, *Salmonella*, and *Neisseria gonorrhoeae*. Many

of these MDR pathogens can cause severe bloodstream infections and pneumonia and are associated with increased morbidity, extended hospital stays, and mortality.[9] The WHO also warns about a lack of new antibiotics to counteract the growing threat of antimicrobial resistance. The agency indicated that of the 51 antibiotics that are currently in clinical development, only eight are sufficiently novel to add value to the existing treatments of antibiotic-resistant pathogens.[10] If this trend continues, an estimated ten million additional deaths will occur because of bacterial infections by the year 2050.[6]

1.2 Plant essential oils as a rich source of natural antimicrobial compounds

The global rise in the multidrug resistance has led to a renewed interest in the use of alternative approaches for controlling microbial pathogens, such as phage therapy and the use of essential oils, whose antimicrobial properties have been recognized in traditional medicine for centuries.[11] Essential oils (EOs) are aromatic and volatile liquids or solids that are extracted from roots, flowers, leaves, and fruits of certain plants. [11–14] Currently, over 3,000 different EOs are known, and about 300 are being produced commercially for culinary purposes or as ingredients of perfumes and cosmetics.[12,15,16] EOs have also been utilized since ancient times due to their analgesic, antioxidant, sedative, anti-inflammatory, spasmolytic and local anesthetic properties.[17] Finally, essential oils represent one of the oldest known groups of antiseptics due to the presence of numerous metabolites with broad-range antimicrobial properties.[6,13,14,18] Essential oils vary in composition depending on the plant species, growing season, the method of extraction, and physiological state of the plant.[6,11,13–15,17–20] Many plants secrete essential oils to defend themselves against invading pathogens and, as a consequence, many EO-derived alcohols, aldehydes, terpenes, ethers, ketones, and phenols have been shown to

have broad range antibacterial, antifungal, antiviral, antiulcer, anthelmintic, and antioxidant properties.[13,14,21] The capacity to kill a wide variety of microorganisms without promoting resistance, and approval by the FDA as generally recognized as safe (GRAS) substances makes EOs an attractive alternative to conventional antibiotics.[11,13,19]

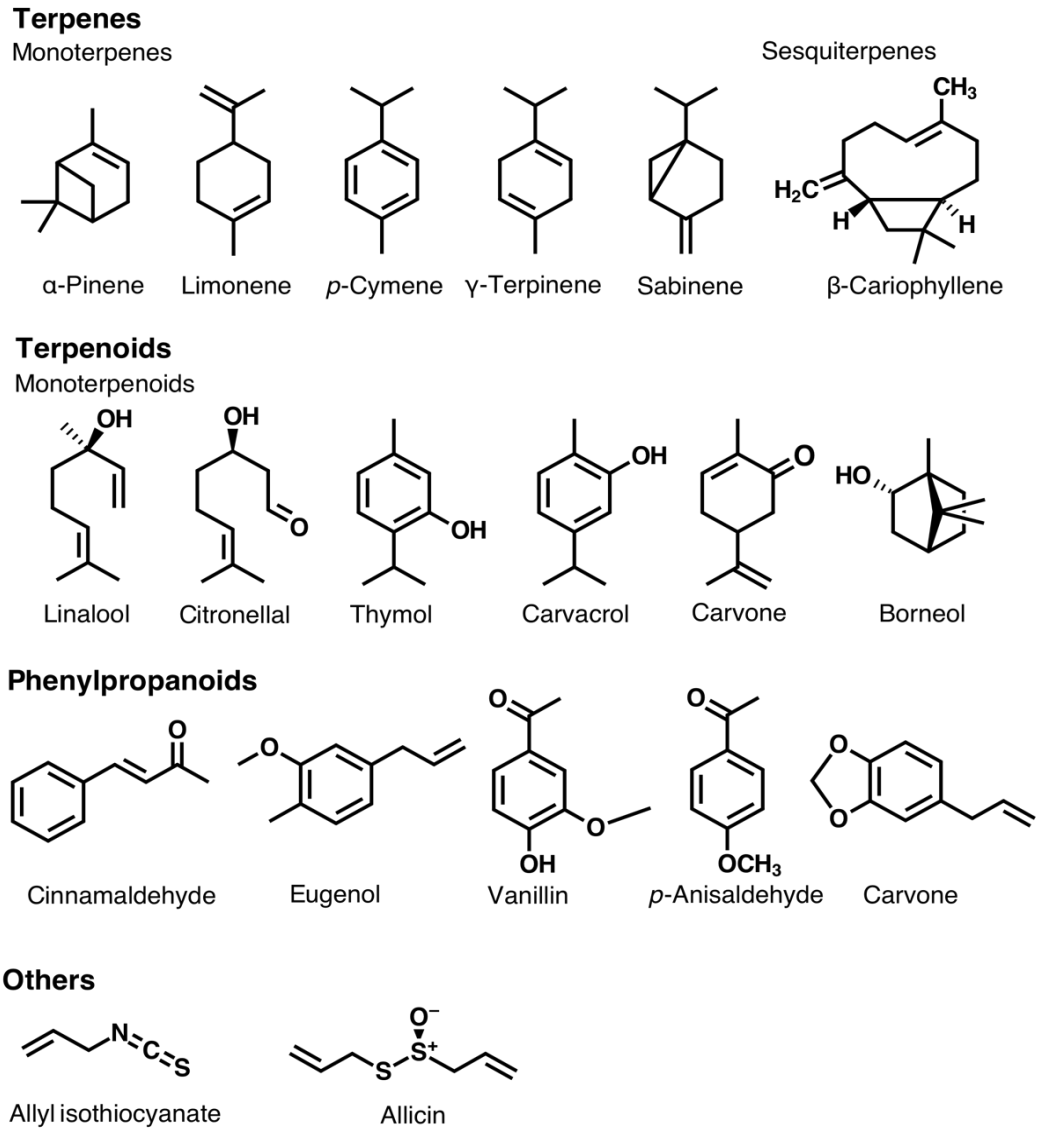

Figure 1.1 Chemical structures of selected constituents of essential oils.

Adapted from Hyldgaard et al., 2012

Plant essential oils contain numerous terpenes, terpenoids, phenylpropanoids, and phenolics, many of which are active against bacteria and fungi (Figure 1.1).[14] My work focused on *p*-anisaldehyde (a biologically active EO constituent from star anise), and structurally related cyanobenzaldehyde (present in the medicinal plant *Saussurea lappa*),[22] *p*-chlorobenzaldehyde, and bromobenzaldehyde (Figure 1.2). These compounds are also naturally present in alcoholic beverages, dairy products, meat, poultry, fruits, vegetables, and spices.

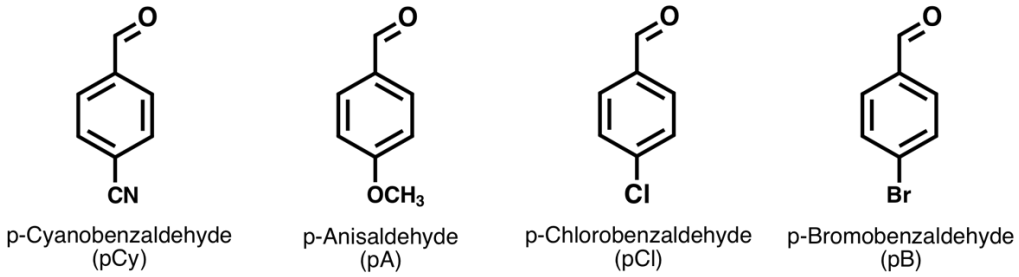

Figure 1.2 Chemical structures of selected benzaldehydes used in this study.

p-Anisaldehyde, along with better-studied cinnamaldehyde and vanillin, belong to a group of plant metabolites known as phenylpropanoids that are named after the six-carbon aromatic phenyl group and three-carbon propene tail produced in the first step of biosynthesis.[14,17] The antimicrobial activity of phenylpropenes depends on the number of substituents on their aromatic ring and is further modulated by experimental conditions and physiology of the target microorganism.[14] The activity of phenylpropanoids is not attributable to a unique mechanism but, is instead a cascade of reactions involving the entire microbial cell.[17] Three different modes of actions (MoAs) have been suggested to explain the antimicrobial activity of cinnamaldehyde. At low concentrations, this metabolite interferes with bacterial cell division by blocking the GTP-dependent

polymerization activity of FtsZ protein.[23] At higher levels, it disrupts cell membranes and acts as an ATPase inhibitor.[24,25] It is currently unclear exactly how cinnamaldehyde disrupts membranes since this compound kills some bacteria by disintegrating the cell envelope, while other species may survive due to the increase in saturated fatty acids in the membrane lipid profile.[26] The mode of action of vanillin is thought to involve the perturbation of membranes and several other intracellular targets.[14] The antibacterial and antifungal activity of *p*-anisaldehyde and structurally-related compounds is well documented, but their mechanism of action remains poorly understood.[27,28]

1.3 *Pseudomonas aeruginosa* as a model multidrug-resistant opportunistic pathogen

P. aeruginosa is a ubiquitous gram-negative microorganism that serves as an important model for opportunistic infections and biofilm research. This bacterium is commonly found in soil, water, or plants, but can readily infect immunocompromised individuals causing septicemia, wound, and urinary tract infections.[5,29] It also causes pneumonia and predominantly responsible for the increased morbidity and mortality of cystic fibrosis patients.[29,30] Over the past several decades, this organism evolved from being primarily a burn wound pathogen into a major threat of nosocomial infections.[6,9] *P. aeruginosa* is now resistant to multiple classes of antibiotics and belongs to a class of pathogens with the increased virulence, persistence and transmissibility known as the ESKAPE group (also encompasses *Enterococcus faecium, S. aureus, Klebsiella pneumoniae, A. baumannii*, and *Enterobacter* species) [5,7,9]. The Centers for Disease Control report that in the US *P. aeruginosa* is responsible for 8% of all hospital-acquired infections and over 400 deaths per year, which are often caused by multidrug-resistant variants of the pathogen. These MDR strains of *P. aeruginosa* are insensitive to nearly all

the available β-lactams and aminoglycosides and thus, are classified by the CDC as a serious threat that requires close monitoring and prevention activities.[5] Once acquired, *P. aeruginosa* is particularly difficult to treat due to its capacity to form thick biofilms which provide additional protection from the environmental stress, immune response, and antimicrobial compounds.

1.4 Cell signaling and RND efflux pumps are potential drug targets to combat *P. aeruginosa* infections

P. aeruginosa secretes an extensive array of virulence factors (multiple exotoxins, rhamnolipids, cyanide, pyocyanin), and their production, as well as the formation of biofilms and surface motility, are coordinately regulated via quorum-sensing (QS).[31,32] *P. aeruginosa* has two hierarchically organized QS circuits (Las and Rhl) that rely on the production, detection, and response to N-3-oxo-dodecanoyl-homoserine lactone (3-oxo-C12-HSL) and N-butanoyl-homoserine lactone (C4-HSL). A third QS system (Pqs) regulates the acquisition of iron, cytotoxicity, and secretion of outer membrane vesicles in response to 2-heptyl-3-hydroxy-4-quinolone.[33] Collectively these quorum sensing signals interact with transcriptional regulators in a concentration-dependent way, thus modulating the expression of pathogenicity related traits and formation of persistent biofilms.[32,34] Human cells lack the acyl-homoserine lactone- and quinolone-based regulation, which makes microbial QS components an attractive target for the development of new antimicrobials.[32]

Several strategies of "quorum quenching" were suggested in *P. aeruginosa*, including the inhibition of synthesis,[35] sequestration,[36] and degradation[37] of acyl homoserine lactones (AHLs). However, the most promising approach involves the use of

antagonistic compounds that compete with AHLs for target receptors. Different classes of synthetic and natural AHL analogs were described, many of which were discovered in plants extract.[38] Some examples of plant-derived QS inhibitors include the polyphenolic compounds baicalin from the roots of *Scutellaria baicalensis*[39] and epigallocatechin from green tea, [40] bergamottin from grapefruit juice,[41] allicin and ajoene from garlic.[42] A group of potent AHL mimics known as halogenated furanones was first discovered in the red alga *Delisea pulchra,* which produces the brominated metabolite (5Z)-4-bromo-5-(bromomethylene)3-butyryl-2(5H)-furanone.[43]

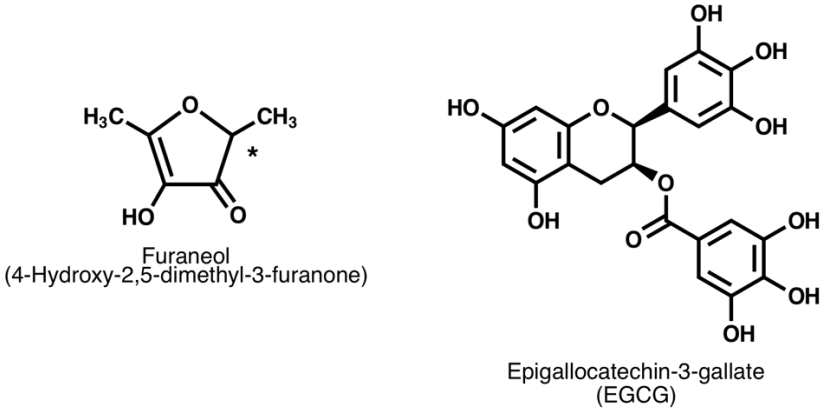

Figure 1.3 Chemical structures of furaneol and epigallocatechin gallate (EGCG).

Although natural halogenated furanones and their synthetic derivatives effectively inhibit biofilms in *P. aeruginosa* and other gram-positive and gram-negative pathogens, the high toxicity of these compounds limits their potential use.[38] In contrast, furaneol (Figure 1.3), a furanone metabolite from strawberries and other fruits, is safe to humans and used as a flavoring agent in the food industry.[44] Recent studies with *P. aeruginosa* also demonstrated that furaneol inhibits the synthesis of virulence factors that are regulated by QS.[31] Because of these attractive properties, part of my work involved

combining furaneol with *p*-anisaldehyde to produce antimicrobial polymers capable of eradicating *P. aeruginosa* biofilms.

The ability to rapidly expel a broad range of antimicrobials out of the cell represents a vital component of the intrinsic and acquired antibiotic resistance in *P. aeruginosa*.[45] This organism has 12 different efflux pumps of the resistance-nodulation-cell division (RND) superfamily, some of which (e.g., MexAB-OprM) are constitutively expressed in wild-type strains and provide the intrinsic resistance to several classes of antibiotics, disinfectants, detergents, dyes, amphiphilic molecules, and QS signals.[46] In contrast, other RND pumps (e.g., MexXY-OprM, MexCD-OprJ, MexEF-OprN) are tightly regulated in wild type strains but can be de-repressed via regulatory mutations resulting in the stable acquired resistance and MDR phenotypes in clinical isolates. Because of the crucial importance of efflux pump transporters for the active drug efflux in many gram-positive and gram-negative bacteria, recent efforts are focused on the development of specific efflux pump inhibitors (EPIs).[47] In theory, such compounds can render obsolete antibiotics effective again and open up extensive opportunities for adjuvant therapy. Despite significant efforts, the identification of chemicals that can bypass efflux pump effects without disrupting the proton motive force continues to be a challenge.[48] Several active synthetic inhibitors proved to be too toxic for clinical applications prompting researchers to screen plant extracts for natural EPIs. The results of these ongoing studies appear to be promising and confirm that plants contain various EPIs, especially for pumps of Gram-positive species.[49] In my project, I used one of these compounds, epigallocatechin gallate (EGCG) (Figure 1.3), which has chemical properties

suitable for the incorporation into PANDAs and has been shown to inhibit efflux pumps in *S. aureus* and interfere with QS and biofilm formation in *P. aeruginosa*.[50,51]

1.5 Research purpose, significance, and broader impacts

Despite the promising antimicrobial potential, the broader implementation of EOs and their constituents is hampered by several technical challenges. In particular, poor water solubility significantly limits the bioavailability and lowers biological and antimicrobial activity of these compounds, whereas volatility is problematic for achieving sustained release and controlled delivery. Recent work in the area of polyactive materials offers a viable solution to these challenges. “Polyactives” refer to polymeric prodrugs that undergo partial or complete degradation to release active therapeutic agents (e.g., anti-inflammatory, antioxidant, antibiotic).[52] The collaborative research by the Mavrodi group and Dr. Derek Patton from the USM School of Polymers and High Performing Materials demonstrated that polymer-based delivery systems could successfully circumvent the aforementioned technical issues and achieve high loading, highly efficient “encapsulation,” solvent-free processing, and rational design of phytochemical release profiles.[53] The collaborators incorporated antimicrobial plant-derived aldehydes into polymer compounds called PANDAs (Pro-Antimicrobial Networks via Degradable Acetals) (Figure 1.4). These materials were designed to release incorporated aldehydes upon exposure to conditions conducive to acetal degradation (e.g., change in humidity and pH), and demonstrated good antimicrobial activity against both bacterial and fungal pathogens, including *P. aeruginosa* PAO1, *Salmonella typhimurium* ATCC 6539, *E. coli* ATCC 43895 (serotype O157:H7), and *Histoplasma capsulatum* G217B, and exhibited a low cytotoxic effect on KB (HeLa) cells. [54]

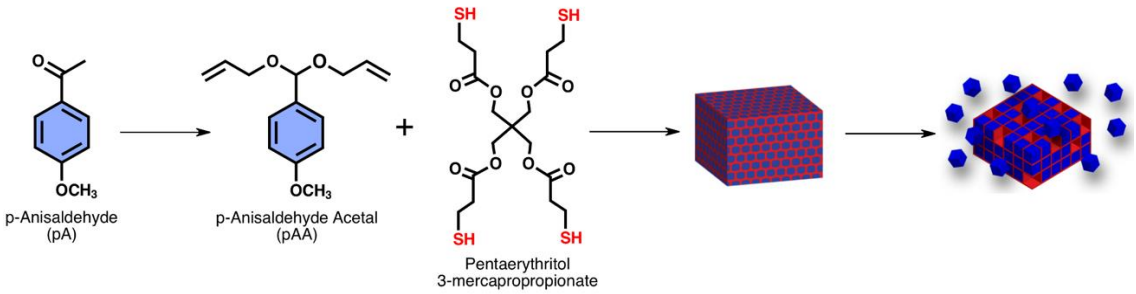

Figure 1.4 Synthesis of Pro-Antimicrobial Networks via Degradable Acetals (PANDAs).

The PANDAs polymers are designed to kill microorganisms via partial degradation and release of plant-derived antimicrobial aldehydes, such as p-anisaldehyde (adapted from Amato et al., 2016).

Based on the results of previous studies, I hypothesized that the antimicrobial efficacy of PANDAs could be further improved by understanding their cellular targets and developing polymeric systems capable of simultaneous delivery of synergistically interacting combinations of antimicrobial phytochemicals. Accordingly, in the first part of my project, I screened combinations of phytoaldehydes for synergistic antimicrobial activity against *P. aeruginosa* by determining their fractional inhibitory concentrations. I then collaborated with the Patton research group on the synthesis of the dual-release PANDA polymer that, upon hydrolysis, releases *p*-bromobenzaldehyde and *p*-anisaldehyde at a synergistic 40:60 ratio. The study demonstrated that the polymer network has potent antimicrobial action and that the aldehydes interact with porins and multidrug efflux pumps of *P. aeruginosa*. Results of these experiments are presented in Chapter II.

Although significant progress has been made in the understanding of the antimicrobial activity of EOs, many aspects of their mode of action remain inconclusive and are investigated in a limited range of organisms. Thus, the second goal of this work was to address these gaps by studying cellular targets of *p*-anisaldehyde and PANDAs in

P. aeruginosa PAO1. I carried out a transposon screen of PAO1 for the hypersensitivity to *p*-anisaldehyde. I screened several plant-derived efflux pump inhibitors and demonstrated that epigallocatechin gallate (EGCG), a polyphenol from green tea, potentiates the activity of *p*-anisaldehyde against *P. aeruginosa*. I also used RNA-seq to study transcriptional responses of *P. aeruginosa* to *p*-anisaldehyde, EGCG, and their combination. My results revealed that *p*-anisaldehyde induces stress response and targets membrane transport, synthesis of lipids, energy metabolism, and biosynthesis of the molybdenum cofactor. EGCG induced oxidative stress and reversed many of the *p*-anisaldehyde-coping responses, which may explain its synergistic effect against *P. aeruginosa*. Results of these experiments are described in Chapter III and will help to understand better molecular mechanisms that govern the susceptibility, adaptation, and resistance of bacteria to antimicrobial phytoaldehydes.

In *P. aeruginosa*, the N-acyl homoserine lactone-mediated QS represents a crucial facet of pathogenicity, because it governs the production of multiple virulence factors and formation of biofilms. Therefore, in the last part of my work, I attempted to potentiate the antimicrobial action of *p*-anisaldehyde and aldehyde-based PANDAs by combining them with furaneol, a natural QS-inhibitor from strawberries. I hypothesized that the presence of furaneol will trigger the transition of bacteria from the surface-attached biofilm to a suspended planktonic mode of growth and will render them more susceptible to the destruction by *p*-anisaldehyde. Results of my experiments, which are presented in chapter IV, supported my hypothesis and revealed that pro-antimicrobial polymers containing a combination of furaneol and *p*-anisaldehyde inhibited the secretion of QS-regulated

virulence factors (pyocyanin and protease), interfered with surface motility, and eradicated established *P. aeruginosa* biofilms.

1.6 References

(1) Nii-Trebi, N. I. Emerging and neglected infectious diseases: insights, advances, and challenges. *Biomed Res. Int.* **2017**, *2017*, 1–15.

(2) Zumla, A.; Rao, M.; Wallis, R. S.; Kaufmann, S. H. E.; Rustomjee, R.; Mwaba, P.; Vilaplana, C.; Yeboah-Manu, D.; Chakaya, J.; Ippolito, G.; Azhar, E.; Hoelscher, M.; Maeurer, M. Host-directed therapies for infectious diseases: current status, recent progress, and future prospects. *lancet infect dis* **2016**, *16*, e47–e63.

(3) Centers for Diseases Control and Prevention. *Preventing Emerging Infectious Diseases: A Strategy for the 21st Century Overview of the Updated CDC Plan*; 1998.

(4) Levy, S.B; Marshall, B. Antibacterial resistance worldwide: causes, challenges and responses. *Nat. Med.* **2004**, *10* (12), S122–S129.

(5) Ventola, C. L. The antibiotic resistance crisis: part 1: causes and threats. *P T* **2015**, *40* (4), 277–283.

(6) Rai, M.; Kon, K. *Fighting Multidrug Resistance with Herbal Extracts, Essential Oils and Their Components*, 1st ed.; Rai, M., Kon, K., Eds.; Elsevier Academic Press: San Diego, CA, 2013.

(7) Gautam, D.; Morten, S. How to fight back against antibiotic resistance. *Am. Sci.* **2014**, *102*, 42–51.

(8) Tacconelli, E.; Carrara, E.; Savoldi, A.; Harbarth, S.; Mendelson, M.; Monnet, D. L.; Pulcini, C.; Kahlmeter, G.; Kluytmans, J.; Carmeli, Y.; Ouellette, M.;

Outterson, K.; Patel, J.; Cavaleri, M.; Cox, E. M.; Houchens, C. R.; Grayson, M. L.; Hansen, P.; Singh, N.; Theuretzbacher, U.; Magrini, N.; Aboderin, A. O.; Al-Abri, S. S.; Awang Jalil, N.; Benzonana, N.; Bhattacharya, S.; Brink, A. J.; Burkert, F. R.; Cars, O.; Cornaglia, G.; Dyar, O. J.; Friedrich, A. W.; Gales, A. C.; Gandra, S.; Giske, C. G.; Goff, D. A.; Goossens, H.; Gottlieb, T.; Guzman Blanco, M.; Hryniewicz, W.; Kattula, D.; Jinks, T.; Kanj, S. S.; Kerr, L.; Kieny, M.-P.; Kim, Y. S.; Kozlov, R. S.; Labarca, J.; Laxminarayan, R.; Leder, K.; Leibovici, L.; Levy-Hara, G.; Littman, J.; Malhotra-Kumar, S.; Manchanda, V.; Moja, L.; Ndoye, B.; Pan, A.; Paterson, D. L.; Paul, M.; Qiu, H.; Ramon-Pardo, P.; Rodríguez-Baño, J.; Sanguinetti, M.; Sengupta, S.; Sharland, M.; Si-Mehand, M.; Silver, L. L.; Song, W.; Steinbakk, M.; Thomsen, J.; Thwaites, G. E.; van der Meer, J. W.; Van Kinh, N.; Vega, S.; Villegas, M. V.; Wechsler-Fördös, A.; Wertheim, H. F. L.; Wesangula, E.; Woodford, N.; Yilmaz, F. O.; Zorzet, A. discovery, research, and development of new antibiotics: The WHO priority list of antibiotic-resistant bacteria and tuberculosis. *Lancet Infect. Dis.* **2018**, *18* (3), 318–327.

(9) Davies, J.; Davies, D. Origins and evolution of antibiotic resistance. *Microbiol. Mol. Biol. Rev.* **2010**, *74* (3), 417–433.

(10) WHO. Antibacterial agents in clinical development: An analysis of the antibacterial clinical development pipeline, including tuberculosis; 2017 pp 1-48.

(11) Hintz, T.; Matthews, K. K.; Di, R. The use of plant antimicrobial compounds for food preservation. *BioMed Res. Int.* **2015**, *2015*, 1–12.

(12) Pandey, A. K.; Kumar, P.; Singh, P.; Tripathi, N. N.; Bajpai, V. K. Essential oils:

sources of antimicrobials and food preservatives. *Front. Microbiol.* **2017**, *7* (2161), 1–14.

(13) Boire, N. A.; Riedel, S.; Parrish, N. M. Essential oils and future antibiotics: New weapons against emerging‘superbugs’? *J. Anc. Dis. Prev. Remedies* **2013**, *1* (2), 1–5.

(14) Hyldgaard, M.; Mygind, T.; Meyer, R. L. Essential oils in food preservation: mode of action, synergies, and interactions with food matrix components. *Front. Microbiol.* **2012**, *3* (12), 1–12.

(15) Bassolé, I. H. N.; Juliani, H. R. Essential oils in combination and their antimicrobial properties. *Molecules* **2012**, *17* (4), 3989–4006.

(16) Langeveld, W. T.; Veldhuizen, E. J. A.; Burt, S. A. Synergy between essential oil components and antibiotics : A Review. *Crit Rev Microbiol* **2014**, *40* (1), 79–94.

(17) Nazzaro, F.; Fratianni, F.; De Martino, L.; Coppola, R.; De Feo, V. Effect of essential oils on pathogenic bacteria. *Pharmaceuticals* **2013**, *6*, 1451–1474.

(18) Nascimento, G. G. F.; Locatelli, J.; Freitas, P. C.; Silva, G. L. Antibacterial activity of plant extracts and phytochemicals on antibiotic-resistant bacteria. *Brazilian J. Microbiol.* **2000**, *31* (4), 247–256.

(19) Mith, H.; Duré, R.; Delcenserie, V.; Zhiri, A.; Daube, G.; Clinquart, A. Antimicrobial activities of commercial essential oils and their components against food-borne pathogens and food spoilage bacteria. *Food Sci. Nutr.* **2014**, *2* (4), 403–416.

(20) Oroojalian, F.; Kasra-Kermanshahi, R.; Azizi, M.; Bassami, M. R. Phytochemical composition of the essential oils from three apiaceae species and their antibacterial

effects on food - borne pathogens. *Food Chem.* **2010**, *120*, 765–770.

(21) Pandey, A. K.; Kumar, P.; Singh, P.; Tripathi, N. N.; Bajpai, V. K. Essential oils: sources of antimicrobials and food preservatives. *Front. Microbiol.* **2016**, *7* (2161), 1–14.

(22) Al Otibi, F.; Rizwana, H.; Alharbi, R. I.; Alshaikh, N.; Albasher, G. Antifungal effect of saussurea lappa roots against phytopathogenic fungi and resulting morphological and ultrastructural changes. *Gesunde Pflanz.* **2019**, 1–11.

(23) Hemaiswarya, S.; Kruthiventi, A. K.; Doble, M. Synergism between natural products and antibiotics against infectious diseases. *Phytomedicine* **2008**, *15*, 639–652.

(24) Gill, A. O.; Holley, R. A. Inhibition of membrane bound atpases of escherichia coli and listeria monocytogenes by plant oil aromatics. *Int. J. Food Microbiol.* **2006**, *111* (2), 170-174.

(25) Gill, A. O.; Holley, R. A. Disruption of *Escherichia coli*, *Listeria monocytogenes* and *Lactobacillus sakei* cellular membranes by plant oil aromatics. *Int. J. Food Microbiol.* **2006**, *108* (1), 1–9.

(26) Pasqua, R. Di; Betts, G.; Hoskins, N.; Edwards, M.; Ercolini, D.; Mauriello, G. Membrane toxicity of antimicrobial compounds from essential oils. *Agric.FoodChem.* **2007**, *55* (12), 4863−4870.

(27) Feron, V. J.; Til, H. P.; De Vrijer, F.; Woutersen, R. A.; Cassee, F. R.; Van Bladeren, P. J. Aldehydes: Occurrence, carcinogenic potential, mechanism of action and risk assessment. *Mutat. Res.* **1991**, *259*, 363–385.

(28) Friedman, M.; Henika, P.; Mandrell, R. Antibacterial activities of phenolic

benzaldehydes and benzoic acids against *Campylobacter jejuni*, *Escherichia coli*, *Listeria monocytogenes*, and *Salmonella enterica*. *J. Food Prot.* **2003**, *66* (10), 1811–1821.

(29) Stover, C. K.; Pham, X. Q.; Erwin, A. L.; Mizoguchi, S. D.; Warrener, P.; Hickey, M. J.; Brinkman, F. L.; Hufnagle, W. O.; Kowalik, D. J.; Lagrou, M.; Garber, R. L.; Goltry, L.; Tolentino, E.; Westbrock-Wadman, S.; Yuan, Y.; Brody, L. L.; Coulter, S. N.; Folger, K. R.; Kas, A.; Larbig, K.; Lim, R.; Smith, K.; Spencer, D.; K-S Wong, G.; Wu, Z.; Paulsenk, I. T.; Reizer, J.; Saier, M. H.; W Hancock, R. E.; Lory, S.; Olson, M. V. Complete genome sequence of *Pseudomonas aeruginosa* PAO1, an opportunistic pathogen. *Nat.* **2000**, *406*, 959–964.

(30) Gallagher, L. A.; Manoil, C. *Pseudomonas aeruginosa* PAO1 kills caenorhabditis elegans by cyanide poisoning. *J. Bacteriol.* **2001**, *183* (21), 6207–6214.

(31) Choi, S.-C.; Zhang, C.; Moon, S.; Oh, Y.-S. Inhibitory effects of 4-hydroxy-2,5-dimethyl-3(2h)-furanone (hdmf) on acyl-homoserine lactone-mediated virulence factor production and biofilm formation in *Pseudomonas aeruginosa* PAO1. *J. Microbiol.* **2014**, *52* (9), 734–742.

(32) Rutherford, S. T.; Bassler, B. L.; Delany, I.; Rappuoli, R.; Seib, K. L.; Ben-tekaya, H.; Gorvel, J.; Ruhe, C. Bacterial Quorum Sensing : Its role in virulence and possibilities for its control. *Cold Spring Harb Perspect Med* **2014**, *2*, 1–26.

(33) Lin, J.; Cheng, J.; Wang, Y.; Shen, X. The *Pseudomonas* Quinolone Signal (PQS): not just for quorum sensing anymore. *Front. Cell. Infect. Microbiol.* **2018**, *8* (230), 1–9.

(34) Smith, K. M.; Bu, Y.; Suga, H. Induction and inhibition of *Pseudomonas*

aeruginosa quorum sensing by synthetic autoinducer Analogs. *Chem. Biol.* **2003**, *10* (1), 81–89.

(35) Parsek, M. R.; Val, D. L.; Hanzelka, B. L.; Cronan, J. E.; Greenberg, E. P. Acyl homoserine-lactone quorum-sensing signal generation. *Proc. Natl. Acad. Sci.* **1999**, *96* (8), 4360–4365.

(36) Whitehead, N. A.; Welch, M.; Salmond, G. P. C. Silencing the majority. *Nat. Biotechnol.* **2001**, *19* (8), 735–736.

(37) Michel, L.; Harms, H.; Heurlier, K.; Michaux, P.; Zala, M.; Ginet, N.; Haas, D.; Défago, G.; Keel, C.; Reimmann, C.; Triandafillu, K.; Krishnapillai, V. Genetically programmed autoinducer destruction reduces virulence gene expression and swarming motility in *Pseudomonas aeruginosa* PAO1. *Microbiology* **2002**, *148* (4), 923–932.

(38) Brackman, G.; Coenye, T. Quorum sensing inhibitors as anti-biofilm agents. *Curr. Pharm. Des.* **2014**, *21* (1), 5–11.

(39) Luo, J.; Dong, B.; Wang, K.; Cai, S.; Liu, T.; Cheng, X.; Lei, D.; Chen, Y.; Li, Y.; Kong, J.; Chen, Y. Baicalin inhibits biofilm formation, attenuates the quorum sensing-controlled virulence and enhances pseudomonas aeruginosa clearance in a mouse peritoneal implant infection model. *PLoS One* **2017**, *12* (4), 1–32.

(40) Huber, B.; Eberl, L.; Feucht, W.; Polster, J. Influence of polyphenols on bacterial biofilm formation and quorum-sensing. *Z. Naturforsch* **2003**, *58*, 879–884.

(41) Girennavar, B.; Cepeda, M. L.; Soni, K. A.; Vikram, A.; Jesudhasan, P.; Jayaprakasha, G. K.; Pillai, S. D.; Patil, B. S. Grapefruit juice and its furocoumarins inhibits autoinducer signaling and biofilm formation in bacteria.

Int. J. Food Microbiol. **2008**, *125* (2), 204–208.

(42) Rasmussen, T. B.; Bjarnsholt, T.; Skindersoe, M. E.; Hentzer, M.; Kristoffersen, P.; Köte, M.; Nielsen, J.; Eberl, L.; Givskov, M. Screening for quorum-sensing inhibitors (QSI) by use of a novel genetic system, the QSI selector. *J. Bacteriol.* **2005**, *187* (5), 1799–1814.

(43) de Nys, R.; Givskov, M.; Kumar, N.; Kjelleberg, S.; Steinberg, P. D. Furanones. *Prog. Mol. Subcell. Biol.* **2006**, *42*, 55–86.

(44) Sung, W. S.; Jung, H. J.; Park, K.; Kim, H. S.; Lee, I.-S.; Lee, D. G. 2,5-Dimethyl-4-hydroxy-3(2h)-furanone (dmhf); antimicrobial compound with cell cycle arrest in nosocomial pathogens. *Life Sci.* **2007**, *80* (6), 586–591.

(45) Poole, K. *Pseudomonas aeruginosa*: Resistance to the max. *Front. Microbiol.* **2011**, *2* (65), 1–13.

(46) Li, X.-Z.; Plésiat, P.; Nikaido, H. The Challenge of efflux-mediated antibiotic resistance in gram-negative bacteria. *Clin. Microbiol. Rev.* **2015**, *28* (2), 337–418.

(47) Schweizer, H. P. Understanding efflux in gram-negative bacteria: opportunities for drug discovery. *Expert Opin. Drug Discov.* **2012**, *7* (7), 633–642.

(48) Lomovskaya, O.; Bostian, K. A. Practical applications and feasibility of efflux pump inhibitors in the clinic—a vision for applied use. *Biochem. Pharmacol.* **2006**, *71* (7), 910–918.

(49) Cheesman, M. J.; Ilanko, A.; Blonk, B.; Cock, I. E. Developing new antimicrobial therapies: are synergistic combinations of plant extracts/compounds with conventional antibiotics the solution? *Pharmacogn. Rev.* **2017**, *11* (22), 57–72.

(50) Steinmann, J.; Buer, J.; Pietschmann, T.; Steinmann, E. Anti-infective properties

of epigallocatechin-3-gallate (egcg), a component of green tea. *Br. J. Pharmacol.* **2013**, *168* (5), 1059–1073.

(51) Stenvang, M.; Dueholm, M. S.; Vad, B. S.; Seviour, T.; Zeng, G.; Geifman-Shochat, S.; Søndergaard, M. T.; Christiansen, G.; Meyer, R. L.; Kjelleberg, S.; Nielsen, P. H.; Otzen, D. E. Epigallocatechin gallate remodels overexpressed functional amyloids in *Pseudomonas aeruginosa* and increases biofilm susceptibility to antibiotic treatment. *J. Biol. Chem.* **2016**, *291* (51), 26540–26553.

(52) Stebbins, N. D.; Faig, J. J.; Yu, W.; Guliyev, R.; Uhrich, K. E. Polyactives: controlled and sustained bioactive release via hydrolytic degradation. *Biomater. Sci.* **2015**, *3* (8), 1171–1187.

(53) Amato, D. N.; Amato, D. V.; Adewunmi, Y.; Mavrodi, O. V.; Parsons, K. H.; Swilley, S. N.; Braasch, D. A.; Walker, W. D.; Mavrodi, D. V.; Patton, D. L. Using aldehyde synergism to direct the design of degradable pro-antimicrobial networks. *ACS Appl. Bio Mater.* **2018**, *1* (6), 1983–1991.

(54) Amato, D. V; Amato, D. N.; Blancett, L. T.; Mavrodi, O. V; Martin, W. B.; Swilley, S. N.; Sandoz, M. J.; Shearer, G.; Mavrodi, D. V; Patton, D. L. A bio-based pro-antimicrobial polymer network via degradable acetal linkages. *Acta Biomater.* **2018**, *67*, 196–205.

CHAPTER II – USING ALDEHYDE SYNERGISM TO DIRECT THE DESIGN OF DEGRADABLE PRO-ANTIMICROBIAL NETWORKS

2.1 Abstract

We describe the design and synthesis of degradable, dual-release, pro-antimicrobial poly (thioether acetal) networks derived from synergistic pairs of aromatic terpene aldehyde derivatives exhibiting a synergistic antimicrobial activity against *Pseudomonas aeruginosa* by determining fractional inhibitory concentrations. Synergistic aldehydes were converted into dialkene acetal monomers and copolymerized at various ratios with a multifunctional thiol via thiol−ene photopolymerization. The step-growth nature of the thiol−ene polymerization ensures every cross-link junction contains a degradable acetal linkage enabling a fully cross-linked polymer network to revert into its small molecule constituents upon hydrolysis, releasing the synergistic aldehydes as active antimicrobial compounds. A three-pronged approach was used to characterize the poly (thioether acetal) materials: (i) determination of the degradation/aldehyde release behavior, (ii) evaluation of the antimicrobial activity, and (iii) identification of the cellular pathways impacted by the aldehydes on a library of mutated bacteria. From this approach, a polymer network derived from a 40:60 *p*-bromobenzaldehyde/*p*-anisaldehyde monomer ratio exhibited potent antimicrobial action against *Pseudomonas aeruginosa*, a common opportunistic human pathogen. From a transposon mutagenesis assay, we showed that these aldehydes target porins and multidrug efflux pumps. The aldehydes released from the poly (thioether acetal) networks exhibited negligible toxicity to mammalian tissue culture cells, supporting the potential development of these materials as dual-release antimicrobial biomaterial platforms.

2.2 Introduction

The rise in antibiotic resistance among pathogens caused by the overuse of antibiotics in medicine and agriculture has been identified by the Infectious Disease Society of America as a significant risk to public health.[1,2] The increase in rates of nosocomial infections caused by pathogens of the ESKAPE group (*Enterococcus faecium*, *Staphylococcus aureus*, *Klebsiella pneumoniae*, *Acinetobacter baumannii*, *Pseudomonas aeruginosa*, and *Enterococcus* sp.) is particularly alarming, considering effective treatment options for these infections are rapidly dwindling due to the high levels of antibiotic resistance.[3] Among the members of the ESKAPE group, *P. aeruginosa* is associated with respiratory tract infections in patients with cystic fibrosis and severe hospital-acquired infections associated with surgical wounds and burns.[4–6] *P. aeruginosa* can efflux, inactivate, or modify a wide range of antibiotics,[7] prompting the search for alternative therapeutic strategies, including the use of antibodies,[8–10] vaccines,[11] antimicrobial peptides,[12] and signaling inhibitors.[13–20] Nevertheless, FDA-approved antibiotics and combinations thereof remain the primary approach for controlling *P. aeruginosa* infections, but the continuous rise in the antimicrobial resistance threatens the long-term efficacy of this approach.[21–37]

Essential oils are plant extracts that contain antimicrobial terpenes, aldehydes, and terpenoids and have emerged as an effective alternative to antibiotics in combating pathogenic microorganisms. The antimicrobial constituents of essential oils often exert multimodal biological activity and can overcome and potentially reverse antimicrobial resistance.[38,39] Prior work has shown that aromatic terpene aldehydes disrupt metabolic functions in bacteria via membrane disruption,[40,41] gene regulation,[42] and modification of

DNA/RNA, proteins, and peptides via Schiff base formation.[43] Recently, we demonstrated the synthesis of degradable poly(thioether acetal) scaffolds, referred to as a pro-antimicrobial network via degradable acetals (PANDA), using aromatic terpene aldehydes as building blocks. The PANDA approach helps to circumvent the low bioavailability, high volatility, and chemical instability of the aldehydes as part of the poly (thioether acetal) network, but provides controlled release of the antimicrobial aldehyde upon acetal hydrolysis.[44,45] Borrowing from the well-established combination therapy approach, we hypothesized that synergistic aldehyde pairs could be used to construct new antimicrobial materials with significantly improved antimicrobial properties. In this article, we systematically investigated aldehyde combinations to identify pairs that exhibited antimicrobial synergism. The identified aldehyde pairs were subsequently converted into diallyl acetal monomers and copolymerized into pro-antimicrobial networks via degradable acetals (co-PANDAs). The acetal linkages present throughout the co-PANDAs allow the network to degrade into aldehydes and alcohols upon exposure to a mild pH (<7.4). To highlight the potential of the new combinatorial antimicrobial platform, we evaluated the activity and cellular targets of co-PANDAs against the important opportunistic pathogen *P. aeruginosa*.

2.3 Materials and methods

2.3.1 Materials

All reagents were obtained from Fisher Scientific at the highest purity available and used without further purification unless otherwise specified. Pentaerythritol tetra(3-mercaptopropionate) (PETMP) was obtained by Bruno Bock. Trimethylolpropane diallyl ether (90%) was purchased from Sigma-Aldrich. Bacto Tryptone, Difco Agar, and

Mueller-Hinton (MH) broth and agar were acquired from Becton Dickinson. The MTT assay kit (3-(4,5-dimethylthiazol-2-yl)-2,5-diphenyltetrazolium bromide) was acquired from Invitrogen.

2.3.2 Characterization

A Bruker Ascend 600 MHz (TopSpin 3.5) spectrometer was used to record $^{1}H/^{13}C$ NMR spectra with chloroform-d. HRMS analysis was completed using positive-ion mode ionization with an Apollo II ion source on a Bruker 12 T APEX-Qe FTICR-MS. Dynamic mechanical analysis (DMA, TA Instruments Q800) was performed in tension mode from −60 to 50 °C at a ramp rate of 3 °C min^{-1}. Real-time Fourier transform IR (RT-FTIR) spectroscopy (Nicolet 8700 FTIR spectrometer with MCT/A detector; 2 scans s^{-1} with a resolution of 4 cm^{-1}) was employed to characterize photopolymerization kinetics by integrating the thiol (2500−2620 cm^{-1}) and alkene (3050−3125 cm^{-1}) peaks to determine conversions. UV light (400 mW cm^{-2}) was supplied by an Excelitas Omnicure S1000. Optical density at 600 nm (OD600) was measured in a BioTek Synergy 2 programmable microplate reader (BioTek Instruments).

2.3.3 Determination of minimum inhibitory concentrations (MICs) of aldehydes

A modified broth microdilution method[46] was used to determine the MICs of pA and pB required to inhibit the growth of *P. aeruginosa* PAO1. Solutions of pA and pB ranging in concentration between 0.5 and 3 mg mL^{-1} were prepared by sonicating for 5 min in the presence of 0.2% agar. Overnight bacterial cultures were then adjusted to 10^5 CFU mL^{-1} in 2× Difco Mueller-Hinton (MH) broth. Next, 50 μL aliquots of bacterial cultures were mixed with equal volumes of aldehyde solutions in a microtiter plate. Bacteria suspended in MH broth without the addition of aldehydes served as a positive

control, while 2× MH broth mixed with aldehydes diluted in 0.2% agar served as a negative control. Microtiter plates were then incubated at 37 °C for 24 h. The MICs were determined by measuring OD_{600} with values < 0.05 considered negative for bacterial growth. Each experiment was repeated three times with three replicates for each treatment.

2.3.4 Identifying synergistic interactions between EO-derived aldehydes

The synergism assay was done via the checkerboard broth microdilution technique.[47] Briefly, solutions of aldehydes were prepared in 0.2% agar at concentrations corresponding to 0.5× MIC, 0.25× MIC, and 0.125× MIC. Next, 50 µL of an overnight bacterial culture adjusted to 10^5 CFU mL^{-1} in 2× MH broth were mixed in a microtiter plate in a checkerboard pattern with 25 µL of two different aldehydes. Bacteria suspended in MH broth without aldehydes and 2× MH broth mixed with aldehydes diluted in 0.2% agar served as the positive and negative controls, respectively. Microtiter plates were incubated at 37 °C for 24 h, and turbidity at 600 nm was measured as described above. The effect of the checkerboard combinations was determined by calculating the fractional inhibitory concentration (FIC) index as follows: $\Sigma FIC = (MIC_A$ in combination/MIC_A alone) + (MIC_B in combination/MIC_B alone). The FIC index was used to interpret the results as follows: FIC index ≤ 0.5 = synergism, 0.5− 0.75 = partial synergy, > 0.75−1 = additive, > 1− 4.0 = indifference, and > 4.0 = antagonism. All treatments were done in triplicates, and experiments were repeated at least three times.

2.3.5 Construction of *P. aeruginosa* PAO1 transposon mutant library

Transposon mutagenesis of *P. aeruginosa* was performed with EZ-Tn5 <TET-1> transposon (Lucigen, WI, USA). Briefly, bacteria were cultured overnight in LB broth at

37 °C with shaking at 250 rpm and prepared for electroporation using the method of Choi et al.[48,49] Then, 100 ng of the EZ-Tn5 <TET-1> DNA was combined with one unit of the EZ-Tn5 transposase, and 0.7 μL of this mix was electroporated into *P. aeruginosa* with an Electroporator 2510 (2.5 kV, 10 μF, 600 Ω) (Eppendorf, NY, USA). The transformed cells were incubated with shaking for 1.5 h in LB broth and spread-plated on LB agar supplemented with 100 μg mL^{-1} of tetracycline. The resultant transposon-bearing clones were individually transferred into 96-well microplates filled with LB-tetracycline broth, incubated overnight at 37 °C, mixed with dimethyl sulfoxide (7% final), and frozen at −80 °C for long-term storage.

2.3.6 Screening transposon mutants hypersensitivity to aldehydes

The transposon mutant library was inoculated into microplates containing 0.2% MH agar amended with 0.6 × MIC of pA and pB using a 96-prong replicator (VP Scientific, San Diego, CA). The inoculated microplates were incubated at 37 °C for 24 h, and bacterial growth was recorded by measuring OD_{600}. The data was normalized by removing the background absorbance, and a factor of inhibition (F_1) was calculated for each mutant as the reciprocal of the OD_{600} ratio between the treated and untreated conditions.[50] All mutants with F1 ≥ 9 were identified and retested again with four different levels (0.6× MIC, 0.8× MIC, 1× MIC, and 1.2× MIC) of pA and pB to confirm their susceptibility. Controls included the wild-type strain PAO1 and mutants grown in MH broth in the absence of aldehyde compounds. Assays were repeated twice with two replicates for each treatment condition.

2.3.7 Identification of transposon insertion sites

Genomic DNA from susceptible mutants was extracted using the UltraClean Microbial DNA Isolation Kit (Qiagen, MD, USA). Five hundred nanograms of each DNA sample were digested to completion with SacII endonuclease and self-ligated with T4 DNA ligase (both from New England Biolabs, MA, USA). The ligation products served as a template for inverse PCR with Q5 High-Fidelity DNA Polymerase (New England Biolabs) and transposon-specific primers TET-1 FP-3 (5′-GCATCTCGGGCACGTTGGGTCCT-3′) and TET-1 RP-3 (5′-GGGGCTGACTTCAGGTGCTACATTT-3′). The resultant amplicons were cleaned with a GeneJET PCR purification spin kit (ThermoFisher, MA, USA) and sequenced with TET-1 FP-3 and TET-1 RP-3 primers. Areas flanking the EZ-Tn5 <TET-1> integration sites were located by BLAST searches against the reference assembly of *P. aeruginosa* PAO1 genome.[51]

2.3.8 Synthesis of *p*-anisaldehyde acetal (pAA)

p-Anisaldehyde (pA) was synthesized according to a literature procedure.[45,52] ^{1}H NMR ($CDCl_3$, 600 MHz): δ 7.45 (dd), 6.93 (dd), 5.97(m), 5.62 (s), 5.35 (dd), 5.17 (dd), 4.07 (d), 3.82 (s). ^{13}C NMR ($CDCl_3$): δ 159.66, 134.16, 130.68, 127.97, 116.67, 113.52, 100.29, 66.00, and 55.22. HRMS (ESI-FTICR-MS): m / z $[M + Na]^+$ calcd for $C_{14}H_{18}O_3Na$, 257.114816; found, 257.114844.

2.3.9 Synthesis of *p*-bromobenzaldehye acetal (pBA)

Trimethylsilyl trifluoromethanesulfonate (TMSOTf) (200 μL, 1.1 mmol) in dry dichloromethane (30 mL) was added to flame-dried round-bottom flask under nitrogen and cooled to −84 °C. Allyloxytrimethylsilane (54.5 mL, 324 mmol) and *p*-

bromobenzaldehyde (pB) (24 g, 129.7 mmol) in 25 mL were then added dropwise, and the solution was stirred for 3 h. The reaction was then warmed to −30 °C, stirred for 1 h, and quenched with pyridine (15 mL). The reaction mixture was poured into a saturated sodium bicarbonate solution (100 mL) and extracted three times with 100 mL of diethyl ether, and the organic layer was separated and dried over anhydrous $MgSO_4$. The crude oil collected after rotary evaporation was purified via column chromatography using ethyl acetate and hexane (1:1). The target compound was a clear oil (79% yield). ^1H ($CDCl_3$, 600 MHz): δ 7.67 (dd), 7.63 (dd), 5.93 (m), 5.66 (s), 5.32 (dd), 5.20 (dd), 4.07 (m). ^{13}C NMR ($CDCl_3$): δ 143.60, 133.97, 132.08, 127.59, 118.62, 117.18, 112.35, and 66.36. HRMS (ESI-FTICR-MS): m / z $[M + Na]^+$ calcd for $C_{13}H_{15}BrO_2Na$, 305.014763; found, 305.014758.

2.3.10 Synthesis of *p*-cyanobenzaldehyde acetal (pCyA)

Following the procedure described for *p*-bromobenzaldehyde, the reaction using TMSOTf (170 μL, 0.88 mmol), allyloxytrimethylsilane (36 mL, 200 mmol), and *p*-cyanobenzaldehyde (pCy) (11.5 g, 88 mmol) afforded pCyA as a clear oil (8.54 g, 42.5% yield). ^1H NMR ($CDCl_3$, 600 MHz): δ 7.35 (dd), 7.24 (dd), 5.78 (m), 5.45 (s), 5.17 (dd), 5.03 (dd), and 3.90 (dd). ^{13}C NMR ($CDCl_3$): δ 137.54, 134.29, 131.36, 128.55, 122.53, 116.93, 99.76, and 66.13. HRMS (ESI-FTICR-MS): m / z $[M + Na]^+$ calcd for C14H15NO2Na, 252.099500; found, 252.099407.

2.3.11 Synthesis of *p*-cinnamaldehyde acetal (CinA)

Following the procedure described for *p*-cyanobenzaldehyde, the reaction using TMSOTf (85 μL, 0.44 mmol), allyloxytrimethylsilane (18.5 mL, 110 mmol), and cinnamaldehyde (Cin) (5.81 g, 44 mmol) afforded CinA as a clear oil (7.47 g, 74% yield).

Column chromatography was carried out using ethyl acetate, hexane, and triethylamine (9:0.5:0.5). ^{1}H ($CDCl_3$, 600 MHz): δ 7.42 (dd), 7.34 (m), 6.77 (dd), 6.24 (dd), 5.97 (m), 5.34 (dd), 5.21 (dd), and 4.15 (dd). ^{13}C NMR (CDCl3): δ 136.09, 134.96, 133.41, 128.62, 128.16, 126.79, 127.06, 116.98, 100.34, and 66.26.

2.3.12 General preparation of co-PANDA disks

Pentaerythritol tetra (3-mercaptopropionate) (PETMP), 4 wt % 2-hydroxy-2-methylpropiophenone (Darocur 1173), and a mixture of two acetals were added to a scintillation vial maintaining a 1:1 thiol to alkene ratio. The thiol−ene formulation was mixed thoroughly, and 30 μL of the mixture was cast between two glass slides separated with a Teflon spacer (0.76 ± 0.02 mm in thickness). The samples were cured using an Omnicure S1000-1B with a 100 W mercury lamp (λmax = 365 nm, 320−500 nm filter) at an intensity of 400 mW cm^{-2} for 40 s. Control disks were prepared similarly by replacing the diallyl acetal monomers with trimethylolpropane diallyl ether.

2.3.13 Degradation of co-PANDA disks

Co-PANDA disks (100 mm3) were submerged in a 100 mL solution of acetonitrile and deionized water (80:20 ratio), and the mixture was continuously shaken (45 rpm) for 48 h. Then, 500 μL aliquots were removed at 0, 0.25, 0.5, 1, 3, 4, 6, 8, 12, 18, 24, and 48 h and deposited into sealed GC−MS vials. GC−MS analysis was performed according to previous literature.[46] The aldehyde release percentages from the 100 mm^3 disks were then applied to estimate the concentration released from a 30 mm^3 disk used in the microbial assays. Dark field images were acquired on a Nikon SMZ-800N stereomicroscope equipped with a Nikon LED dark field base and a Moticam 1080

HDMI camera (1/ 2.8″ CMOS sensor). Disk diameters were measured using Motic Images Plus 3.0 software.

2.3.14 Determining the antimicrobial activity of PANDAs and co-PANDAs via zone of inhibition assays

Cultures of the wild-type *P. aeruginosa* PAO1 (WT) and its *mexA* and *oprF* mutants were adjusted in MH broth to OD_{600} of 0.1. Two hundred microliters of the diluted bacteria were mixed with 4 mL of molten soft agar maintained at 55 °C, and the mixture was poured on the surface of MH agar plates. Then, 60 mm^3 PANDA disks (prepared with either pAA or pBA) and co-PANDA disks (prepared with 40:60 pBA/pAA) were fabricated and placed on the overlaid plates. Plates were incubated for 24 h prior to determining the zone of inhibition (ZOI). Three replicates were carried out for each treatment and each bacterium, and the experiment was repeated twice.

2.3.15 Determining the MIC of PANDAs and co-PANDAs via a broth macrodilution assay

To determine the optimal pBA/pAA ratio for preparing co-PANDAs, the two aldehydes were copolymerized at ratios of 100:0, 70:30, 60:40, 50:50, 40:60, 30:70, and 0:100 and compared for the antimicrobial activity. The overnight cultures of the wild-type *P. aeruginosa* and its *mexA* and *oprF* mutants were diluted in MH broth to 10^5 CFU mL^{-1}. Four milliliter aliquots of each bacterium were combined with disks of the polymer material that ranged in size between 10 and 80 mm^3 (PANDAs) or between 10 and 40 mm^3 (co-PANDAs). MICs of the PANDA and co-PANDA disks were determined after 24 h of incubation at 37 °C.

2.3.16 Evaluation of kill kinetics via terminal dilution assay

The kill kinetics were determined by measuring the viability of *P. aeruginosa* following the exposure to co-PANDAs for 0, 4, 8, 12, and 24 h. Bacterial cultures were adjusted to 10^5 CFU mL^{-1} and combined with 60 mm^3 co-PANDA disks in a volume of 4 mL, and the mixtures were incubated with shaking for 24 h at 37 °C. At different time points, six 100 μL aliquots of bacteria were transferred to a 96-well microtiter plate prefilled with 200 μL of MHB and serially diluted. The inoculated microtiter plates were incubated for 48 h at 37 °C, after which the OD_{600} was measured. The population of viable bacteria was determined using the following formula: $\frac{\text{CFU}}{\text{mL}} = \frac{10 \times 3^{\text{TD}}}{1\ \text{mL}}$ where TD stands for the highest dilution with bacterial growth in microtiter plates. The average of the six replicates was used to calculate the CFU mL^{-1}.

2.3.17 Direct contact mammalian cell viability test

The effect of the co-PANDAs on mammalian cells was assessed by measuring the viability of KB cells in a direct contact ISO 10993-5 assay. The KB cells were maintained and proliferated at 37 °C in 5% CO_2 in a humidified atmosphere in the RPMI 1640 medium supplemented with 10% FBS. For viability tests, KB cells (1 M cells mL−1, 100 μL) were seeded in 96-well microtiter plates, incubated 24 h, and then overlaid with 6 mm^3 co-PANDA disks. Treatments exposed to 6 mm^3 nondegradable thiol−ene control disks were used as a control, and cells with no treatment served as a blank reference. Three replicates were measured to calculate percent survival and standard deviation. After 24 h incubation, cell viability was determined using a Vybrant MTT Cell Proliferation Assay Kit (Invitrogen) following the manufacturer's protocol.

MTT absorbance was measured using a Biotek Synergy2 microplate reader. All assays were performed in triplicate, and the experiment was repeated twice.

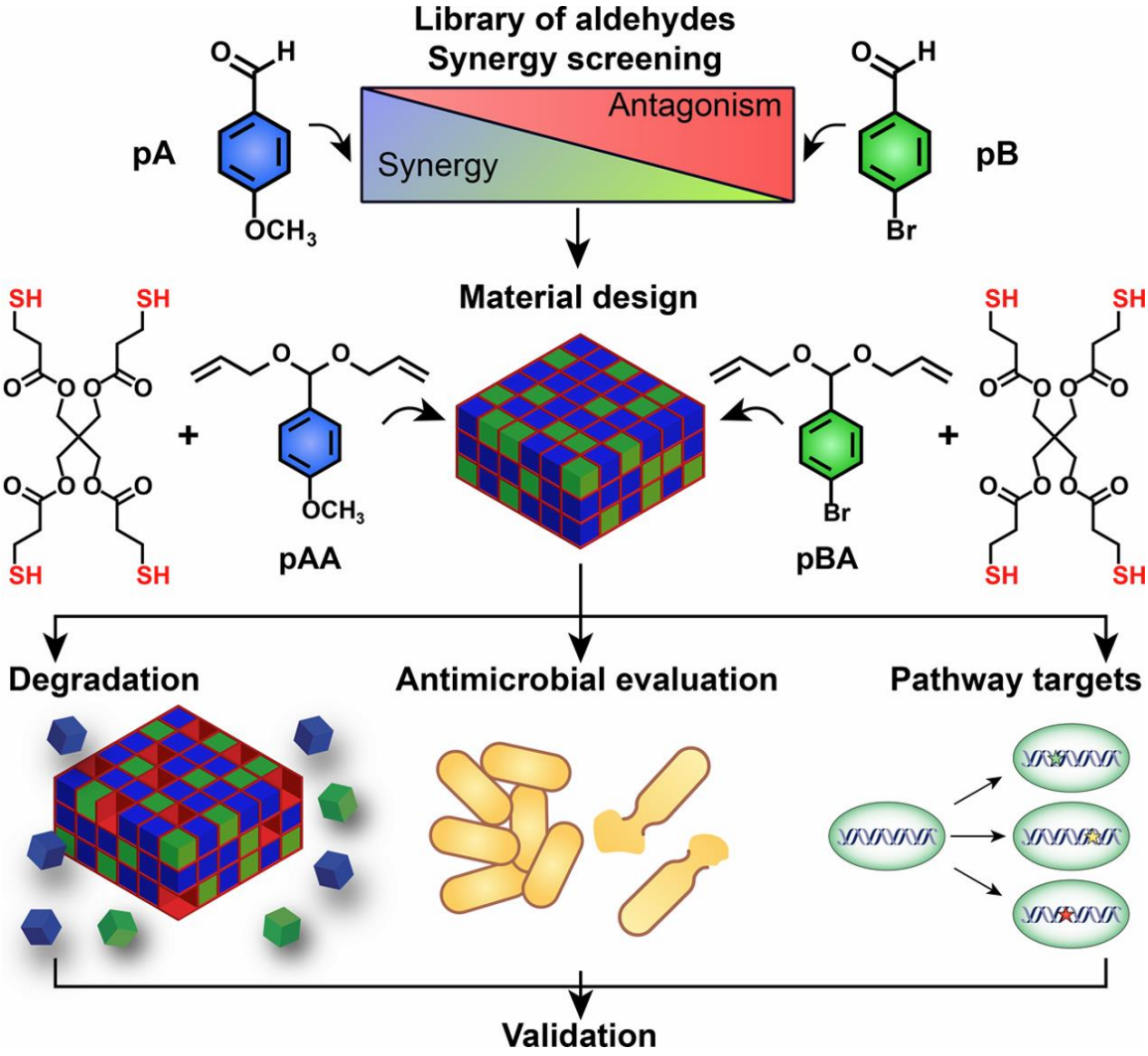

Scheme 2.1 *Outline of the Approach for Designing an Antimicrobial Material from Screening Synergistic Aldehyde.*

2.4 Results and discussion

The overall experimental strategy is outlined schematically in Scheme 2.1. This strategy involved screening aldehyde pairs for antimicrobial synergy, followed by direct conversion of aldehydes into polymerizable dialkene acetal monomers. The acetal monomers were then copolymerized at different ratios into cross-linked polymer

networks and subsequently used to (i) determine concentrations of released aldehydes, (ii) evaluate the antimicrobial activity of the copolymerized networks, and (iii) identify microbial pathways targeted by individual aldehydes, as well as their combinations in the wildtype and mutant derivatives of *P. aeruginosa*. Initially, we identified synergistic combinations of aldehydes by measuring the fractional inhibitory concentration (FIC) of cinnamaldehyde (Cin), *p*-cyanobenzaldehyde (pCy), *p*-anisaldehyde (pA), *p*-chlorobenzaldehyde (pCl), and *p*-bromobenzaldehyde (pB) pairs against *P. aeruginosa* PAO1 (Table 1). From the screening, only Cin/pA (FIC = 0.75), pB/pCy (FIC = 0.75), and pB/pA (FIC = 0.75, Figure 2.1a), pairs exhibited partial synergism and served as raw material candidates for degradable matrix synthesis. The synergistic aldehydes were converted into polymerizable acetal monomers with allyloxytrimethylsilane in the presence of trimethylsilyl trifluoromethanesulfonate in reasonable yields (∼40−55% after column). The resulting dialkene acetal monomers (e.g., *p*-bromobenzaldehyde acetal (pBA) and *p*-anisaldehyde acetal (pAA), cinnamaldehyde acetal (CinA) and *p*-anisaldehyde acetal (pAA), and *p*-bromobenzaldehyde acetal (pBA) and *p*-cyanobenzaldehyde acetal (pCyA)) were then copolymerized into polymer networks in a variety of ratios with a tetrafunctional thiol cross-linker (PETMP) at a 1:1 SH/ene stoichiometry.

Table 2.1 *Summary of Synergistic Screening of Aldehyde Pairs.*

Aldehydes Pairs	Lowest ΣFIC	Interaction
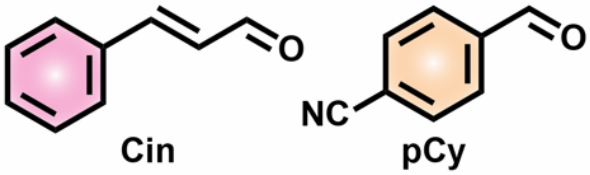	1	Indifference
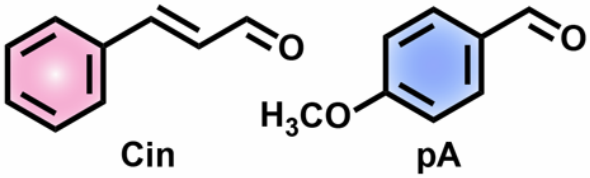	0.75	Synergy
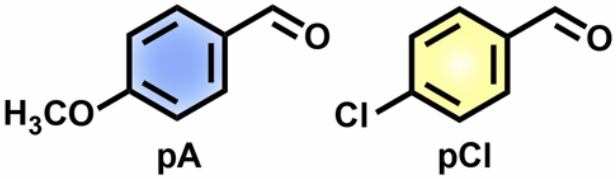	1	Indifference
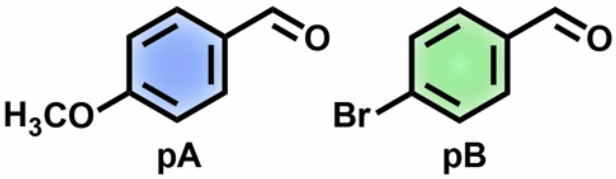	0.75	Synergy
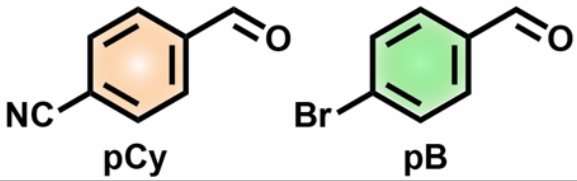	0.75	Synergy
Cinnamaldehyde (Cin), p-Cyanobenzaldehyde (pCy), p-Chlorobenzaldehyde (pCl), p-Anisaldehyde (pA), p-Bromobenzaldehyde (pB)		

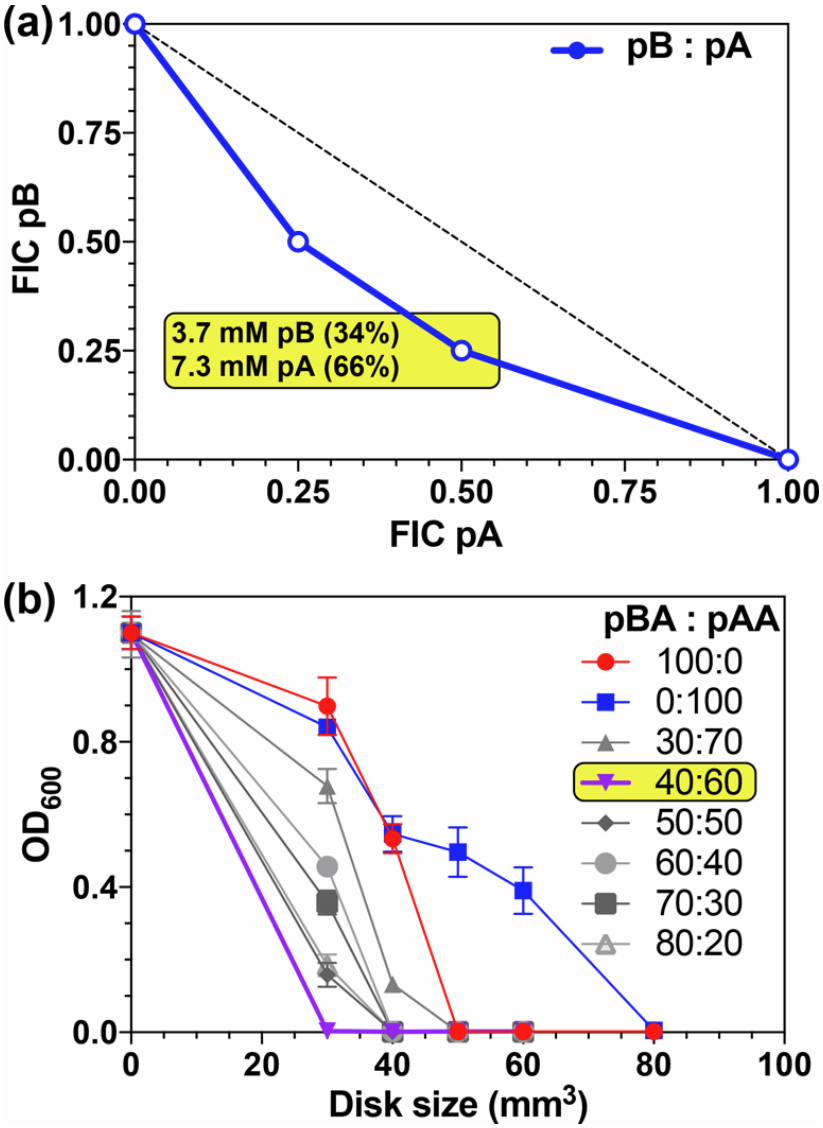

Figure 2.1 Antimicrobial properties of small molecules and matrices.

(a) Graph showing synergistic interactions between pB and pA against *P. aeruginosa* PAO1. The highlighted box shows the determined synergistic concentrations and molar ratio of pA and pB at the FIC value used in this study. (b) Optical density measurements as a function of disk size for co-PANDA pBA/pAA matrices of different ratios. The highlighted box indicates the most effective synergistic composition of pB and pA, which was used throughout the study.

Preliminary degradation studies were carried out in 1 N HCl simply to accelerate the degradation process. Under these conditions, networks composed of 50:50 pBA/pCyA and 50:50 CinA/pAA both required greater than 2 days to reach the point of visual degradation. Real-time FTIR studies revealed that CinA/pAA was the only

composition in which the SH exhibited complete conversion, while the alkene did not fully polymerize (Figure A.1 a, b). We speculate that the internal alkene of CinA could be a competing site for radical addition, which would lead to the formation of irreversible cross-links and thereby slow rate of degradation. Additionally, the rate of acetal degradation increases with decreasing pH, and therefore, the 2-day onset of degradation for both pCB/pCyA and CinA/pAA under 1 N HCl conditions precludes their use as a release platform against *P. aeruginosa* (growth conditions ~ pH 7). However, 50:50 pBA/pAA disks degraded even under PBS (pH 7.4); thus, the pBA/pAA system remained the primary focus in subsequent antimicrobial tests. Additionally, the pBA/pAA co-PANDA resins reached a high conversion upon UV exposure (Figure A.2) and yielded materials with a glass transition temperature below room temperature (Figure A.3). The antimicrobial properties of pBA/pAA matrices that comprised different acetal mole ratios were compared by establishing the minimum amount of co-PANDA material required for the complete inhibition of *P. aeruginosa* PAO1 after an overnight exposure (Figure 2.1b). Results of this experiment revealed that at a 30 mm^3 disk size all co-PANDAs exhibited a lower *P. aeruginosa* OD_{600} reading (lower OD_{600} reading = lower bacterial concentration) than PANDAs containing either only pAA or pBA. Moreover, among all of the tested pBA/pAA ratios, the 40:60 co-PANDA required the smallest disk size (30 mm^3) to achieve full inhibition of *P. aeruginosa* PAO1, compared to the other co-PANDAs (MICs = 40−50 mm^3), pure pAA (80 mm^3) and pBA (50 mm^3) PANDA disks. The fact that the 40:60 co-PANDA required the smallest disk size to inhibit the growth of *P. aeruginosa* PAO1 is not coincidental, as this ratio closely matched the synergistic 34:66 pB/pA mole ratio determined from the aldehyde FIC study (as previously shown in Figure 2.1a). This

result suggests that both aldehydes are released from the 40:60 pBA/pAA co- PANDA at concentrations similar to the FIC study. The concentration of aldehydes released from the 40:60 pBA/pAA co-PANDA over time was measured by GC−MS.

Due to low solubility of both aldehydes in water, an 80:20 acetonitrile/H_2O mixture was necessary to ensure sink conditions for aldehyde release. The co-PANDA disks (100 mm^3) were submerged in a sealed vial with 100 mL of degradation media, and aliquots were removed and analyzed via GC−MS to determine the concentrations of pA and pB released over time (Figure 2.2a). Although the degradation media is not identical to growth media in the bacteria experiments, the concentrations/percent released obtained from the release data are assumed to be similar and serve as an estimate for the concentration of aldehydes released to the bacteria. Within the first hour, the co-PANDA disks released 0.71 ± 0.11 mg mL^{-1} of pB (29% acetal degradation) and 1.02 ± 0.12 mg mL^{-1} of pA (41% acetal degradation). After the initial burst release, the degradation begins to slow over the full 48 h study. The determined release values (0.71 ± 0.11 mg mL^{-1} of pB and 1.02 ± 0.12 mg mL^{-1} of pA) were in excellent agreement with the FIC values for both pB (0.69 mg mL^{-1}) and pA (1.00 mg mL^{-1}) corroborating that the 40:60 co-PANDA disk released the synergistic pair of aldehydes near the concentration necessary to inhibit bacteria observed in the testing of small molecule experiments. Additionally, dark field optical micrographs of a 40:60 co-PANDA disk exposed to the same degradation medium were used to determine the average co-PANDA disk diameter over time. As shown in Figure 2.2b, the average disk diameter rapidly decreases within the first 5 h, which coincides with the burst release observed in the GC− MS data (Figure 2.2a). After the initial burst, both the optical images and GC−MS show a slower change

in disk diameter and aldehyde released. From an antimicrobial perspective, the burst release of both pA and pB at inhibitory concentrations is essential for exerting synergistic antimicrobial activity. It is important to state that if the disks did not burst to inhibitory concentrations, no significant antimicrobial activity would be observed. Additionally, the slow release kinetics observed after the initial burst (> 4 h), limits the 40:60 co-PANDA's ability to continually deliver inhibitory levels of aldehydes over the long term.

Despite the progress in the understanding of the biological activity of plant terpene aldehydes, these compounds have been investigated in a limited range of microorganisms and many aspects of their antimicrobial action remain inconclusive. We addressed these gaps by conducting an analysis of cellular pathways targeted by pA and pB and their co-PANDA matrices in *P. aeruginosa*. Screening a small transposon insertion library of *P. aeruginosa* for tolerance to subinhibitory concentrations (0.6× MIC) of pA and pB yielded 141 mutants with an increased sensitivity (factor of inhibition $F1 \geq 1$) to one or both aldehydes. Nineteen mutants with F_1 values of ≥ 9 were selected for further work and identification of genes affected by transposon insertions (Figure A.4). Results of the analysis revealed that pA and pB target a diverse range of cytoplasmic and membrane pathways, including those involved in the central intermediary metabolism, biosynthesis of cofactors, and various transport functions.

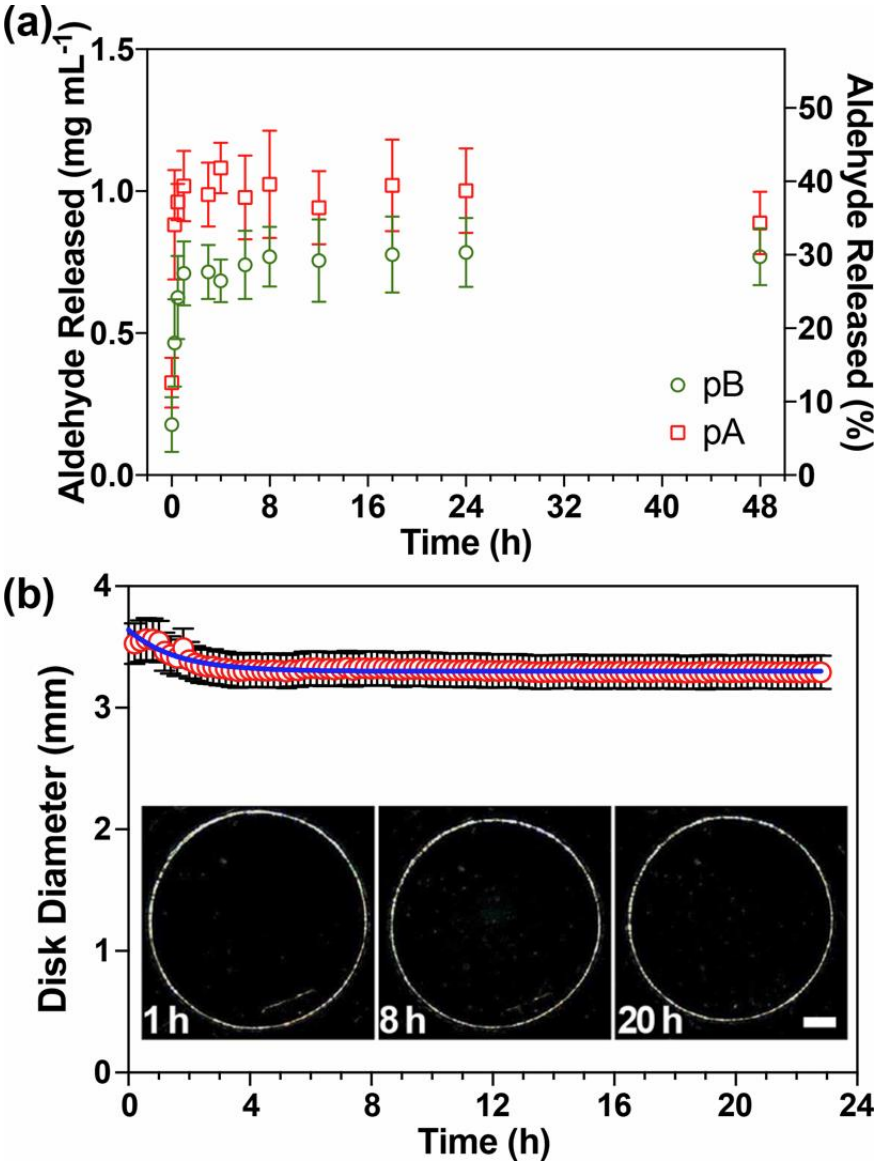

Figure 2.2 Degradation behavior for 40:60 pBA/pAA co-PANDA disks in 80:20 ACN/H_2O.

(a) Determined amounts and percentages of pA and pB released from co-PANDA disks (n = 5). (b) Average disk diameters measured from dark field images (inset images) taken over time (n = 5). Scale bar = 0.5 mm. The blue line is inserted to guide the reader's eye.

The hypersusceptibility phenotype was linked to genes operating in global regulation, twinarginine (Tat) protein secretion pathway, respiratory chain, biosynthesis of molybdenum cofactor, and transport of various small molecules and antimicrobials.

Several mutants were deficient in the production of conserved hypothetical proteins. We are currently working on a paper that will present the detailed analysis of these pathways and discuss the effects of phytoaldehydes on the transcriptome of *P. aeruginosa*. Here, we further concentrated our attention on two mutants that carried mutations in genes encoding porin proteins OprF and MexA, which are components of the multidrug efflux pump MexAB−OprM (Figure A.4). Both proteins play an essential role in the intrinsic and adaptive resistance of *P. aeruginosa* to a variety of antimicrobial agents. The major porin OprF mediates the passage of small hydrophilic molecules and contributes to the low outer membrane permeability in this pathogen.[53] Rapid efflux of antimicrobials by the resistance-nodulation-cell division (RND) systems, such as MexAB−OprM complements the action of *P. aeruginosa* porins.[54] Although previous studies implicated OprF and MexAB−OprM as important determinants of resistance to several classes of antibiotics,[55] our results are the first to report that outer membrane porins and RND efflux pumps play a crucial role in the resistance of *P. aeruginosa* to aromatic terpenes.

We further employed the *oprF* and *mexA* mutants to assess the susceptibility of *P. aeruginosa* to pBA- and pAA-containing polymer materials. The zone of inhibition (ZOI) assays revealed that the inactivation of *oprF* and *mexA* increased the sensitivity to both PANDA and co-PANDA matrices (Figure 3a). Importantly, the co-PANDA disks simultaneously releasing both pA and pB created a larger zone of inhibition in all tested strains compared to PANDA disks of equal size that were synthesized with only pBA or pAA. In contrast, the control disks (no degradable acetals) did not exhibit antimicrobial activity against any of the bacterial strains. To determine the minimum inhibitory concentrations, we cultured the wild-type *P. aeruginosa* and its *mexA* and *oprF* mutants

in liquid growth medium in the presence of 40:60 pBA/pAA co- PANDA disks of different sizes. Results of this experiment demonstrated that a co-PANDA disk of 30 mm^3 was sufficient to inhibit the growth of both mutants and the wild-type strain (Figure 2.3b). Overall, the *mexA*-deficient strain exhibited the highest sensitivity to the co-PANDA disks followed by the *oprF* mutant and the wild-type strain, which agreed with results of the screening for susceptibility to pA and pB (Figure A.4). To investigate whether the co-PANDAs exert a bactericidal or bacteriostatic effect, we exposed *P. aeruginosa* to 60 mm^3 co- PANDA disks for varying times and estimated the number of viable bacteria by a terminal dilution assay (Figure 2.3c). After 12 h of exposure, the co-PANDA disks exhibited a bactericidal 5 log reduction in bacterial concentration, while the control disks were unable to inhibit the growth of bacteria. In general, the mutants were more susceptible to co-PANDA than the wild-type parental strain (*mexA* > *oprF* > WT). These findings were in good agreement with results of the screening of transposon mutants for sensitivity to aldehydes, where the *mexA* mutant was more sensitive to both aldehydes than its *oprF* counterpart.

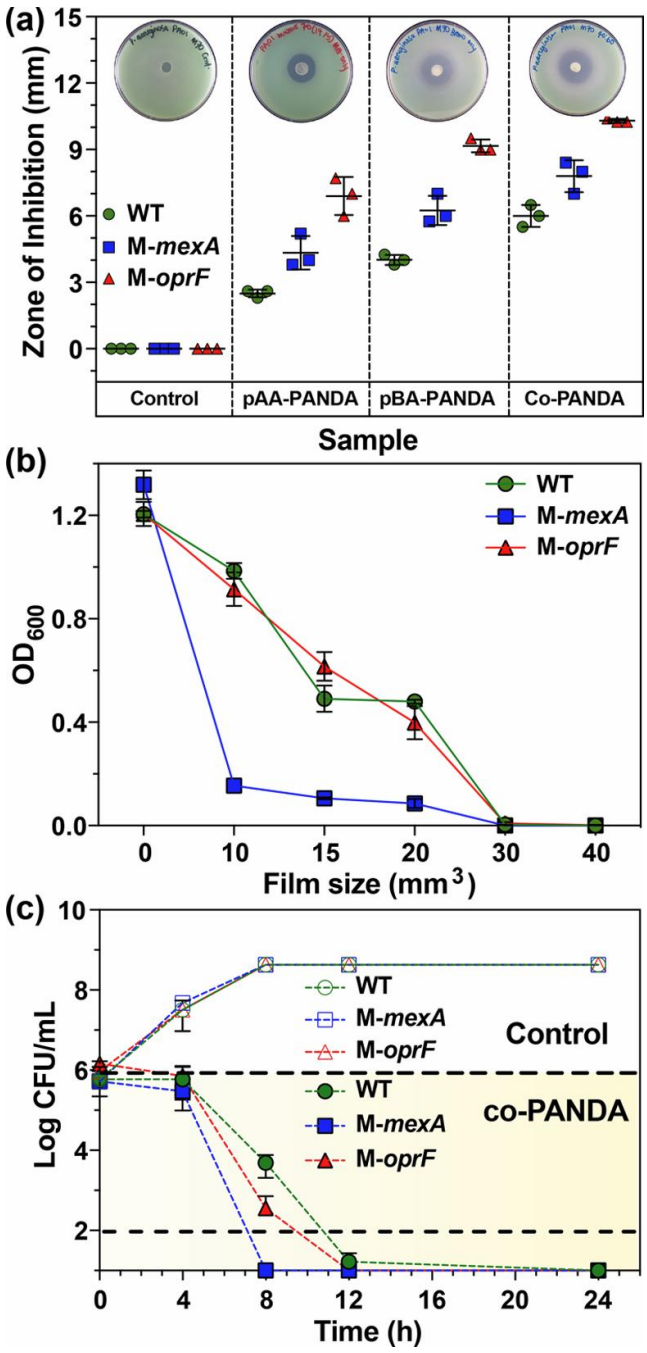

Figure 2.3 Antimicrobial action of PANDAs and the 40:60 pBA/PAA co-PANDAs against the wild-type *P. aeruginosa* PAO1 and its *mexA* and *oprF* mutant.

(a) Zone of inhibition assay. (b) Minimum inhibition disk size assay. (c) Kinetic bactericidal assay. Controls were a nondegradable thiol−ene disk of the same size. The upper dashed line represents the initial bacterial concentration as a reference, while the lower dashed line represents the limit of detection for the assay.

Finally, an MTT assay with KB cells (a type of HeLa cell) was used to assess the cytotoxicity of the 40:60 pBA/pAA co-PANDA material. The co-PANDA disk size was scaled down to 6 mm^3 for the MTT assay with 10^4 cells in 100 μL well volumes. The results of the assay, shown in Figure 2.4, revealed that the 40:60 pBA/pAA co-PANDA caused a decrease in the cell viability to 76% relative to the blank. However, the viability was still above 70%, which meets the ISO 10993-5 criteria for cytocompatibility for materials. A bright field image of control cells (no treatment) after 24 h is shown in Figure 2.4b. Bright field images of the KB cells incubated with a co-PANDA showed no signs of cell lysis, reduction of growth, or zones of inhibition after 24 h of exposure to the 40:60 pBA/pAA co-PANDA disks (Figure 2.4c).[56]

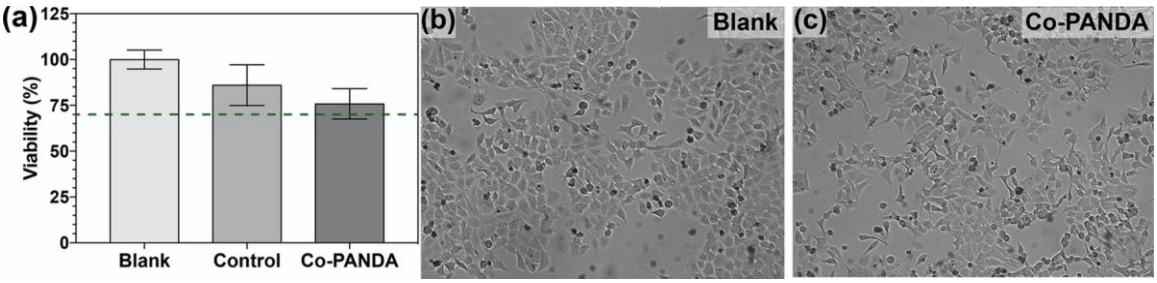

Figure 2.4 MTT cytocompatibility results of co-PANDA materials.

(a) HeLa cells challenged with either a 40:60 pBA/pAA co-PANDA, a nondegradable control, or a blank control. The lower limit of viability for cytocompatibility established by ISO 10993-5 (0.7 × negative control) is represented by the dashed line. (b) Bright field image of control cells (no treatment) after 24 h. (c) Bright field image of cells incubated with a co-PANDA disk after 24 h.

2.5 Conclusion

In summary, we have shown a rational design for a dual-release antimicrobial material. The synergistic screening of multiple aldehydes led to a few select pairs that were converted into monomers and then copolymerized into cross-linked co-PANDAs. After the co-PANDA degradation behavior was understood, the pBA/pAA co-PANDA emerged with the greatest potential for antimicrobial activity (MIC levels released within

1 h). The most potent co-PANDA ratio (40:60 pBA/pAA) closely matched the most potent aldehyde synergy ratio (36:64 pB/pA). The antimicrobial activity of the 40:60 pBA/pAA co-PANDA was evaluated against wild-type and *mexA* and *oprF* mutants of *P. aeruginosa*. Both mutants were more susceptible to aldehydes than the parental strain, suggesting that outer membrane porins and MDR efflux pumps play an important role in resistance of *P. aeruginosa* to antimicrobial terpene aldehydes. Lastly, co-PANDAs exhibited negligible toxicity to mammalian tissue culture cells. These degradable, dual-release antimicrobial materials should elicit interest for a broad range of biomaterial applications (e.g., wound care, surgical tool coatings, etc.).

2.6 References

(1) Levy, S. B.; Marshall, B. Antibacterial Resistance Worldwide: Causes, Challenges and Responses. *Nat. Med.* **2004**, 10, S122−S129.

(2) Marshall, B. M.; Levy, S. B. Food Animals and Antimicrobials: Impacts on Human Health. *Clin. Microbiol. Rev.* **2011**, 24 (4), 718−733.

(3) Boucher, H. W.; Talbot, G. H.; Bradley, J. S.; Edwards, J. E.; Gilbert, D.; Rice, L. B.; Scheld, M.; Spellberg, B.; Bartlett, J. Bad Bugs, No Drugs: No ESKAPE! An Update from the Infectious Diseases Society of America. *Clin. Infect. Dis.* **2009**, 48 (1), 1−12.

(4) Oliver, A.; Cantón, R.; Campo, P.; Baquero, F.; Blázquez, J. High Frequency of Hypermutable Pseudomonas aeruginosa in Cystic Fibrosis Lung Infection. *Science*. **2000**, 288 (5469), 1251−1253.

(5) Wang, C. Y.; Jerng, J. S.; Cheng, K. Y.; Lee, L. N.; Yu, C. J.; Hsueh, P. R.; Yang, P. C. Pandrug-Resistant Pseudomonas Aeruginosa Among Hospitalised Patients:

Clinical Features, Risk-Factors and Outcomes. *Clin. Microbiol. Infect*. **2006**, 12 (1), 63−68.

(6) Appelgren, P.; Björnhagen, V.; Bragderyd, K.; Jonsson, C. E.; Ransjö, U. A Prospective Study of Infections in Burn Patients. *Burns*. **2002**, 28 (1), 39−46.

(7) Mah, T.-F.; Pitts, B.; Pellock, B.; Walker, G. C.; Stewart, P. S.; O'Toole, G. A. A Genetic Basis for Pseudomonas Aeruginosa Biofilm Antibiotic Resistance. *Nature*. **2003**, 426, 306−310.

(8) DiGiandomenico, A.; Keller, A. E.; Gao, C.; Rainey, G. J.; Warrener, P.; Camara, M. M.; Bonnell, J.; Fleming, R.; Bezabeh, B.; Dimasi, N.; Sueman, B.R.; Hillard, J.; Guenther, C.M.; Datta, V.; Zhao, W.; Gao, C.; Yu, X.Q.; Suzich, J.A.; Stover, C.K. A Multifunctional Bispecific Antibody Protects Against Pseudomonas aeruginosa. *Sci. Transl. Med.* **2014**, 6 (262), 262ra155−262ra155.

(9) Secher, T.; Fas, S.; Fauconnier, L.; Mathieu, M.; Rutschi, O.; Ryffel, B.; Rudolf, M. The Anti-Pseudomonas Aeruginosa Antibody Panobacumab is Efficacious on Acute Pneumonia in Neutropenic Mice and has Additive Effects with Meropenem. PLoS One. 2013, 8 (9), No. e73396.

(10) Baer, M.; Sawa, T.; Flynn, P.; Luehrsen, K.; Martinez, D.; Wiener-Kronish, J. P.; Yarranton, G.; Bebbington, C. An Engineered Human Antibody Fab Fragment Specific for Pseudomonas Aeruginosa Pcrv Antigen has Potent Antibacterial Activity. *Infect. Immun.* **2009**, 77 (3), 1083−1090.

(11) Westritschnig, K.; Hochreiter, R.; Wallner, G.; Firbas, C.; Schwameis, M.; Jilma, B. A Randomized, Placebo-Controlled Phase I Study Assessing the Safety and Immunogenicity of a Pseudomonas Aeruginosa Hybrid Outer Membrane Protein

OprF/I Vaccine (IC43) In Healthy Volunteers. *Hum. Vaccines Immunother.* **2014**, 10 (1), 170−183.

(12) Luther, A.; Moehle, K.; Chevalier, E.; Dale, G.; Obrecht, D. Protein Epitope Mimetic Macrocycles as Biopharmaceuticals. *Curr. Opin. Chem. Biol.* **2017**, 38, 45−51.

(13) Starkey, M.; Lepine, F.; Maura, D.; Bandyopadhaya, A.; Lesic, B.; He, J.; Kitao, T.; Righi, V.; Milot, S.; Tzika, A.; Rahme, L. Identification of Anti-virulence Compounds That Disrupt Quorum- Sensing Regulated Acute and Persistent Pathogenicity. *PLoS Pathog*. **2014**, 10 (8), e1004321.

(14) Kaufmann, G. F.; Sartorio, R.; Lee, S.-H.; Mee, J. M.; Altobell, L. J.; Kujawa, D. P.; Jeffries, E.; Clapham, B.; Meijler, M. M.; Janda, K. D. Antibody Interference with N-Acyl Homoserine Lactone-Mediated Bacterial Quorum Sensing. *J. Am. Chem. Soc.* **2006**, 128 (9), 2802−2803.

(15) O'Loughlin, C. T.; Miller, L. C.; Siryaporn, A.; Drescher, K.; Semmelhack, M. F.; Bassler, B. L. A Quorum-Sensing Inhibitor Blocks Pseudomonas aeruginosa Virulence and Biofilm Formation. *Proc. Natl. Acad. Sci. U. S. A.* **2013**, 110 (44), 17981−17986.

(16) Czaplewski, L.; Bax, R.; Clokie, M.; Dawson, M.; Fairhead, H.; Fischetti, V. A.; Foster, S.; Gilmore, B. F.; Hancock, R. E.; Harper, D.; Henderson, I.R.; Hilpert, K.; Jones, B.; Kadioglu, A.; Knowles, D.; Ólafsdóttir, S.; Payne, D.; Projan, S.; Shaunak, S.; Silverman, J.; Thomas, CM.; Trust, T.J.; Warn, P.; Rex, J.H. Alternatives to Antibiotics- A Pipeline Portfolio Review. *Lancet Infect. Dis.* **2016**, 16 (2), 239−251.

(17) Anantharajah, A.; Faure, E.; Buyck, J. M.; Sundin, C.; Lindmark, T.; Mecsas, J.; Yahr, T. L.; Tulkens, P. M.; Mingeot- Leclercq, M.-P.; Guery, B.; Van Bambeke, F. Inhibition of the Injectisome and Flagellar Type III Secretion Systems by INP1855 Impairs Pseudomonas Aeruginosa Pathogenicity and Inflammasome Activation. *J. Infect. Dis.* **2016**, 214 (7), 1105−1116.

(18) Williams, J. D.; Torhan, M. C.; Neelagiri, V. R.; Brown, C.; Bowlin, N. O.; Di, M.; McCarthy, C. T.; Aiello, D.; Peet, N. P.; Bowlin, T. L.; Moir, D.T. Synthesis and Structure−Activity Relationships of Novel Phenoxyacetamide Inhibitors of the Pseudomonas Aeruginosa Type III Secretion System (T3SS). *Bioorg. Med. Chem.* **2015**, 23 (5), 1027−1043.

(19) Seiple, I. B.; Zhang, Z.; Jakubec, P.; Langlois-Mercier, A.; Wright, P. M.; Hog, D. T.; Yabu, K.; Allu, S. R.; Fukuzaki, T.; Carlsen, P. N.; Kitamura, Y.; Zhou, X.; Condakes, M.L.; Szczypiński, F.T.; Green, W.D.; Myers, A.G. A Platform For The Discovery Of New Macrolide Antibiotics. *Nature*. **2016**, 533 (7603), 338−345.

(20) Dickey, S. W.; Cheung, G. Y.; Otto, M. Different Drugs for Bad Bugs: Antivirulence Strategies in the Age of Antibiotic Resistance. *Nat. Rev. Drug Discovery*. **2017**, 16 (7), 457−471.

(21) Mouton, J. W.; Ambrose, P. G.; Canton, R.; Drusano, G. L.; Harbarth, S.; MacGowan, A.; Theuretzbacher, U.; Turnidge, J. Conserving Antibiotics for The Future: New Ways to Use Old and New Drugs from a Pharmacokinetic and Pharmacodynamic Perspective. *Drug Resist. Updates.* **2011**, 14 (2), 107−117.

(22) Cassir, N.; Rolain, J.-M.; Brouqui, P. A New Strategy to Fight Antimicrobial Resistance: The Revival of Old Antibiotics. *Front. Microbiol.* **2014**, 5 (551), 1−15.

(23) Berditsch, M.; Jäger, T.; Strempel, N.; Schwartz, T.; Overhage, J.; Ulrich, A. S. Synergistic Effect of Membrane-Active Peptides Polymyxin B and Gramicidin S on Multidrug-Resistant Strains and Biofilms of Pseudomonas Aeruginosa. *Antimicrob. Agents Chemother.* **2015**, 59 (9), 5288−5296.

(24) Ejim, L.; Farha, M. A.; Falconer, S. B.; Wildenhain, J.; Coombes, B. K.; Tyers, M.; Brown, E. D.; Wright, G. D. Combinations of Antibiotics and Nonantibiotic Drugs Enhance Antimicrobial Efficacy. *Nat. Chem. Biol.* **2011**, 7 (6), 348−350.

(25) Cherian, P. T.; Deshpande, A.; Cheramie, M. N.; Bruhn, D. F.; Hurdle, J. G.; Lee, R. E. Design, Synthesis and Microbiological Evaluation of Ampicillin−Tetramic Acid Hybrid Antibiotics. *J. Antibiot.* **2017**, 70 (1), 65−72.

(26) Lambert, R.; Hanlon, G.; Denyer, S. The Synergistic Effect of EDA/Antimicrobial Combinations on Pseudomonas aeruginosa. *J. Appl. Microbiol.* **2004**, 96 (2), 244−253.

(27) Lyu, Y.; Domalaon, R.; Yang, X.; Schweizer, F. Amphiphilic Lysine Conjugated to Tobramycin Synergizes Legacy Antibiotics Against Wild-Type and Multidrug-Resistant Pseudomonas aeruginosa. *Pept. Sci.* **2018**, e23091.

(28) Jenkins, R.; Cooper, R. Improving Antibiotic Activity Against Wound Pathogens with Manuka Honey In Vitro. *PLoS One*. **2012**, 7 (9), No. e45600.

(29) Borselli, D.; Lieutaud, A.; Thefenne, H.; Garnotel, E.; Pagès, J.- M.; Brunel, J. M.; Bolla, J.-M. Polyamino-Isoprenic Derivatives Block Intrinsic Resistance of *P. aeruginosa* to Doxycycline and Chloramphenicol In Vitro. *PLoS One.* **2016**, 11 (5), No. e0154490.

(30) Zheng, Z.; Tharmalingam, N.; Liu, Q.; Jayamani, E.; Kim, W.; Fuchs, B. B.; Zhang, R.; Vilcinskas, A.; Mylonakis, E. Synergistic Efficacy of Aedes Aegypti Antimicrobial Peptide Cecropin A2 and Tetracycline Against Pseudomonas aeruginosa. Antimicrob. Agents Chemother. 2017, 61 (7), e00686.

(31) Chan, B. K.; Sistrom, M.; Wertz, J. E.; Kortright, K. E.; Narayan, D.; Turner, P. E. Phage Selection Restores Antibiotic Sensitivity In MDR Pseudomonas aeruginosa. *Sci. Rep.* **2016**, 6 (26717), 1−8.

(32) Chaudhry, W. N.; Concepción-Acevedo, J.; Park, T.; Andleeb, S.; Bull, J. J.; Levin, B. R. Synergy and Order Effects of Antibiotics and Phages in Killing Pseudomonas aeruginosa Biofilms. *PLoS One.* **2017**, 12 (1), No. e0168615.

(33) Duncan, B.; Li, X.; Landis, R. F.; Kim, S. T.; Gupta, A.; Wang, L.-S.; Ramanathan, R.; Tang, R.; Boerth, J. A.; Rotello, V. M. Nanoparticle-Stabilized Capsules for the Treatment of Bacterial Biofilms. *ACS Nano*. **2015**, 9 (8), 7775−7782.

(34) Zhitnitsky, D.; Rose, J.; Lewinson, O. The Highly Synergistic, Broad Spectrum, Antibacterial Activity of Organic Acids and Transition Metals. *Sci. Rep.* **2017**, 7 (44554), 1−13.

(35) Breidenstein, E. B.; de la Fuente-Núñez, C.; Hancock, R. E. Pseudomonas aeruginosa: All Roads Lead to Resistance. *Trends Microbiol.* **2011**, 19 (8), 419−426.

(36) Tang, S. Y.; Zhang, S. W.; Wu, J. D.; Wu, F.; Zhang, J.; Dong, J. T.; Guo, P.; Zhang, D. L.; Yang, J. T.; Zhang, W. J. Comparison of Mono- and Combination Antibiotic Therapy for the Treatment of Pseudomonas Aeruginosa Bacteraemia: A

Cumulative Meta-Analysis of Cohort Studies. *Exp. Ther. Med.* **2018**, 15 (3), 2418−2428.

(37) Chamot, E.; El Amari, E. B.; Rohner, P.; Van Delden, C. Effectiveness of Combination Antimicrobial Therapy for Pseudomonas Aeruginosa Bacteremia. *Antimicrob. Agents Chemother*. **2003**, 47 (9), 2756−2764.

(38) Burt, S. Essential Oils: Their Antibacterial Properties and Potential Applications in Foods-A Review. *Int. J. Food Microbiol.* **2004**, 94 (3), 223−253.

(39) Yap, P. S. X.; Yiap, B. C.; Ping, H. C.; Lim, S. H. E. Essential Oils, a New Horizon in Combating Bacterial Antibiotic Resistance. Open Microbiol. J. 2014, 8, 6−14.

(40) Chen, X.; Zhang, X.; Meng, R.; Zhao, Z.; Liu, Z.; Zhao, X.; Shi, C.; Guo, N. Efficacy of a Combination Of Nisin and P-Anisaldehyde Against Listeria Monocytogenes. *Food Control.* **2016**, 66, 100−106.

(41) Shi, C.; Zhao, X.; Meng, R.; Liu, Z.; Zhang, G.; Guo, N. Synergistic Antimicrobial Effects of Nisin and P-Anisaldehyde on Staphylococcus aureus in Pasteurized Milk. *LWT–Food Sci. Technol.* **2017**, 84 (SupplementC), 222−230.

(42) Yu, L.; Guo, N.; Yang, Y.; Wu, X.; Meng, R.; Fan, J.; Ge, F.; Wang, X.; Liu, J.; Deng, X. Microarray Analysis of P-Anisaldehyde- Induced Transcriptome of Saccharomyces Cerevisiae. *J. Ind. Microbiol. Biotechnol*. **2010**, 37 (3), 313−322.

(43) Natsch, A.; Gfeller, H.; Haupt, T.; Brunner, G. Chemical Reactivity and Skin Sensitization Potential for Benzaldehydes: Can Schiff Base Formation Explain Everything? *Chem. Res. Toxicol*. **2012**, 25 (10), 2203−2215.

(44) Amato, D. N.; Amato, D. V.; Mavrodi, O. V.; Martin, W. B.; Swilley, S. N.; Parsons, K. H.; Mavrodi, D. V.; Patton, D. L. Pro-Antimicrobial Networks via

Degradable Acetals (PANDAs) Using Thiol−Ene Photopolymerization. *ACS Macro Lett*. **2017**, 6 (2), 171− 175.

(45) Amato, D. V.; Amato, D. N.; Blancett, L. T.; Mavrodi, O. V.; Martin, W. B.; Swilley, S. N.; Sandoz, M. J.; Shearer, G.; Mavrodi, D. V.; Patton, D. L. A Bio-Based Pro-Antimicrobial Polymer Network via Degradable Acetal Linkages. *Acta Biomater*. **2018**, 67, 196−205.

(46) Amato, D. N.; Amato, D. V.; Mavrodi, O. V.; Braasch, D. A.; Walley, S. E.; Douglas, J. R.; Mavrodi, D. V.; Patton, D. L. Destruction of Opportunistic Pathogens via Polymer Nanoparticle-Mediated Release of Plant-Based Antimicrobial Payloads. *Adv. Healthcare Mater*. **2016**, 5 (9), 1094−1103.

(47) Schwalbe, R.; Steele-Moore, L.; Goodwin, A. C. *Antimicrobial Susceptibility Testing Protocols*; CRC Press, 2007.

(48) Choi, K.-H.; Kumar, A.; Schweizer, H. P. A 10-min Method for Preparation of Highly Electrocompetent Pseudomonas Aeruginosa Cells: Application for DNA Fragment Transfer Between Chromosomes and Plasmid Transformation. *J. Microbiol. Methods*. **2006**, 64 (3), 391−397.

(49) Choi, K.-H.; Schweizer, H. P. An Improved Method for Rapid Generation of Unmarked Pseudomonas Aeruginosa Deletion Mutants. *BMC Microbiol*. **2005**, 5 (1), 30.

(50) Campen, R. L.; Ackerley, D. F.; Cook, G. M.; O'Toole, R. F. Development of a Mycobacterium Smegmatis Transposon Mutant Array for Characterizing the Mechanism of Action of Tuberculosis Drugs: Findings with Isoniazid and Its Structural Analogues. *Tuberculosis*. **2015**, 95 (4), 432−439.

(51) Winsor, G. L.; Griffiths, E. J.; Lo, R.; Dhillon, B. K.; Shay, J. A.; Brinkman, F. S. L. Enhanced Annotations and Features for Comparing Thousands Of Pseudomonas Genomes in the Pseudomonas Genome Database. *Nucleic Acids Res*. **2016**, 44 (D1), D646− D653.

(52) Tsunoda, T.; Suzuki, M.; Noyori, R. A Facile Procedure for Acetalization Under Aprotic Conditions. *Tetrahedron Lett*. **1980**, 21 (14), 1357−1358.

(53) Hancock, R. E. Resistance Mechanisms in Pseudomonas Aeruginosa and Other Non-fermentative Gram-Negative Bacteria. Clin. Infect. Dis. 1998, 27 (1), S93−S99.

(54) Li, X.-Z.; Zhang, L.; Poole, K. Interplay Between the MexAMexB- OprM Multidrug Efflux System and the Outer Membrane Barrier in the Multiple Antibiotic Resistance of Pseudomonas aeruginosa. *J. Antimicrob. Chemother*. **2000**, 45 (4), 433−436.

(55) Dötsch, A.; Becker, T.; Pommerenke, C.; Magnowska, Z.; Jänsch, L.; Häussler, S. Genomewide Identification of Genetic Determinants of Antimicrobial Drug Resistance in Pseudomonas aeruginosa. *Antimicrob. Agents Chemother*. **2009**, 53 (6), 2522−2531.

(56) ISO, 10993-5:2009 *Biological Evaluation of Medical Devices− Part 5: Tests for in Vitro Cytotoxicity*; International Organization for Standardization: Geneva, 2009.

CHAPTER III –THE ANTIMICROBIAL ACTIVITY AND CELLULAR PATHWAYS TARGETED BY P-ANISALDEHYDE AND EPIGALLOCATECHIN GALLATE IN THE OPPORTUNISTIC HUMAN PATHOGEN PSEUDOMONAS AERUGINOSA.

3.1 Abstract

Plant-derived aldehydes are constituents of essential oils that possess broad-spectrum antimicrobial activity and kill microorganisms without promoting resistance. In our previous study, we incorporated *p*-anisaldehyde from star anise into a polymer network called PANDAs (Pro-Antimicrobial Networks via Degradable Acetals) and used it as a novel drug delivery platform. PANDAs released *p*-anisaldehyde upon a change in pH and humidity, and controlled growth of the multi-drug resistant pathogen *Pseudomonas aeruginosa* PAO1. In this study, we identified cellular pathways targeted by PANDAs, by generating 10,000 transposon mutants of PAO1 and screened them for hypersensitivity to *p*-anisaldehyde. To improve the antimicrobial efficacy of *p*-anisaldehyde, we combined it with epigallocatechin gallate (EGCG), a polyphenol from green tea, and demonstrated that it acts synergistically with *p*-anisaldehyde in killing *P. aeruginosa*. We then used RNA-seq to profile transcriptomic responses of *P. aeruginosa* to *p*-anisaldehyde, EGCG, and their combination of thereof. The exposure to *p*-anisaldehyde altered the expression of genes involved in the modification of cell envelope, membrane transport, drug efflux, energy metabolism, molybdenum cofactor biosynthesis, and stress response. We also demonstrated that the addition of EGCG reversed many *p*-anisaldehyde-coping effects and induced oxidative stress. Our results provide an insight into the antimicrobial activity of *p*-anisaldehyde and its interactions with EGCG and may aid in the rational identification of new synergistically acting

combinations of plant metabolites. Our study also confirms the utility of the thiol-ene polymer platform for the sustained and effective delivery of hydrophobic and volatile antimicrobial compounds.

3.2 Introduction

Pseudomonas aeruginosa is a ubiquitous gram-negative bacterium that serves as an important model for opportunistic infections and biofilm research [34,35]. This organism is commonly found in soil, water, and plants, but can readily infect immunocompromised individuals causing septicemia and wound or urinary tract infections [8]. It also responsible for pneumonia and causes increased morbidity and mortality in cystic fibrosis patients. *P. aeruginosa* is resistant to multiple classes of antibiotics and belongs to a class of pathogens with increased virulence, persistence and transmissibility known as the ESKAPE group (also encompasses *Enterococcus faecium, Staphylococcus aureus, Klebsiella pneumoniae, Acinetobacter baumannii*, and *Enterobacter* species) [10]. The Centers for Disease Control and Prevention (CDC) reports that, in the U.S. alone, *P. aeruginosa* is associated with 8% of all hospital-acquired infections and over 400 deaths per year, which are often caused by multi-drug resistant (MDR) strains [30]. These MDR variants are insensitive to nearly all the available β-lactams and aminoglycosides and are classified by the CDC as a serious threat that requires close monitoring and prevention activities [53]. Therefore, there is a need for the development of antimicrobial agents, which do not promote antibiotic resistance and may help to mitigate the spread of MDR phenotypes in *P. aeruginosa* and other bacterial pathogens.

Plant essential oils (EOs) represent a rich source of alcohols, aldehydes, terpenes, ethers, ketones, and phenolic compounds with antimicrobial, antifungal, and antiparasitic

activity [23]. The antiseptic properties and low toxicity of EOs prompted their use in traditional food preservation and folk medicine [43]. However, despite the demonstrated biological activity, the wider acceptance of EOs and their constituents as antimicrobial agents is limited by the hydrophobicity, chemical instability, high concentrations needed to achieve sufficient antimicrobial effect, and lack of understanding of the mode of action. In our previous work, we addressed some of these issues by incorporating the antimicrobial EO constituent *p*-anisaldehyde into a polymer network called PANDAs (Pro-Antimicrobial Networks via Degradable Acetals) [3,5]. The resultant polymer material was designed to act as a pro-drug that releases *p*-anisaldehyde upon a change in pH and humidity. The incorporation into PANDAs increased the bioavailability and antimicrobial efficacy of *p*-anisaldehyde and related phytoaldehydes against *P. aeruginosa*, *Escherichia coli, Burkholderia cenocepacia*, *Staphylococcus aureus*, and *Candida albicans.* We also demonstrated that the inactivation of the MexAB-OprM multidrug efflux pump sensitizes *P. aeruginosa* to the action of *p*-anisaldehyde.

MexAB-OprM is a member of the resistance-nodulation-cell-division (RND) superfamily of multidrug efflux pumps, which are recognized as essential contributors to the emergence of MDR phenotypes in pathogenic bacteria. These membrane transporters extrude a broad spectrum of antimicrobial compounds [17], intercellular signals, and virulence factors [2,40], which makes them an attractive target for the development of anti-resistance drugs. Such drugs, known as efflux pump inhibitors (EPIs), interfere with the function, expression, or assembly of RND pumps, and can significantly reduce or completely reverse resistance against otherwise ineffective antibiotics [47]. Despite the development of a number of effective synthetic and semi-synthetic EPIs, none of these

compounds are currently used in the treatment of bacterial infections because of the instability, low selectivity, and cytotoxic side effects [48]. Plants, like animals, are attacked by bacterial pathogens and have evolved defense mechanisms to counteract such infections. This fact has prompted numerous plant-based studies aimed at the isolation of natural EPIs with lower toxicity and better tolerability. These efforts produced a growing list of promising candidates, some of which were patented and are being evaluated against different pathogens [15,41].

In this study, we used *P. aeruginosa* PAO1 as a model to identify cellular pathways targeted in bacterial pathogens by *p*-anisaldehyde and structurally related compounds. We first subjected PAO1 to transposon mutagenesis and screened the resultant library of mutants for susceptibility to sub-inhibitory concentrations of *p*-anisaldehyde and the new *p*-anisaldehyde-containing antimicrobial polymer. This new polymer network relies solely on diffusion to control the release of the active *p*-anisaldehyde from a non-degradable thiol-ene thermoset matrix. The synthesis of the polymer was performed using only commercially available polyfunctional alkenes and polyfunctional thiols, which have eliminated the need to prepare and purify hydrolytically unstable monomers required for release of *p*-anisaldehyde. The new approach minimized the susceptibility of the monomers to atmospheric conditions during the network cure process and improved the batch-to-batch variability. The resultant polymer material had antimicrobial efficacy nearly identical to that of the previously reported degradable systems [3,5].

We also screened a panel of plant-derived EPIs for the ability to potentiate the antimicrobial activity of phytoaldehydes and demonstrated that epigallocatechin gallate

(EGCG), a polyphenol from green tea, acts synergistically with *p*-anisaldehyde and significantly reduces its minimal inhibitory concentration against *P. aeruginosa*. Finally, we profiled the transcriptomes of *P. aeruginosa* grown in the presence of *p*-anisaldehyde, EGCG, and a combination of thereof to gain insight into the possible mode of action of these plant-derived antimicrobial compounds. Our results revealed that *p*-anisaldehyde alters the expression of genes involved in the membrane transport, lipids biosynthesis, stress response, energy metabolism, and biosynthesis of the molybdenum cofactor. The addition of EGCG reversed many of the *p*-anisaldehyde-coping responses and induced oxidative stress, which may contribute to the synergistic antimicrobial effect against *P. aeruginosa*.

3.3 Materials and Methods

3.3.1 Bacterial strain, growth conditions and compounds

All experiments conducted in this study were performed with the reference strain *Pseudomonas aeruginosa* PAO1. The organism was routinely cultured at 37 °C in Difco Luria-Bertani (LB) medium (Becton Dickinson, Franklin Lakes, NJ), while Mueller-Hilton II (MH) broth and agar (Becton Dickinson) were used for all antimicrobial assays. The selection of transposon mutants was performed by amending the growth medium with tetracycline (Tc) (Thermo Scientific, Waltham, MA) at the concentration of 100 μg mL^{-1}. *p*-Anisaldehyde (pA), epigallocatechin gallate (EGCG), geraniol, daidzein, berberine, curcumin, 2-hydroxy-2-methylpropionate (Darocur 1173), and 1,3,5-triallyl-1,3,5-triazine-2,4,6(1H,3H,5H)-trione (TTT) were obtained from Thermo Scientific in the highest purity available and used without further purification. The stock solution of *p*-anisaldehyde was prepared by ultrasonicating the compound for 5 min in 0.2% (w/v)

agar. The stock solutions of EGCG (10 mg mL^{-1}), geraniol (5 mg mL^{-1}), daidzein (5 mg mL^{-1}), berberine (2 mg mL^{-1}), and curcumin (5 mg mL^{-1}) were prepared by dissolving the chemicals in dimethyl sulfoxide (DMSO) (Alfa Aesar, Haverhill, MA).

3.3.2 Construction of the transposon mutant library

The transposon mutagenesis was conducted by electroporating *P. aeruginosa* with transposomes, which are stable complexes formed between the EZ-Tn*5* <TET-1> transposon and the EZ-Tn*5* Transposase (both from Lucigen, Middleton, WI). Briefly, cells from an overnight culture of PAO1 were collected and washed twice in 0.3 M sucrose. One hundred microliters of electrocompetent bacteria, equivalent to 10^{10} viable cells, were mixed with 0.7 μL of the EZ-Tn5™ <TET-1> transposomes in a 2-mm gap width electroporation cuvette. The mixture was electroporated with an Electroporator 2510 (Eppendorf, Hauppauge, NY) at 2.5 kV, 10 μF, and 600 Ω. The transformed cells were immediately suspended in LB broth, incubated with shaking at 37 °C for 1.5 h, spread plated onto LB-Tc_{100}, and incubated at 37 °C until the appearance of individual colonies. The tetracycline-resistant colonies were transferred individually into 96-well microtiter plates prefilled with LB broth amended with 7% DMSO and stored at -80 °C. A total of 10,000 transposon-bearing mutants were collected, which is estimated to cover approximately 83% of the PAO1 genome using the formula: $m = 1 - e^{-L/G}$, where *G* is equal to the number of genes in the PAO1 genome (5,572 protein-coding genes) and for a given size library (L) [13].

3.3.3 Screening of the transposon library for the sensitivity to *p*-anisaldehyde

The transposon mutants of PAO1 were screened for hypersensitivity to *p*-anisaldehyde by replicating the library with a 96-prong replicator (VP Scientific, San Diego, CA) into microplates pre-filled with MH broth supplemented with 0.6× MIC (1.2 mg mL^{-1}), 0.75× MIC (1.5 mg mL^{-1}), and 0.85× MIC (1.7 mg mL^{-1}) of *p*-anisaldehyde. The inoculated plates were incubated at 37 °C for 24 h, and bacterial growth was recorded by measuring optical density at 600 nm (OD_{600}) using a Synergy 2 reader (BioTek Instruments, Winooski, VT). The sensitivity of individual mutants was determined by defining their factor of inhibition (F_1) values, which are calculated as the reciprocal of the OD_{600} ratio between the treated and untreated conditions [13]. All mutants with F_1 values of ≥ 9 were considered as hyper susceptible to *p*-anisaldehyde. The screening was performed twice in duplicates for each tested concentration of *p*-anisaldehyde.

3.3.4 Mapping transposon insertion sites in hypersensitive mutants

Genomic DNA was extracted from overnight cultures of the sensitive mutants grown in LB broth using a DNeasy UltraClean Microbial Kit (Qiagen, Germantown, MD), and 250 ng of the DNA was digested with the restriction endonuclease *Sac*II (New England Biolabs, MA, USA). The endonuclease reaction was incubated for 3 hours at 37 °C, and the enzyme was inactivated at 65°C for 20 min. The digested DNA was self-ligated with T4 DNA ligase (New England Biolabs) by incubating it overnight at 16°C. The ligation products served as a template for inverse PCR with the Q5 High-Fidelity DNA Polymerase (New England Biolabs), and transposon-specific primers (Table 1). Cycling conditions included 98 °C for 30 s, followed by 34 cycles of 98 °C for 10 s, 72

°C for 2 min and 72 °C for 2 min, and a final extension at 72 °C for 5 min. The PCR amplicons were purified using a GeneJET PCR Purification Kit (Thermo Scientific) and sequenced at Eurofins MWG Operon (Huntsville, AL). Areas flanking the EZ-Tn*5* <TET-1> integration sites were mapped to the *P. aeruginosa* PAO1 genome using the BLASTn web tool of the *Pseudomonas* database.[17]

3.3.5 Synthesis of *p*-anisaldehyde-releasing polymeric discs

A stock resin solution was prepared by adding 2 g of TTT (8.04 mmol, 24.12 mmol ene), 2.95 g of PETMP (6.03 mmol, 24.12 mmol SH), and 118 mg Darocur 1173 (0.72 mmol, 3 mol percent relative to SH) to a scintillation vial and mixing thoroughly. Two-gram portions of the resin were then mixed with 800 mg *p*-anisaldehyde (28.6 wt %) to form the active resin. Eighty microliter aliquots of resin were dispensed onto glass slides spaced with Teflon spacers (0.75 mm in thickness) and cured using an OmniCure S1000-1B light source (Lumen Dynamics, Mississauga, Ontario, Canada) with a 100 W mercury lamp (λmax = 365 nm, 320–500 nm filter) for 20 s at an intensity of 200 mW cm^{-2}. Control disks were prepared in the same fashion from the stock resin. Network conversion was confirmed via kinetic data collected through real-time FTIR (RT-FTIR) spectroscopy to monitor the disappearance of thiol and alkene functional groups. RT-FTIR spectra were recorded using a Nicolet 8700 FTIR spectrometer (Thermo Scientific) equipped with a KBr beam splitter and MCT/A detector using an OmniCure S1000 320–500 nm filtered ultraviolet light source. Each sample was exposed to a UV light with an intensity of 200 mW cm^{-2}. Series scans were collected with a data spacing of 2 scans per second with a resolution of 4 cm^{-1}. Thiol conversion was monitored via integration of the SH peak between 2500 and 2620 cm^{-1} and alkene conversion was monitored via the peak

between 3050 and 3125 cm^{-1}. Evaluating the sensitivity of transposon mutants to the of *p*-anisaldehyde-releasing polymeric discs

The antimicrobial activity of polymeric discs against the wild type PAO1 strain and select hypersensitive mutants was determined via a zone of inhibition (ZOI) assay. Briefly, overnight bacterial cultures were adjusted to OD_{600} of 0.1, and then further diluted 1:5 with fresh MH broth. Aliquots (200 µL) of diluted bacterial suspensions were mixed with 4 mL of lukewarm molten soft agar and overlaid on MH agar, after which an 80 mm^3 *p*-anisaldehyde polymeric disc was placed at the center of each inoculated plate. Plates were incubated for 24 h at 37 °C, and the ZOI was measured in mm. In order to compare the sensitivity of mutants, the average ZOI of each mutant was normalized to that of the WT strain, which represented the level of sensitivity of 100%. All treatments were replicated three times, and each mutant was tested twice.

3.3.6 Screening plant-derived EPIs for synergistic interactions with *p*-anisaldehyde

Several plant-derived EPIs were evaluated for the synergistic antimicrobial activity with *p*-anisaldehyde using a modified broth microdilution technique [4]. This was done by determining the MIC of *p*-anisaldehyde against *P. aeruginosa* PAO1 in the presence of non-inhibitory concentrations of EGCG (150 µg mL^{-1}), daidzein (1 mg mL^{-1}), curcumin (400 µg mL^{-1}), berberine (400 µg mL^{-1}), or geraniol (600 µg mL^{-1}). The positive control was treated with the uncoupler of proton motive force carbonyl cyanide m-chlorophenylhydrazone (CCCP) (25 µg mL^{-1}), whereas the negative control was treated with *p*-anisaldehyde, and bacteria cultured in the unamended MH medium served as growth control. The assay was conducted in 96 well-microtiter plates, which were incubated at 37 °C for 24 hours before measuring OD_{600} to determine the nature of

interactions (OD_{600} < 0.05 was considered negative for bacterial growth). Each experiment was repeated three times, with three replicates per treatment.

3.3.7 Confirmation of synergistic interactions between EGCG and *p*-anisaldehyde

The synergistic interaction between EGCG and *p*-anisaldehyde was verified using a broth microdilution checkerboard technique. Stock concentrations of both compounds were diluted to MIC, ½ MIC, ¼ MIC, and $^1/_8$ MIC, which corresponds to 300, 150, 75 and 37.5 μg mL^{-1} for EGCG, and 2, 1, 0.5 and 0.25 mg mL^{-1} of *p*-anisaldehyde. Next, 25-μL aliquots of both compounds were combined in a checkerboard manner with 50 μL of bacterial suspension adjusted to 10^5 CFU mL^{-1}. Negative control included both compounds mixed with MH broth, while bacteria grown in the absence of EGCG and *p*-anisaldehyde served as a positive control. Microtiter plates were incubated at 37 °C for 24 h, and OD_{600} was measured to determine the fractional inhibitory concentration (FIC) [3], with FIC ≤ 0.5 and FIC ≥ 4 indicating, respectively, synergism and antagonism. Each treatment included three replicates, and the entire experiment was repeated three times.

3.3.8 Extraction and processing of RNA

Overnight broth culture of WT *P. aeruginosa* PAO1 was diluted to an OD_{600} 0.01, after which 100 μL aliquots of the bacterial suspension were dispensed into wells of a 96 well-microtiter plate and incubated statically at 37 °C. At an OD_{600} of 0.6, each microtiter plate well received 100 μL of MH broth amended with ½ MIC concentrations of *p*-anisaldehyde (1 mg mL^{-1}), EGCG (150 μg mL^{-1}), or a combination of both compounds. The experiment included three biological replicates of each treatment plus a control, which was cultured in unamended MH broth. After 1 h of exposure to antimicrobials at 37 °C, approximately 2.5×10^8 cells were fixed by mixing with two volumes of

RNAprotect Bacteria Reagent (Qiagen), and total RNA was extracted using RNeasy Mini Kit (Qiagen) according to the manufacturer's instructions. Total RNA was treated with RNase-free DNase I (Ambion, Austin, TX) and purified with RNA Clean and Concentrator-25 columns (Zymo Research, Irvine, CA). The concentration of RNA was measured using a NanoDrop OneC spectrophotometer (Thermo Scientific) and a QuantiFlour RNA System (Promega, Madison, WI), while its integrity was determined using an Agilent 2100 Bioanalyzer and an RNA 6000 Nano Kit (both from Agilent Technologies, Santa Clara, CA). Samples of total RNA (RIN > 9; $A_{260}/_{280}$ ratio ~2.0) were shipped to the Center for Genome and Research and Biocomputing (Oregon State University, Corvallis, OR), where they were treated with a Ribo-Zero rRNA Removal Kit (Bacteria) (Illumina, San Diego, CA), and the efficacy of ribodepletion was confirmed using a Bioanalyzer RNA 6000 Pico Kit (Agilent Technologies). The stranded RNA-Seq libraries were prepared, quantified by qPCR, and sequenced on a HiSeq 3000 instrument (Illumina) in 150 bp single-end mode.

3.3.9 Bioinformatic analysis of transcriptomic data

The analysis of RNA-seq data was performed using the KBase suite of expression analysis tools [7]. Briefly, the raw reads in fastq format were filtered and processed with Trimmomatic [9], and the quality of filtered data was assessed with FastQC (https://www.bioinformatics.babraham.ac.uk/projects/fastqc/). The processed reads were then aligned to the reference PAO1 genome (GenBank accession number NC_002516.2, downloaded from http://www.pseudomonas.com) with HISAT2-v2.10 [25], and full-length transcripts were assembled with StringTie v1.3.3b[39]. The differential expression analysis of the assembled transcripts was carried out with DESeq2 v1.20.0[32], and genes

demonstrating greater than a 1.5-fold (log2) difference in expression and an adjusted p value ≤ 0.05 between control and experimental treatments were used in downstream analysis. The functional annotation and gene enrichment analysis were performed with the Blast2GO suite.[20]

3.3.10 RT-qPCR analysis of genes encoding components of RND efflux pumps

The response of *P. aeruginosa* RND efflux pump genes to *p*-anisaldehyde, EGCG, and a combination of both compounds was validated by the quantitative reverse transcription PCR (RT-qPCR). Briefly, 1 μg of total RNA was converted to cDNA using the iScript Reverse Transcription Supermix (Bio-Rad, Hercules, CA, USA), and used in the RT-qPCR assay performed with the Luminaris Probe qPCR Master Mix (Thermo Scientific) and oligonucleotide primers and probes targeting *mexA*, *mexC*, *mexE*, *mexX*, *mexK*, *muxB*, and PA1541 (Table A.1). Samples of RNA untreated with reverse transcriptase served as a negative control to confirm the absence of contaminating genomic DNA. The analysis was performed with a CFX96 Real-Time PCR Detection System and CFX Maestro software (Bio-Rad). The expression of selected RND efflux genes was normalized to that of the housekeeping gene *rpoD*.

3.4 Results

3.4.1 Selection and characterization of mutants with hypersensitivity to *p*-anisaldehyde

The screening of the transposon mutant library yielded 39 clones that failed to grow in the presence of *p*-anisaldehyde. All hypersensitive mutants had F_1 values ≥ 9 and were at least 1.2 times more sensitive to *p*-anisaldehyde than the wild type PAO1 strain (Fig. 3.1A). Most of these mutants were sensitive to 1.5 mg mL^{-1} of *p*-anisaldehyde

(0.75× MIC of the wild type strain), while the growth of two mutants was completely inhibited at 1.2 mg mL^{-1}. The hypersensitive mutants were further tested for the sensitivity to the *p*-anisaldehyde-containing polymeric discs. Our results confirmed that most of them were significantly more sensitive to the polymeric discs ($P < 0.05$), with the most sensitive mutants manifesting a 2.6-fold increase in the zone of inhibition compared to the WT strain (Fig. 3.1B). The mapping of transposon insertion sites by inverse PCR and DNA sequencing revealed that the sensitivity to *p*-anisaldehyde was caused by mutations in 27 unique *P. aeruginosa* genes. The majority (40%) of the affected genes function in the energy metabolism and generation of ATP or participate in the uptake of molybdenum and synthesis of the molybdenum cofactor (Table 3.1). Other identified genes are involved in signal transduction, nucleotide metabolism, or membrane transport of small molecules. Interestingly, among mutants with increased sensitivity to *p*-anisaldehyde-containing polymeric discs were two isolates that carried mutations in *mexB*, which encodes the periplasmic linker component of the RND efflux pump MexAB-OprM (Table 3.1).

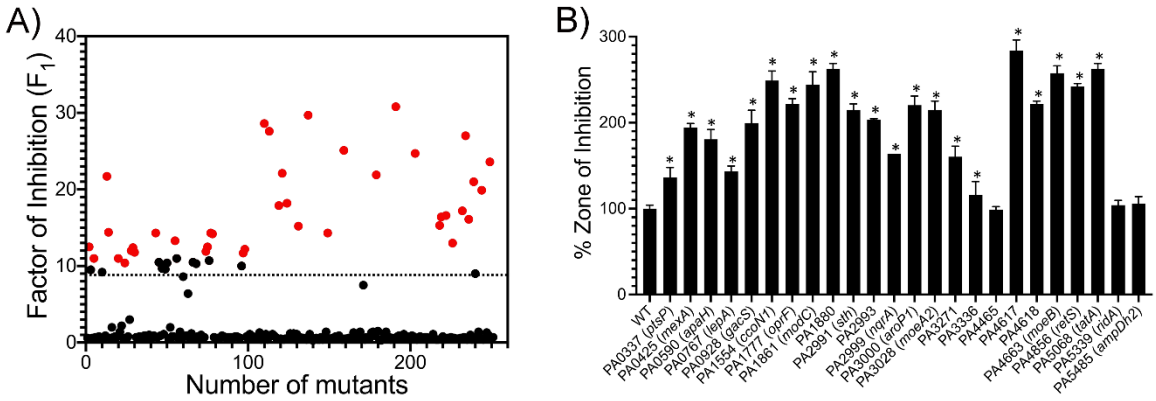

Figure 3.1. The sensitivity of transposon mutants to *p*-anisaldehyde.

(A) The distribution of F1 values of mutants after first round of screening. Red dots indicate mutants with F1 ≥ 9 that were selected for further analysis. (B) The inhibition of growth caused by *p*-anisaldehyde polymeric discs in selected transposon mutants (F1 ≥ 9) and the wild type PAO1 strain. Asterisks indicate mutants that were more sensitive to *p*-anisaldehyde than parental strain (one-tailed t-test at $P<0.05$).

Table 3.1 *Genes disrupted by EZ-Tn5<TET-1> in transposon mutants with increased sensitivity to p-anisaldehyde.*

Functional category	**PA number**	**Gene name**	**Predicted function**	**Number of mutants**
Membrane transport	PA1777	*oprF*	Outer membrane porin F	1
	PA3000	*aroP1*	Aromatic amino acid permease	1
	PA3336		Major facilitator superfamily (MFS) transporter	1
	PA5068	*tatA*	Sec-independent protein translocase	2
Signal transduction	PA0928	*gacS*	Two-component sensor kinase	1
	PA3271		Two-component sensor kinase	1
	PA4856	*retS*	Hybrid sensor histidine kinase/response regulator	1
Energy metabolism	PA1554	*ccoN1*	Cbb3-type cytochrome c oxidase subunit I	1
	PA4465		Nucleotide-binding protein	1
	PA0337	*ptsP*	Phosphoenolpyruvate-protein phosphotransferase	2
	PA1880		Probable oxidoreductase	2
	PA2993		FAD:protein FMN transferase	1
	PA2994	*nqrF*	Na(+)-translocating NADH-quinone reductase subunit F	3
	PA2995	*nqrE*	Na(+)-translocating NADH-quinone reductase subunit E	1

Table 3.1 (Continued)

Functional category	PA number	*Gene name*	Predicted function	Number of mutants
	PA2999	*nqrA*	Na(+)-translocating NADH-quinone reductase subunit A	3
Transport of molybdenum and synthesis of Mo co-factor	PA1861	*modC*	Molybdenum import ATP-binding protein	3
	PA1862	*modB*	Molybdenum transport system permease	1
	PA3028	*moeA2*	Molybdopterin molybdenumtransferase	2
	PA3029	*moaB2*	Molybdenum cofactor biosynthesis protein B	1
	PA4663	*moeB*	Molybdopterin biosynthesis MoeB protein	1
Response to antibiotics	PA0425	*mexA*	MexAB-OprM efflux system, periplasmic linker component	2
	PA5485	*ampDh2*	N-acetylmuramoyl-L-alanine amidase	1
Nucleotide metabolism and modification	PA0590	*apaH*	Bis(5'-nucleosyl)-tetraphosphatase	1
	PA2991	*sth*	Soluble pyridine nucleotide transhydrogenase	1
	PA5339	*ridA*	2-aminoacrylate deaminase	1
	PA4617		rRNA large subunit methyltransferase G	1
Unknown	PA4618		Hypothetical protein	2

3.4.2 Epigallocatechin gallate potentiates the activity of *p*-anisaldehyde in *P. aeruginosa*

Since the transposon screen suggested the possible importance of RND efflux pumps for the resistance to phytoaldehydes, we tested a panel of known plant-derived EPIs for the ability to sensitize *P. aeruginosa* to *p*-anisaldehyde. The testing involved measuring the MIC of *p*-anisaldehyde in the presence of non-inhibitory concentrations of selected EPIs. Results of that screen revealed that the addition of daidzein had no effect, while berberine, curcumin, and geraniol exhibited partial synergism and moderately decreased the MIC of *p*-anisaldehyde in the wild-type PAO1 (Table 3.2). In contrast, the green tea polyphenol epigallocatechin gallate (EGCG) significantly reduced the MIC of *p*-anisaldehyde and exhibited a strong synergistic effect similar to that of the proton motive force uncoupler CCCP. Broth microdilution checkerboard assay between EGCG and *p*-anisaldehyde confirmed that both compounds interact synergistically with the ∑FIC value of 0.5 (data not shown).

Table 3.2 *The effect of plant-derived EPIs on the MIC of p-anisaldehyde in P. aeruginosa PAO1.*

EPI	Concentration ($\mu g\ mL^{-1}$)	MIC of *p*-anisaldehyde ($mg\ mL^{-1}$)	Type of interaction
None	N/A	2.0	N/A
CCCP	25	0.6	Synergism
EGCG	150	0.8	Synergism
Daidzein	400	2	Indifference
Berberine	400	1.5	Synergism
Curcumin	400	1.5	Synergism
Geraniol	400	1.5	Synergism

3.4.3 The effect of *p*-anisaldehyde on the transcriptome of *P. aeruginosa* PAO1

In order to gain further insight into the antimicrobial activity of *p*-anisaldehyde, we profiled and compared transcriptomes of *P. aeruginosa* treated with *p*-anisaldehyde, EGCG, and a combination of both compounds. The RNA-seq generated a total of 554 million filtered reads, which were mapped to the reference PAO1 genome. Statistical analysis using the cut off criteria of $|\log_2 FC| \geq 1.5$ and FDR ≤ 0.05 revealed that the highest number of differentially expressed genes (DEGs) was associated with exposure to *p*-anisaldehyde, which affected the expression of 264 genes, or 5% of the entire genome (Fig. 3.2A). The treatment with EGCG and a combination of both compounds altered, respectively, the expression of 28 and 86 genes. We also performed the pairwise comparison between the *p*-anisaldehyde and combination treatments to understand molecular mechanisms responsible for the synergistic effect of epigallocatechin gallate.

P. aeruginosa responded to *p*-anisaldehyde by upregulating the expression of 128 genes, many of which function in energy metabolism, membrane transport, signal transduction, and stress response. The overall highest levels of induction were observed in genes encoding components of RND multidrug efflux pumps, the two-component response regulator PhoP (PA1179), and several conserved hypothetical proteins. The 137 downregulated genes included those encoding various transporters, and components of energy metabolism pathways, type III secretion apparatus, and respiratory nitrate reductase. Interestingly, a significant proportion (32%) of DEGs that responded to *p*-anisaldehyde genes encoded conserved hypothetical proteins of unknown function. We also matched the genes that were differentially expressed in response to *p*-anisaldehyde to genetic loci identified during the transposon screen. Results of this comparison revealed

that the two datasets shared three genes, which encoded a cytochrome oxidase (PA1554), a predicted oxidoreductase (PA1880), and a two-component sensor (PA3271) (Fig. 3.2B).

The Blast2GO analysis of *p*-anisaldehyde DEGs identified the intrinsic component of the membrane, plasma membrane, and cell periphery as dominant GO terms in the cellular component category. The most common GO terms in molecular function and biological processes categories were, respectively, the binding of an organic cyclic compound, and cellular metabolic processes (Fig. 3.3A). A similar pattern of GO terms was observed in the Blast2GO profiling of genes interrupted by insertions of the EZ-Tn*5* <TET-1> transposon in *p*-anisaldehyde-sensitive mutants. Finally, the gene enrichment analysis of upregulated DEGs revealed the overrepresentation (Fisher's exact test; FDR $\leq$ 0.05) of genes involved in the biosynthesis of lipids and response to chemicals and antibiotics. In contrast, the downregulated DEGs were enriched in genes associated with ion transmembrane transport and translation (Fig. 3.3B).

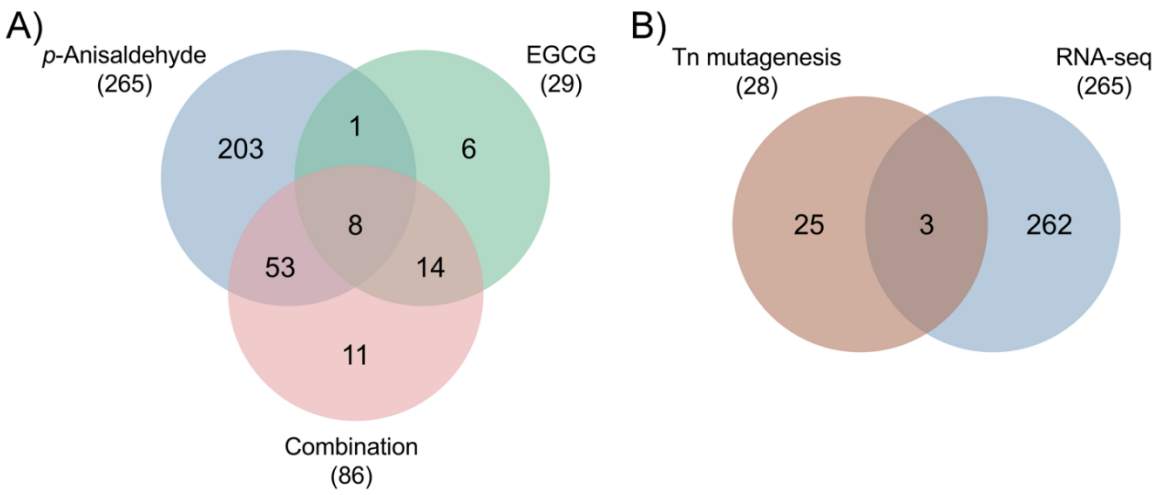

Figure 3.2 Venn diagram comparing the number of differentially expressed genes between *P. aeruginosa* exposed to *p*-anisaldehyde, EGCG, and the combination of thereof.

(A) The comparison of genes implicated in the response to *p*-anisaldehyde in transposon mutants and cultures profiled by RNA-seq (B).

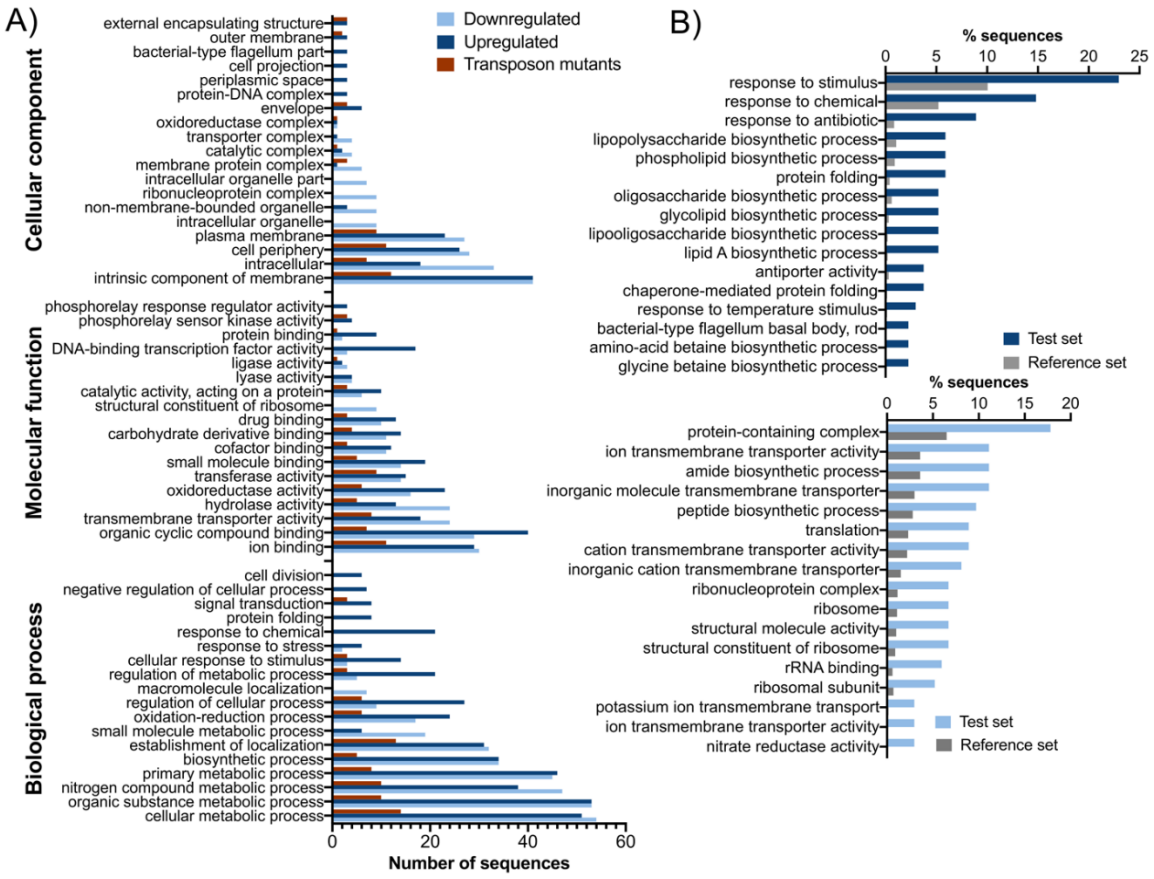

Figure 3.3. GO classification of DEGs in response to *p*-anisaldehyde.

(A) Functional annotation analysis of DEGs and transposon mutagenesis genes. (B) Gene enrichment analysis of DEGs using the Fishers exact test (FDR ≤ 0.05).

3.4.4 EGCG modulates transcriptional changes caused by *p*-anisaldehyde in *P. aeruginosa*

In contrast to *p*-anisaldehyde, the exposure of PAO1 to subinhibitory levels of epigallocatechin gallate altered the expression of only 28 genes, one-third of which were classified as conserved hypothetical. Among the upregulated DEGs with predicted functions were those encoding the RND efflux pump MuxABC-OpmB, transcriptional regulators (PA2525-PA2528 and PA2825), and components of the cell envelope and oxidative stress defense systems (PA0848, PA0849, PA4612, and PA4613). The six

downregulated DEGs encoded a DNA mismatch repair protein (PA4946), an MFS transporter (PA2314), 1-phosphofructokinase (PA3561), and a FAD-binding subunit of glycolate oxidase (PA5354). The common GO terms in the cellular component category were linked with cell envelope, while the molecular function was associated with binding of heterocyclic compounds, oxidoreductase activity, transporter and peroxidase activity (Fig. 3.4A). The dominant biological processes involved the response to chemical, regulation of cellular processes, and cellular detoxification. Gene enrichment analysis showed that most EGCG DEGs were involved in response to toxic substances and oxidative stress, while downregulated genes were associated with lipid biosynthesis and carbohydrate metabolism (Fig. 3.4B).

Interestingly, the treatment of *P. aeruginosa* with a combination of *p*-anisaldehyde and EGCG altered the expression of 86 genes. The majority of these genes (76 in total) were also present in *p*-anisaldehyde or EGCG datasets, and only 11 were uniquely associated with the mixed treatment (Fig. 3.2A). Three of these unique DEGs were downregulated and encoded a hypothetical protein (PA5406), a ribosomal protein (PA4433), and the cell division protein FtsE (PA0374). The unique upregulated genes encoded a hydrocarbon reductase (PA5236), an MFS transporter (PA5030), and a fosfomycin resistance protein (PA1129). The gene enrichment analysis of the combination treatment revealed an overrepresentation of DEGs involved in the transmembrane transport, response to antibiotics and efflux, iron binding, and peptide biosynthesis (Figure 3.5).

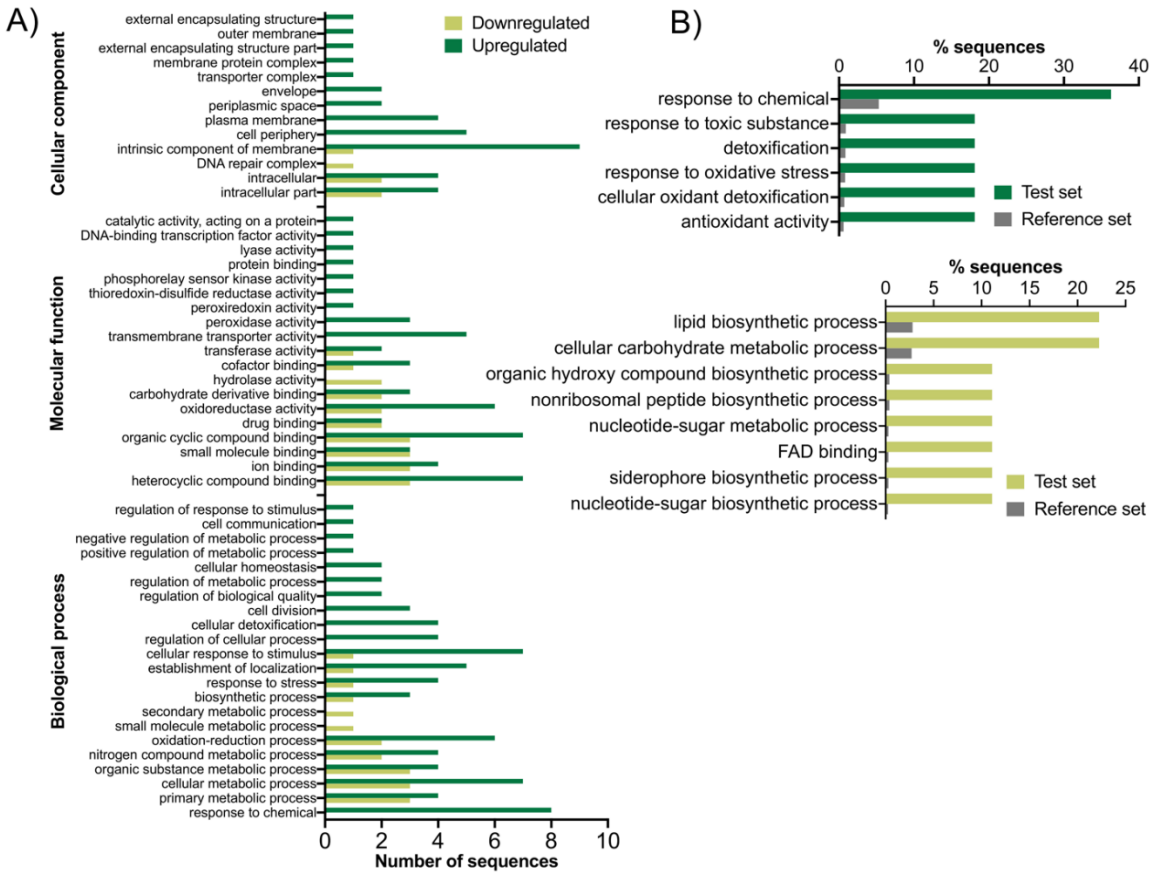

Figure 3.4. Gene ontology (GO) classification of *P. aeruginosa* genes that were differentially expressed in response to epigallocatechin gallate (A), and gene enrichment analysis of EGCG DEGs using Fishers exact test (FDR ≤ 0.05) (B).

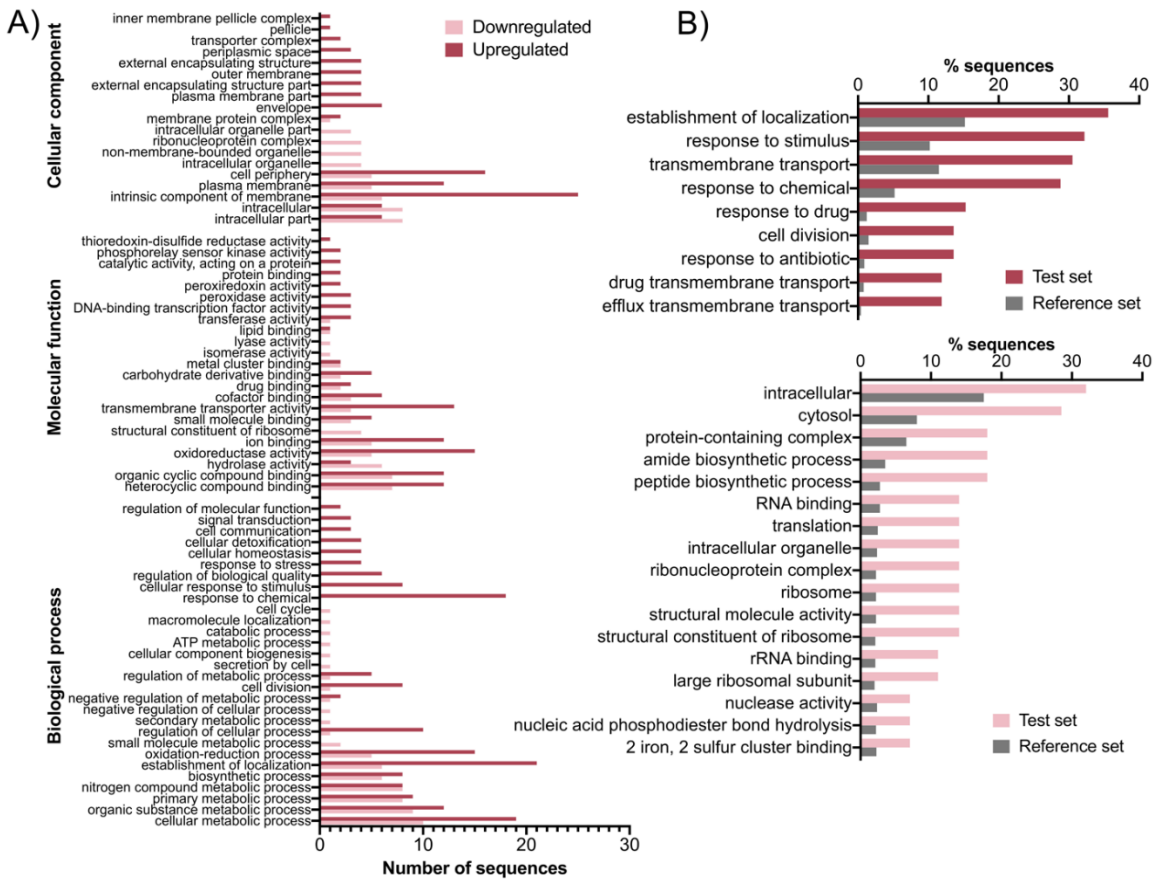

Figure 3.5 Gene ontology (GO) classification of *P. aeruginosa* genes that were differentially expressed in response to a combination of *p*-anisaldehyde and epigallocatechin gallate (A), and gene enrichment analysis of DEGs using Fishers exact test (FDR ≤ 0.05) (B).

3.4.5 The interaction between *p*-anisaldehyde and EGCG affects multiple categories of cellular pathways in *P. aeruginosa*

Our transcriptomic analysis revealed that *p*-anisaldehyde strongly induced genes encoding the RND efflux pumps MexCD-OprJ, MexEF-OprN, and MexKJ, as well as the putative transporter of the small multidrug resistance (SMR) family PA1541. Additionally, genes that encode regulators of the *mexAB-oprM* operon (i.e., the repressor gene *mexR* (PA3720), the antirepressor gene *armR* (PA3719), and *nalC* (PA3721)) were

differentially expressed in *p*-anisaldehyde-treated cells. In contrast, the treatment with EGCG induced only one RND pump, MuxABC, suggesting that this transporter plays a specific role in the efflux of epigallocatechin gallate. We further validated the RNA-seq data by RT-qPCR with oligonucleotide primers and probes targeting components of seven clinically relevant *P. aeruginosa* efflux pumps. The results of this experiment revealed a strong induction of *mexC*, *mexE*, and *mexK* in response to *p*-anisaldehyde, which was in agreement with the results of RNA-seq (Fig. 3.6). Interestingly, although, *mexC*, *mexE*, and *mexK* were also upregulated in the combination treatment, the addition of EGCG resulted in significantly lower levels of expression compared to the *p*-anisaldehyde-only treatment. Contrary to results of the transposon mutagenesis, we failed to detect any measurable induction of genes encoding components of the MexAB-OprM efflux pump. We attribute this discrepancy to differences in the length of the exposure to *p*-anisaldehyde between the transposon screen and gene expression experiments.

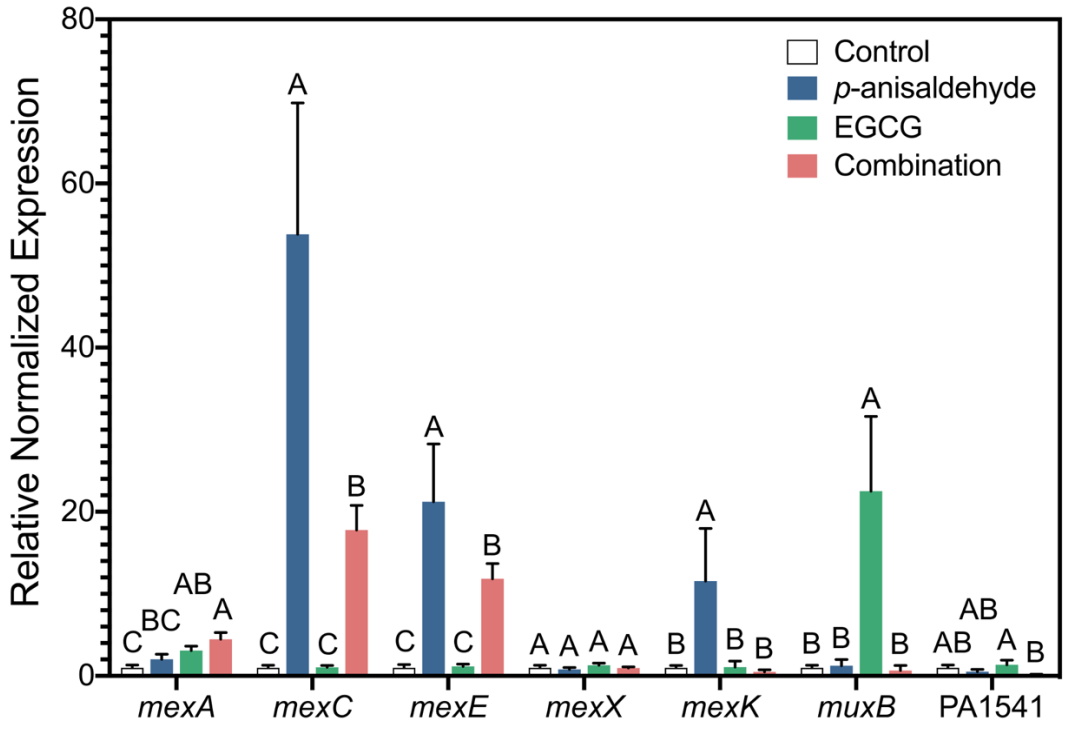

Figure 3.6. Relative expression of RND-type efflux pump genes in response to *p*-anisaldehyde, EGCG, and a combination of both compounds.

Bars with different letters indicate significant differences in gene expression as determined by Tukey-Kramer HSD test ($P < 0.05$).

In addition to RND pumps, we observed that the presence of *p*-anisaldehyde modulated the expression of almost 30 other membrane transporter genes. The enrichment analysis of these DEGs revealed an overrepresentation of pathways associated with the transmembrane transport of ions and inorganic molecules (Fig. 3.3B). Like in the case of RND pumps, some of these genes were also differentially expressed between the *p*-anisaldehyde and *p*-anisaldehyde/EGCG treatments. The comparison of gene expression profiles also revealed five ABC transporter genes (*agtA*, *agtB*, *ihpM*, *gltG*, and *yrbE*) that were downregulated by *p*-anisaldehyde, but that effect was significantly reversed in cultures treated with a combination of *p*-anisaldehyde and EGCG (Fig. 7). The effect was especially pronounced in the case of *yrbE* (PA4455),

which encodes an ABC transporter involved in resistance to acidified nitrite, EDTA, and several antibiotics [33]. A similar response to *p*-anisaldehyde and EGCG was observed in genes encoding components of the potassium translocating ATPase KdpFABC. Conversely, the addition of EGCG significantly induced the cation diffusion facilitator (CDF) transporter gene *yiiP*, whose expression was unaffected by *p*-anisaldehyde.

Our analysis also revealed that *p*-anisaldehyde and EGCG differentially modulate the activity of several genes involved in the modification of the *P. aeruginosa* cell envelope. The exposure to *p*-anisaldehyde induced genes of the *arnBCADTEF* cluster, which functions to modify the lipid A component of the lipopolysaccharide thereby leading to increased resistance to cationic antimicrobial peptides [26]. This induction was not observed in the EGCG-treated cells, and the treatment with both compounds significantly reduced the expression of *arnBCF* (Fig. 3.7). Similar alterations were observed in the expression level of the *oprH-phoPQ* operon, which encodes an outer membrane protein H and a two-component signal transduction system that regulates the activity of the *arnBCADTEF* operon [19]. Interestingly, *oprH*, which was induced by *p*-anisaldehyde but expressed weaker in the presence of EGCG, represents part of the Mg^{2+} stimulon and contributes to the resistance to polymyxin B and aminoglycosides [18].

p-anisaldehyde and EGCG differentially affected expression of multiple cellular pathways associated with the stress response. The comparative analysis revealed that genes encoding several oxidative stress response enzymes, molecular chaperones, and a component of the DNA mismatch repair system were differentially expressed between the *p*-anisaldehyde, EGCG, and combination treatments. The EGCG and combination treatments upregulated genes encoding the KatB catalase (PA4613) [11] and its accessory

ankyrin-like protein AnkB (PA4612) [22], the alkyl hydroperoxide-reducing protein AhpB (PA0848), the thioredoxin reductase TrxB2 (PA0849) [45], and two proteins, PA3237 and PA3287, that are upregulated in response to H_2O_2 [1,37] (Fig. 3.7). In contrast, *p*-anisaldehyde upregulated the expression of molecular chaperones GroES and GroEL, but this effect was reversed by the presence of EGCG. In *mutL*, which functions to stabilize components of the mismatch repair machinery, the combination treatment completely negated the effect of individual *p*-anisaldehyde and EGCG treatments, which both strongly downregulated this gene.

Finally, our results revealed that the treatment with *p*-anisaldehyde and EGCG modulated the expression of the *narK1K2GHJI* operon (PA3872-PA3877), which encodes the respiratory nitrate reductase and nitrate transporter (Fig. 3.7). Whereas *p*-anisaldehyde significantly repressed genes of the nitrate reductase pathway, the combination treatment significantly reduced this effect, while EGCG alone has little effect on the expression of this pathway.

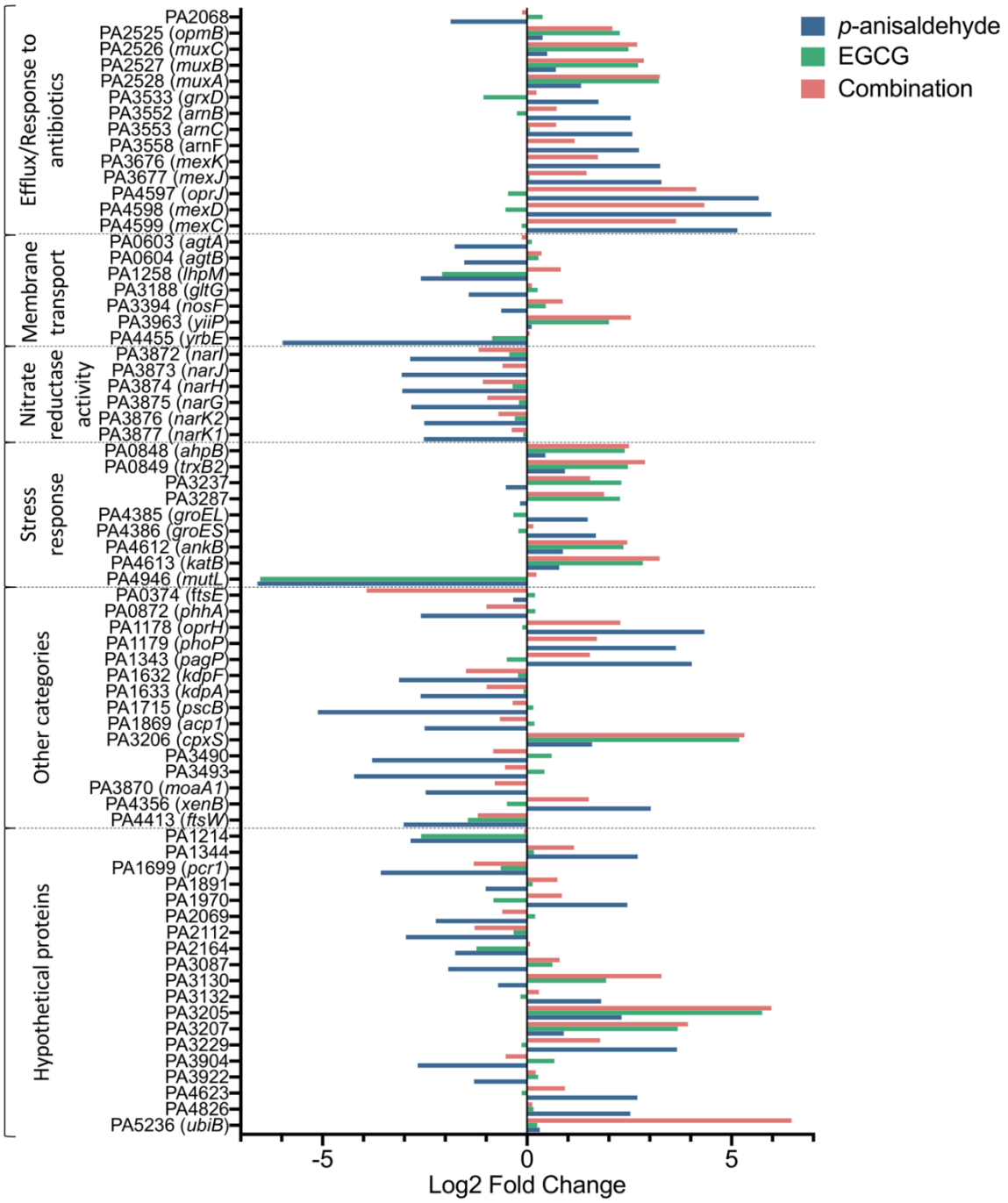

Figure 3.7. Changes in the *P. aeruginosa* transcriptome in response to *p*-anisaldehyde, EGCG, and the combination of both compounds.

3.5 Discussion

In this study, we used a combination of transposon mutagenesis and RNA-seq to characterize cellular pathways targeted by *p*-anisaldehyde and epigallocatechin gallate in the multidrug-resistant human pathogen *P. aeruginosa*. *p*-anisaldehyde is a constituent of essential oils and a member of the phenylpropanoid family of metabolites, which are synthesized by plants as derivatives of the amino acid phenylalanine [54]. Therefore, our findings provide insight into the biological activity of a larger group of structurally related compounds with antimicrobial, antifungal, and antibiofilm properties [24,44]. Although the antimicrobial activity of EOs is traditionally attributed to their ability to affect the integrity of cellular membranes [36], our results revealed that *p*-anisaldehyde interferes with a much broader range of cellular pathways. We observed that the exposure to *p*-anisaldehyde resulted in the downregulation of genes encoding cytochrome oxidases (*cyoA*, *ccoN1*), a phosphofructokinase (*fruK*), a pyruvate carboxylase (*pycA*), and the NADH:ubiquinone oxidoreductase NqrAEF. In the course of our transposon screen, we recovered several mutants with defects in genes involved in the transport of molybdenum and biosynthesis of the molybdenum cofactor. Molybdenum cofactor is an essential component of several important molybdoenzymes, including respiratory nitrate reductases [29]. Our transcriptomic data revealed that exposure to *p*-anisaldehyde significantly downregulated the *narK1K2GHJI* operon that in *P. aeruginosa* encodes components of the inner membrane-bound nitrate reductase complex. This dissimilatory nitrate reductase catalyzes the respiratory reduction of nitrate to nitrite and helps generate ATP in the absence of oxygen [52]. Interestingly, nitrate reduction decreases the *trans* fatty acid content and inhibits the formation of biofilms in *P. aeruginosa* [38]. The biofilm

lifestyle and alterations in the fatty acid profile are associated with the response to environmental stress and toxic substances [21]. Hence, it is plausible that the repression of nitrate reductase represents a defense response to *p*-anisaldehyde by favoring the formation of resistant biofilms and densely packed membranes with higher *trans* fatty acid content.

Other notable categories of defense response to *p*-anisaldehyde in *P. aeruginosa* included the upregulation of molecular chaperones and efflux transport. The treatment with *p*-anisaldehyde upregulated genes encoding chaperons DnaK, DnaJ, and GroES, which function to refold and destroy damaged proteins and are induced by heat shock, oxidative stress, disinfectants, heavy metals, and antibiotics [14,28,57]. We further observed an upregulation of *betAB* genes (PA5372, PA5373) that encode enzymes involved in the conversion of choline to glycine betaine, a key microbial compatible solute. The intracellular accumulation of glycine betaine and related compounds confers tolerance to osmotic, thermal, oxidative, and denaturant forms of stress [12,42,55]. Our transposon screen and RNA-seq also revealed that *p*-anisaldehyde upregulates multiple transporters and including efflux pumps of the RND superfamily. We also observed the induction of genes encoding the MexCD-OprJ, MexEF-OprN, and MexKJ efflux pumps, and recovered a transposon mutant with a defect in MexAB-OprM. These pumps expel antibiotics, metabolic inhibitors, detergents, biocides, quorum sensing signals, and some virulence factors [27,46]. A recent study by Tetard et al. [51] reported the upregulation of the same group of RND pumps in *P. aeruginosa* PA14 treated with cinnamaldehyde. Taken collectively with our results, this observation strongly suggests that active efflux represents a key mechanism of resistance to antimicrobials of the phenylpropanoid group. In addition to

efflux pumps, *P. aeruginosa* harbors an extensive array of intrinsic (chromosomally-encoded) and imported (encoded by mobile elements) serine-based and metallo-β-lactamases and aminoglycosides inactivating enzymes, which contribute to the emergence of MDR (multidrug-resistant), XDR (extensively drug-resistant), and even PDR (pandrug-resistant) strains [8]. Our experiments with *p*-anisaldehyde revealed no changes in the expression of genes involved in the enzymatic inactivation of antibiotics, thus supporting the notion that essential oils may be useful in curbing the spread of antibiotic resistance.

Individual EO constituents are often less potent than antibiotics, which presents practical problems for their use as antimicrobials or food preservatives. A possible way to overcome this obstacle involves the exploitation of synergistic effects between different EO constituents. Although a number of synergistic combinations of compounds were identified by trial and error [23], the molecular mechanisms behind such interactions remain poorly understood. The results of this study may help to address this gap in knowledge by probing synergistic interactions between *p*-anisaldehyde and EGCG. The RNA-seq profiling revealed that the two compounds target very different sets of cellular pathways in *P. aeruginosa*. Interestingly, we included EGCG in our experiments as a potential efflux pump inhibitor [49,50], and then observed the induction of the RND efflux pump MuxABC-OpmB. Although the expression of other efflux pump genes was not affected (or even somewhat repressed in cultures treated with a combination of *p*-anisaldehyde and EGCG), we feel that the EPI properties of epigallocatechin gallate should be investigated further. The analysis of genes differentially expressed in the presence of EGCG also revealed components of several pathways (*katB, ahpB, trxB2,* PA2826,

PA3237, PA3287) that are associated in *P. aeruginosa* with the response to oxidative stress and exposure to H_2O_2 [1]. These findings provide an insight into the antimicrobial mode of action of epigallocatechin gallate and agree with reports of the intercellular release of H_2O_2 in *E. coli* O157:H7 treated with subinhibitory levels of EGCG [16], and results of Liu et al. [31], who profiled the transcriptomic response of *P. fluorescens* to EGCG. Surprisingly, apart from the oxidative stress genes, our RNA-seq data did not significantly overlap with the *P. fluorescens* dataset, which had over 400 genes whose expression was altered in response to EGCG. We attribute these discrepancies to differences in the biology of the two Pseudomonas species, higher concentrations of EGCG used by Liu et al. [31], and more stringent fold change cutoff used in our study ($|\log_2 FC| \geq 1.5$ vs. $|\log_2 FC| \geq 1$) to identify the differentially expressed *P. aeruginosa* genes.

Collectively, our results suggest that *p*-anisaldehyde affects *P. aeruginosa* by first interfering with the integrity of its cell envelope, which then allows it to accumulate intracellularly and adversely affect proteins, by causing their misfolding and aggregation. In contrast, epigallocatechin gallate poisons bacteria by inducing oxidative stress, which may explain its ability to complement and potentiate the antimicrobial action of *p*-anisaldehyde. The synergistic antimicrobial effect is further enhanced by the capacity of EGCG to partially or completely reverse the upregulation of many genes by *p*-anisaldehyde, including those encoding various transporters and key RND efflux pumps. Interestingly, the treatment with a combination of *p*-anisaldehyde and EGCG also significantly repressed a gene (PA0374) encoding FtsE, which is membrane protein located in the septal ring. This may represent yet another facet of the synergism because studies in *E. coli* and several other species demonstrated that *ftsE* mutants grow poorly

and exhibit division defects [6]. In gram-negative bacteria, the failure to complete cell division is associated with increased sensitivity to antibiotics, detergents, and defensins [56].

In conclusion, this study provides an insight into the antimicrobial activity of *p*-anisaldehyde and its synergistic interactions with epigallocatechin gallate. Our results may aid in the rational identification of new synergistically acting combinations of plant metabolites and their exploitation for the control of pathogenic microorganisms. Our study also confirms the utility of the thiol-ene polymer platform for the sustained and effective delivery of hydrophobic and volatile antimicrobial compounds.

3.6 References

1. Aharoni, N., H. Mamane, D. Biran, A. Lakretz, and E. Z. Ron. 2018. Gene expression in *Pseudomonas aeruginosa* exposed to hydroxyl-radicals. Chemosphere 199:243-250.
2. Alcalde-Rico, M., S. Hernando-Amado, P. Blanco, and J. L. Martínez. 2016. Multidrug efflux pumps at the crossroad between antibiotic resistance and bacterial virulence. Front. Microbiol. 7:1483.
3. Amato, D. N., D. V. Amato, Y. Adewunmi, O. V. Mavrodi, K. H. Parsons, S. N. Swilley, D. A. Braasch, W. D. Walker, D. V. Mavrodi, and D. L. Patton. 2018. Using aldehyde synergism to direct the design of degradable pro-antimicrobial networks. ACS Appl. Bio Mater. 1:1983-1991.
4. Amato, D. N., D. V. Amato, O. V. Mavrodi, D. A. Braasch, S. E. Walley, J. R. Douglas, D. V. Mavrodi, and D. L. Patton. 2016. Destruction of opportunistic

pathogens via polymer nanoparticle-mediated release of plant-based antimicrobial payloads. Adv. Healthc. Mater. 5:1094-1103.

5. Amato, D. N., D. V. Amato, O. V. Mavrodi, W. B. Martin, S. N. Swilley, K. H. Parsons, D. V. Mavrodi, and D. L. Patton. 2017. Pro-Antimicrobial Networks via Degradable Acetals (PANDAs) using thiol-ene photopolymerization. ACS Macro Lett. 6:171-175.
6. Arends, S. J., R. J. Kustusch, and D. S. Weiss. 2009. ATP-binding site lesions in FtsE impair cell division. J. Bacteriol. 191:3772-3784.
7. Arkin, A. P., R. W. Cottingham, C. S. Henry, N. L. Harris, R. L. Stevens, S. Maslov, P. Dehal, D. Ware, F. Perez, S. Canon, M. W. Sneddon, M. L. Henderson, W. J. Riehl, D. Murphy-Olson, S. Y. Chan, R. T. Kamimura, S. Kumari, M. M. Drake, T. S. Brettin, E. M. Glass, D. Chivian, D. Gunter, D. J. Weston, B. H. Allen, J. Baumohl, A. A. Best, B. Bowen, S. E. Brenner, C. C. Bun, J. M. Chandonia, J. M. Chia, R. Colasanti, N. Conrad, J. J. Davis, B. H. Davison, M. DeJongh, S. Devoid, E. Dietrich, I. Dubchak, J. N. Edirisinghe, G. Fang, J. P. Faria, P. M. Frybarger, W. Gerlach, M. Gerstein, A. Greiner, J. Gurtowski, H. L. Haun, F. He, R. Jain, M. P. Joachimiak, K. P. Keegan, S. Kondo, V. Kumar, M. L. Land, F. Meyer, M. Mills, P. S. Novichkov, T. Oh, G. J. Olsen, R. Olson, B. Parrello, S. Pasternak, E. Pearson, S. S. Poon, G. A. Price, S. Ramakrishnan, P. Ranjan, P. C. Ronald, M. C. Schatz, S. M. D. Seaver, M. Shukla, R. A. Sutormin, M. H. Syed, J. Thomason, N. L. Tintle, D. Wang, F. Xia, H. Yoo, S. Yoo, and D. Yu. 2018. KBase: The united states department of energy systems biology knowledgebase. Nat. Biotech. 36**:**566-569.

8. Bassetti, M., A. Vena, A. Croxatto, E. Righi, and B. Guery. 2018. How to manage *Pseudomonas aeruginosa* infections. Drugs Context 7:212527.
9. Bolger, A. M., M. Lohse, and B. Usadel. 2014. Trimmomatic: a flexible trimmer for Illumina sequence data. Bioinformatics 30:2114-2120.
10. Boucher, H. W., G. H. Talbot, J. S. Bradley, J. E. Edwards, D. Gilbert, L. B. Rice, M. Scheld, B. Spellberg, and J. Bartlett. 2009. Bad bugs, no drugs: no ESKAPE! An update from the Infectious Diseases Society of America. Clin. Infect. Dis. 48:1-12.
11. Brown, S. M., M. L. Howell, M. L. Vasil, A. J. Anderson, and D. J. Hassett. 1995. Cloning and characterization of the *katB* gene of *Pseudomonas aeruginosa* encoding a hydrogen peroxide-inducible catalase: purification of KatB, cellular localization, and demonstration that it is essential for optimal resistance to hydrogen peroxide. J. Bacteriol. 177:6536-6544.
12. Caldas, T., N. Demont-Caulet, A. Ghazi, and G. Richarme. 1999. Thermoprotection by glycine betaine and choline. Microbiology 145:2543-2548.
13. Campen, R. L., D. F. Ackerley, G. M. Cook, and R. F. O'Toole. 2015. Development of a *Mycobacterium smegmatis* transposon mutant array for characterising the mechanism of action of tuberculosis drugs: Findings with isoniazid and its structural analogues. Tuberculosis 95:432-439.
14. Cardoso, K., R. F. Gandra, E. S. Wisniewski, C. A. Osaku, M. K. Kadowaki, V. Felipach-Neto, L. F. Haus, R. De Cá, and C. Simão Rde. 2010. DnaK and GroEL are induced in response to antibiotic and heat shock in *Acinetobacter baumannii*. J. Med. Microbiol. 59:1061-1068.

15. Cheesman, M. J., A. Ilanko, B. Blonk, and I. E. Cock. 2017. Developing new antimicrobial therapies: are synergistic combinations of plant extracts/compounds with conventional antibiotics the solution? Pharmacognosy Rev. 11:57-72.
16. Cui, Y., Y. J. Oh, J. Lim, M. Youn, I. Lee, H. K. Pak, W. Park, W. Jo, and S. Park. 2012. AFM study of the differential inhibitory effects of the green tea polyphenol (-)-epigallocatechin-3-gallate (EGCG) against gram-positive and gram-negative bacteria. Food Microbiol. 29:80-87.
17. Delmar, J. A., C. C. Su, and E. W. Yu. 2014. Bacterial multidrug efflux transporters. Annu. Rev. Biophys. 43:93-117.
18. Edrington, T. C., E. Kintz, J. B. Goldberg, and L. K. Tamm. 2011. Structural basis for the interaction of lipopolysaccharide with outer membrane protein H (OprH) from *Pseudomonas aeruginosa*. J. Biol. Chem. 286:39211-39223.
19. Francis, V. I., E. C. Stevenson, and S. L. Porter. 2017. Two-component systems required for virulence in *Pseudomonas aeruginosa*. FEMS Microbiol. Lett. 364. doi: 10.1093/femsle/fnx104.
20. Gotz, S., J. M. Garcia-Gomez, J. Terol, T. D. Williams, S. H. Nagaraj, M. J. Nueda, M. Robles, M. Talon, J. Dopazo, and A. Conesa. 2008. High-throughput functional annotation and data mining with the Blast2GO suite. Nucleic Acids Res. 36:3420-3435.
21. Heipieper, H. J., F. Meinhardt, and A. Segura. 2003. The *cis-trans* isomerase of unsaturated fatty acids in *Pseudomonas* and *Vibrio*: biochemistry, molecular biology and physiological function of a unique stress adaptive mechanism. FEMS Microbiol. Lett. 229:1-7.

22. Howell, M. L., E. Alsabbagh, J. F. Ma, U. A. Ochsner, M. G. Klotz, T. J. Beveridge, K. M. Blumenthal, E. C. Niederhoffer, R. E. Morris, D. Needham, G. E. Dean, M. A. Wani, and D. J. Hassett. 2000. AnkB, a periplasmic ankyrin-like protein in *Pseudomonas aeruginosa*, is required for optimal catalase B (KatB) activity and resistance to hydrogen peroxide. J.. Bacteriol. 182:4545-4556.
23. Hyldgaard, M., T. Mygind, and R. L. Meyer. 2012. Essential oils in food preservation: mode of action, synergies, and interactions with food matrix components. Front. Microbiol. 3:12.
24. Ilijeva, R., and G. Buchbauer. 2016. Biological properties of some volatile phenylpropanoids. Nat. Prod. Commun. 11:1619-1629.
25. Kim, D., B. Langmead, and S. L. Salzberg. 2015. HISAT: a fast spliced aligner with low memory requirements. Nat. Methods 12:357-360.
26. King, J. D., D. Kocíncová, E. L. Westman, and J. S. Lam. 2009. Lipopolysaccharide biosynthesis in *Pseudomonas aeruginosa*. Innate Immun. 15:261-312.
27. Kvist, M., V. Hancock, and P. Klemm. 2008. Inactivation of efflux pumps abolishes bacterial biofilm formation. Appl. Environ. Microbiol. 74:7376-7382.
28. Laport, M. S., L. L. Dos Santos, J. A. Lemos, M. do Carmo F. Bastos, R. A. Burne, and M. Giambiagi-deMarval. 2006. Organization of heat shock *dnaK* and *groE* operons of the nosocomial pathogen *Enterococcus faecium*. Res. Microbiol. 157:162-168.
29. Leimkühler, S., L. Leimkühler, and C. Iobbi-Nivol. 2016. Bacterial molybdoenzymes: old enzymes for new purposes. FEMS Microbiol. Rev. 43:1-18.

30. Lister, P. D., D. J. Wolter, and N. D. Hanson. 2009. Antibacterial-resistant *Pseudomonas aeruginosa*: clinical impact and complex regulation of chromosomally encoded resistance mechanisms. Clin. Microbiol. Rev. 22:582-610.

31. Liu, X., B. Shen, P. Du, N. Wang, J. Wang, J. Li, and A. Sun. 2017. Transcriptomic analysis of the response of *Pseudomonas fluorescens* to epigallocatechin gallate by RNA-seq. PloS One 12:e0177938.

32. Love, M. I., W. Huber, and S. Anders. 2014. Moderated estimation of fold change and dispersion for RNA-seq data with DESeq2. Genome Biol. 15:550.

33. McDaniel, C., S. Su, W. Panmanee, G. W. Lau, T. Browne, K. Cox, A. T. Paul, S. H. Ko, J. E. Mortensen, J. S. Lam, D. A. Muruve, and D. J. Hassett. 2016. A putative ABC transporter permease is necessary for resistance to acidified nitrite and EDTA in *Pseudomonas aeruginosa* under aerobic and anaerobic planktonic and biofilm conditions. Front. Microbiol. 7:291.

34. McDougald, D., J. Klebensberg, T. Tolker-Nielsen, J. S. Webb, T. Conibear, S. A. Rice, S. M. Kirov, C. Matz, and S. Kjelleberg. 2008. *Pseudomonas aeruginosa*: a model for biofilm formation, p. 215-253. *In* B. H. A. Rehm (ed.), Pseudomonas. Model Organism, Pathogen, Cell Factory. Wiley-VCH, Weinheim, Germany.

35. Moradali, M. F., S. Ghods, and B. H. Rehm. 2017. *Pseudomonas aeruginosa* lifestyle: a paradigm for adaptation, survival, and persistence. Front. Cell Infect. Microbiol. 7:39.

36. Nazzaro, F., F. Fratianni, L. De Martino, R. Coppola, and V. De Feo. 2013. Effect of essential oils on pathogenic bacteria. Pharmaceuticals 6:1451-1474.

37. Palma, M., D. DeLuca, S. Worgall, and L. E. Quadri. 2004. Transcriptome analysis of the response of *Pseudomonas aeruginosa* to hydrogen peroxide. J. Bacteriol. 186:248-252.

38. Pederick, V. G., B. A. Eijkelkamp, M. P. Ween, S. L. Begg, J. C. Paton, and C. A. McDevitt. 2014. Acquisition and role of molybdate in *Pseudomonas aeruginosa*. Appl. Environ. Microbiol. 80:6843-6852.

39. Pertea, M., G. M. Pertea, C. M. Antonescu, T. C. Chang, J. T. Mendell, and S. L. Salzberg. 2015. StringTie enables improved reconstruction of a transcriptome from RNA-seq reads. Nat. Biotechnol. 33:290-295.

40. Piddock, L. J. 2006. Multidrug-resistance efflux pumps - not just for resistance. Nat. Rev. Microbiol. 4:629-636.

41. Prasch, S., and F. Bucar. 2015. Plant derived inhibitors of bacterial efflux pumps: an update. Phytochem. Rev. 14:961–974.

42. Quale, J., Bratu, S., Gupta, J., Landman D. 2006. Interplay of efflux system, *ampC*, and *oprD* expression in carbapenem resistance of *Pseudomonas aeruginosa* clinical isolates. Antimicrob. Agents Chemother. 50:1633-1641.

43. Randall, K., M. Lever, B. A. Peddie, and S. T. Chambers. 1996. Natural and synthetic betaines counter the effects of high NaCl and urea concentrations. Biochim. Biophys. Acta 1291:189-194.

44. Raut, J. S., and S. M. Karuppayil. 2014. A status review on the medicinal properties of essential oils. Ind. Crop Prod. 62: 250-264.

45. Raut, J. S., R. B. Shinde, N. M. Chauhan, and S. M. Karuppayil. 2014. Phenylpropanoids of plant origin as inhibitors of biofilm formation by *Candida albicans*. J. Microbiol. Biotechnol. 24:1216-1225.

46. Salunkhe, P., T. Topfer, J. Buer, and B. Tummler. 2005. Genome-wide transcriptional profiling of the steady-state response of *Pseudomonas aeruginosa* to hydrogen peroxide. J. Bacteriol. 187:2565-2572.

47. Schaible, B., C. T. Taylor, and K. Schaffer. 2012. Hypoxia increases antibiotic resistance in *Pseudomonas aeruginosa* through altering the composition of multidrug efflux pumps. Antimicrob. Agents Chemother. 56:2114-2118.

48. Schweizer, H. P. 2012. Understanding efflux in Gram-negative bacteria: opportunities for drug discovery. Expert Opin. Drug Discov. 7:633-642.

49. Spengler, G., A. Kincses, M. Gajdacs, and L. Amaral. 2017. New roads leading to old destinations: efflux pumps as targets to reverse multidrug resistance in bacteria. Molecules 22:468.

50. Stavri, M., L. J. Piddock, and S. Gibbons. 2007. Bacterial efflux pump inhibitors from natural sources. J. Antimicrob. Chemother. 59:1247-1260.

51. Sudano Roccaro, A., A. R. Blanco, F. Giuliano, D. Rusciano, and V. Enea. 2004. Epigallocatechin-gallate enhances the activity of tetracycline in staphylococci by inhibiting its efflux from bacterial cells. Antimicrob. Agents Chemother. 48:1968-1973.

52. Tetard, A., A. Zedet, C. Girard, P. Plesiat, and C. Llanes. 2019. Cinnamaldehyde induces expression of efflux pumps and multidrug resistance in *Pseudomonas aeruginosa*. Antimicrob. Agents Chemother. 63:e01081-01019.

53. Van Alst, N. E., L. A. Sherrill, B. H. Iglewski, and C. G. Haidaris. 2009. Compensatory periplasmic nitrate reductase activity supports anaerobic growth of *Pseudomonas aeruginosa* PAO1 in the absence of membrane nitrate reductase. Can. J. Microbiol. 55:1133-1144.

54. Ventola, C. L. 2015. The antibiotic resistance crisis: part 1: causes and threats. P T 40:277-283.

55. Vogt, T. 2010. Phenylpropanoid biosynthesis. Mol. Plant 3:2-20.

56. Wargo, M. J. 2013. Homeostasis and catabolism of choline and glycine betaine: lessons from *Pseudomonas aeruginosa*. Appl. Environ. Microbiol. 79:2112-2120.

57. Yakhnina, A. A., H. R. McManus, and T. G. Bernhardt. 2015. The cell wall amidase AmiB is essential for *Pseudomonas aeruginosa* cell division, drug resistance, and viability. Mol. Microbiol. 97:957-973.

58. Yamaguchi, Y., T. Tomoyasu, A. Takaya, M. Morioka, and T. Yamamoto. 2003. Effects of disruption of heat shock genes on susceptibility of *Escherichia coli* to fluoroquinolones. BMC Microbiol. 3:16.

CHAPTER IV – SYNTHESIS AND FUNCTIONAL EVALUATION OF PRO-ANTIMICROBIAL POLYMERS THAT TARGET THE PRODUCTION OF BIOFILMS AND VIRULENCE FACTORS IN THE HUMAN PATHOGEN PSEUDOMONAS AERUGINOSA

4.1 Abstract

Pseudomonas aeruginosa is a ubiquitous gram-negative opportunistic pathogen that poses a significant threat to public health. This organism has a large repertoire of regulatory genes, an impressive array of virulence traits, and forms antibiotic-resistant biofilms that make infections difficult to eradicate. In *P. aeruginosa*, the production of many virulence factors is regulated in the cell density-dependent way by quorum sensing (QS). The QS also controls the synthesis of rhamnolipids, which mediate the formation of microcolonies during the biofilm establishment, as well as growth and dispersion of mature biofilms. In this study, we combined furaneol (a natural plant-derived QS inhibitor) with *p*-anisaldehyde (an antimicrobial constituent of essential oil from star anise) to disrupt quorum sensing and biofilm formation in *P. aeruginosa* PAO1. We hypothesized that furaneol would trigger the transition of bacteria from the recalcitrant surface-attached biofilm to the suspended planktonic mode of growth, which would render them vulnerable to destruction by *p*-anisaldehyde. Results of our experiments revealed that the treatment of *P. aeruginosa* with furaneol effectively disrupted the secretion of QS-regulated virulence factors, surface motility, and formation of static biofilms. We then used thiol-ene chemistry to produce antimicrobial polymers, which enable high loading, efficient "encapsulation," and sustained release of furaneol and *p*-anisaldehyde. The exposure of *P. aeruginosa* PAO1 to furaneol/*p*-anisaldehyde

polymeric discs strongly repressed the production of pyocyanin, reduced the exoprotease activity, prevented bacteria from colonizing the solid surface, and completely eradicated established biofilms. Our results will facilitate the development of polymeric systems capable of dual phytochemical delivery and controlling microbial growth without promoting antibiotic resistance.

4.2 Introduction

Pseudomonas aeruginosa is a ubiquitous gram-negative opportunistic pathogen that causes life-threatening infections in individuals with burn wounds, cancer, cystic fibrosis, and AIDS.[1,2] This organism utilizes numerous organic compounds as energy sources, has a large repertoire of regulatory genes, and an impressive array of virulence traits, which collectively allow *P. aeruginosa* to successfully adapt to both environmental and pathogenic lifestyles.[3] Moreover, the ability of *P. aeruginosa* to form biofilms enhances its resistance to antimicrobial agents and makes infections very difficult to eradicate.[4] In many bacterial pathogens, the successful colonization of a host organism requires intimate contact between bacterial cells and host tissues. In *P. aeruginosa*, the contact with rigid surfaces induces virulence in multiple models of infection.[5] The initial contact with host tissues involves type IV pili, which are the most important adhesin of *P. aeruginosa*. In addition to binding to the host epithelial cells, type IV pili are also involved in special forms of surface motility known as twitching and swarming.[6] The twitching motility uses only type IV pili, which act as grappling hooks that pull the bacterial cell along a solid surface, whereas the swarming motility uses type IV pili, flagella, and rhamnolipids, and is induced by certain N and C sources. Both twitching and swarming types of motility are linked to the formation of *P. aeruginosa* biofilms.[7]

Quorum sensing (QS) is an intercellular mechanism of communication that allows bacteria to coordinate gene expression in response to cell density. This regulatory mechanism involves the production, sensing, and response to signaling molecules called autoinducers (AIs), which bind to their cognate response regulators that affect the transcription of target genes.[2,8–10] In *P. aeruginosa*, QS governs the production of many virulence factors, especially those involved in acute infections.[11] Quorum sensing also controls the synthesis of rhamnolipids, which mediate the formation of microcolonies during the biofilm establishment, as well as growth and dispersion of mature biofilms.[12] Structural components of the biofilm EPS matrix, such as polysaccharide Pel and extracellular DNA, are also under QS control. *P. aeruginosa* produces three different autoinducer molecules: N-(3-oxo-dodecanoyl)-L-homoserine lactone, N-butyryl-L-homoserine lactone, and 2-heptyl-3-hydroxy-4-quinolone. These autoinducers control, respectively, the Las, Rhl, and PQS parts of the QS network.[2,8,10] Due to the high clinical relevance of regulated traits and the absence of homologs in humans and higher animals, QS is considered a promising target for adjuvant therapy of *P. aeruginosa* infections.[11]

Several strategies have been suggested for the interference with QS in *P. aeruginosa*, including the inhibition and degradation of AI synthesis, inhibition of AI binding to response regulator, and competitive exclusion of AIs.[4] The use of compounds that compete with AIs for target receptors represents an intuitive way of disrupting the function of QS circuits, and the identification of such AI mimics can be performed in a high-throughput fashion using libraries of small molecules.[13] Living organisms represent a rich source of potential AI analogs, and numerous active agonists and antagonists of QS were discovered in bacteria, fungi, and especially plants. For example, brominated

furanones in the red algae *Delisea pulchra* were among the first recognized small molecule inhibitors of QS.[14] The original discovery prompted chemical synthesis research that produced dozens of halogenated furanone compounds, many of which exhibit excellent activity at disrupting QS in *P. aeruginosa* and *Aliivibrio fischeri*.[15] Unfortunately, halogenated furanones proved to be toxic, which precludes their application for therapeutic purposes.[4] Recently, a natural furanone compound, 4-hydroxy-2,5-dimethyl-3-furanone (also known as furaneol, or strawberry furanone), was shown to interfere with QS traits in *P. aeruginosa*.[16] Unlike its halogenated counterparts, furaneol is a non-toxic metabolite and used in the perfume industry and as a food flavoring agent.

In this study, we combined furaneol with the antimicrobial essential oil constituent *p*-anisaldehyde to produce antimicrobial polymer materials capable of disrupting quorum sensing and biofilm formation in *P. aeruginosa*. Our previous research has identified the plant polyphenol epigallocatechin gallate (EGCG) as a compound that potentiates the antimicrobial activity of *p*-anisaldehyde (Adewunmi et al., unpublished). Hence, in this work, we also tested the efficacy of epigallocatechin gallate (EGCG) in combination with *p*-anisaldehyde against *P. aeruginosa* biofilms. The efficient target delivery of furaneol and *p*-anisaldehyde was achieved by incorporating them into a thiol-ene polymer network, an approach that we successfully used in previous studies to stabilize hydrophobic and volatile plant antimicrobials.[17,18] However, in contrast to previously used pro-antimicrobial polymers that require degradation in order to release *p*-anisaldehyde, we describe here the synthesis of a non-degradable thiol-ene thermoset matrix that relies solely on diffusion to control the release of bioactive compounds. We

then evaluated the ability of the new polymer containing furaneol and *p*-anisaldehyde to interfere with QS and disrupt the release of virulence factors and formation of biofilm in the reference strain *P. aeruginosa* PAO1.

4.3 Materials and Methods

4.3.1 Materials, bacterial strains, and culture conditions

Pseudomonas aeruginosa PAO1 was used in all experiments listed in this study. The strain was routinely cultured at 37℃ in Luria-Bertani (LB) medium, while the Mueller-Hilton II (MH) broth and agar (all from Becton Dickinson, Franklin Lakes, NJ) were used in all antimicrobial assays. The production of pyocyanin production was measured in King's medium A (KMA).[19] *p*-Anisaldehyde, 2-hydroxy-2-methylpropionate (Darocur 1173), 1,3,5-triallyl-1,3,5-triazine-2,4,6(1*H*,3*H*,5*H*)-trione (TTT), EGCG, and 4-Hydroxy-2,5-dimethyl-3(2H)-furanone (furaneol) were obtained from Thermo Fisher Scientific (Waltham, MA) in the highest purity available and used without further purification. Pentaerythritol tetrakis (3-mercaptopropionate) (PETMP) was provided by Bruno Bock (Marschacht, Germany) and used as supplied. As needed, 10 mg mL^{-1} stock concentrations of *p*-anisaldehyde, EGCG, and furaneol were prepared in fresh MHB, DMSO, and water, respectively.

4.3.2 Static biofilm assays

We measured the activity of *p*-anisaldehyde, EGCG, furaneol, and their respective combinations on surface-attached biofilms formed by *P. aeruginosa* PAO1 using the protocol of O'Toole.[20] Overnight bacterial cultures were adjusted to an OD_{600} of 0.1 and then diluted 1:10 in MHB supplemented with furaneol (3 mg mL^{-1}), EGCG (150 μg mL^{-1}), *p*-anisaldehyde (1 mg mL^{-1}), a combination of *p*-anisaldehyde and EGCG (1 mg mL^{-1}

and 150 μg mL^{-1}, respectively), or a combination of *p*-anisaldehyde and furaneol (1 and 3 mg mL^{-1}, respectively). One hundred microliter aliquots of diluted bacteria were dispensed into wells of a 96-well Serocluster PVC microplate (Corning Costar, Tewksbury, MA) and the inoculated plates were incubated at 37°C for 24 h. After that, the plates were rinsed twice in RO water to remove unattached cells and media components. To stain the biofilms, 125 μL of 0.1 % crystal violet was added to each well and allowed to incubate for 15 min. Crystal violet was then discarded, and the microplates were rinsed four times with RO water and dried for 2 h. In order to quantify the biofilms, 125 μL of 30% acetic acid were added to each well of the microtiter plates and left for 15 mins. The solution was transferred to a CytoOne flat-bottom 96-well microtiter plate (USA Scientific, Ocala, FL), and the amount of solubilized dye was measured at 550 nm using 30% acetic acid as a blank and bacteria grown in the absence of compounds served as the positive control. Experiments were repeated at least three times with 10 replicates for each treatment.

4.3.3 Swimming, twitching, and swarming motility assays

The effect of furaneol on the swimming and swarming motility was determined using a protocol of Ha et al.[21,22], while the twitching motility assay was carried out as described by Turnbull and Whitchurch.[22,23] The assays were performed in M8 medium (0.2% glucose, 0.5% casamino acid, and 1mM MgSO4) supplemented with 0.3% agar for swimming, 0.8% for swarming, and 1% for twitching motility. The culture medium was further amended with 0, 2, or 4 mg mL^{-1} of furaneol. Twitching motility was determined by stab-inoculating the center of the plate with a sterile toothpick dipped in the overnight culture of *P. aeruginosa* PAO1. Swarming motility was determined by spotting 2.5 μL of

overnight culture in the center of a plate. Swimming motility was determined by stab inoculating M8 agar with a toothpick without touching the bottom of the plate. All plates were incubated at 37°C, and the diameter of colonies was measured after 24 h of growth.

4.3.4 Quantification of pyocyanin

Pyocyanin production was determined as described by Kern et al.[22,24] Briefly, *P. aeruginosa* was cultured at 37°C with shaking at 220 rpm for 24 h in KMA with and without furaneol. After incubation, each 3-mL culture was mixed with 1.5 mL of chloroform and vigorously vortexed for 30 s. After incubation for 10 min at room temperature, the bottom organic layer was aspirated and clarified by spinning for 5 min at 6,000× g. The chloroform extracts were then acidified with 200 μL of 0.1 N HCl, and their absorbance was measured at 520 nm. The absorbance values were multiplied by 17.072 to determine the concentration of pyocyanin in μg mL^{-1}. Experiments were repeated three times, with five replicates per treatment.

4.3.5 Determination of the exoprotease activity

In order to determine the effect of furaneol on protease production, bacterial cultures were grown and treated with furaneol as described above for pyocyanin production. Protease activity was determined using azocasein (Thermo Fisher) as a described by Andrejko et al.[25] One day old cultures were centrifuged at 12,000× g for 10 min at 4°C, and 250 μL of the supernatant were mixed with equal volume of azocasein (5 mg mL^{-1} in water) and incubated for 1 h at 37°C. The reaction was stopped with 250 μL of 20% trichloroacetic acid and allowed to stand for 15 min to ensure complete inactivation.[26] The samples were then centrifuged again for 10 mins at 20,000× g, and

750 μL of the supernatant were mixed with 375 μL of 0.5 M NaOH. The protease activity was quantified by measuring absorbance at 366 nm.[27] The experiment was repeated twice, with five replicates per treatment.

4.3.6 Preparation of polymeric antimicrobial discs

A stock resin solution was prepared by combining and mixing thoroughly 2.00 grams of TTT (8.04 mmol, 24.12 mmol ene), 2.95 grams of PETMP (6.03 mmol, 24.12 mmol SH), and 495 mg Darocur 1173 (3.01 mmol, 10% w/w, 12.5 mol percent relative to SH). The polymer matrix containing a combination of furaneol and *p*-anisaldehyde was prepared using 100 mg furaneol (17.8% total resin mass), 125 mg *p*-anisaldehyde (21.4% w/w), and 336 mg stock resin (60% w/w). Preliminary experiments indicated that the addition of hydrophilic furaneol to thiol-ene networks accelerates the release of *p*-anisaldehyde. Therefore, to match the release profile of the combination matrix, the *p*-anisaldehyde-only polymer was prepared using 160 mg of *p*-anisaldehyde (28.6% w/w) and 400 mg stock resin (31.4% w/w). Finally, the furaneol-only polymer network was prepared using 100 mg of furaneol (17.8% w/w) and 462 mg of stock resin (82.2% w/w). Aliquots (60, 70, or 80 μL) of each material were dispensed onto glass slides separated with 0.75-mm thick PTFE spacers and cured for 120 s with an Omnicure S1000-1B UV light source (100 W mercury lamp, λmax = 365 nm, 320–500 nm filter) at an intensity of 200 mW cm^{-2}. A similar approach was used to prepare from the stock resin inactive control discs.

4.3.7 Evaluation of the effect of polymeric antimicrobial discs on the production of pyocyanin and exoprotease

Overnight bacterial cultures were diluted to 10^7 CFUs mL^{-1} in KMA or MHB broth for the production of pyocyanin and exoprotease, respectively, and dispensed in 4 mL aliquots into culture tubes. Polymeric antimicrobial discs (60 mm^3) containing furaneol, *p*-anisaldehyde, or a combination of both compounds were placed in the inoculated tubes, which were then incubated for 24 h at 37°C with shaking at 220 rpm. The amount of secreted pyocyanin and exoprotease activity was measured as described above. Negative control included polymeric discs without bioactive compounds. All treatments were replicated five times, and the entire experiment was repeated twice.

4.3.8 Biofilm assays

We used a modified procedure of Haney et al.[28] to evaluate the ability of the polymers containing furaneol and *p*-anisaldehyde to inhibit the establishment of surface-attached biofilms. Briefly, MHB cultures of *P. aeruginosa* were adjusted to 10^7 CFUs mL^{-1} and dispensed in 100-µL aliquots into wells of a 96-well Serocluster PVC microplate (Corning Costar). Polymeric discs containing furaneol, *p*-anisaldehyde, or a combination of both compounds were then aseptically placed into each microplate well. Three different disc sizes (1.5, 1.75, and 2 mm^3) were used in these experiments, and discs without furaneol or *p*-anisaldehyde served as a vehicle control. The microplates were incubated for 24 h at 37°C, after which the plates were gently rinsed twice with RO water, and allowed to dry overnight at room temperature to fix bacterial biofilms.[29] The dry biofilms were stained for 45 min with 125 µL of 0.1 % crystal violet, after which the dye was discarded, and microplates were rinsed three times with RO water and dried for

2 h. The retained dye was solubilized with 30% acetic acid and quantified by measuring absorbance at 550 nm.

We also tested the ability of polymeric discs to eradicate mature *P. aeruginosa* biofilms. Static biofilms were established by growing bacteria for 24 h at 37°C in a microplate prefilled with MHB. Following the incubation, culture liquid containing planktonic cells was removed, and each well was gently rinsed and filled with 100 μL of fresh culture medium. Antimicrobial polymeric discs were placed into microplate wells, and the plates were incubated statically at 37°C for 24 h and processed as described above. The amount of eradicated biofilm was calculated relative to the amount of biofilm grown in the presence of vehicle control. All experiments were repeated five times with five replicates per treatment.

4.3.9 Confocal microscopy

Biofilms for microscopic observations were grown identically to the eradication assay, except that the experiment was performed in Nunc MicroWell 96-well optical bottom microplates (ThermoFisher). The established biofilms were exposed to antimicrobial discs for 3 h at 37°C, after which microplate wells were carefully rinsed twice with sterile PBS and stained using a LIVE/DEAD bacterial viability kit (Thermo Fisher).[30] Briefly, 2× stocks of SYTO-9 and propidium iodide were dissolved in 5 mL of sterile RO water, and 200 μL of the dye mixture were added to each microplate well and incubated at room temperature in the dark for 45 min. The dye was then carefully aspirated, and microplate wells were rinsed with sterile PBS and filled with 100 μL of fresh MHB. The confocal microscopy was performed using a Zeiss 510 UV/META LSM microscope (Zeiss, Oberkochen, Germany) with the excitation/emission maxima set to

480/500 nm for green fluorescence, and 490/635 nm for red fluorescence. Images were captured at 40× magnification, and three-dimensional images (z-stacks) of adhered biofilms were captured and compiled using the Zen software (Zeiss).

4.4 Results and Discussion

The overall goal of this study was to improve the antimicrobial efficacy of *p*-anisaldehyde thiol-ene polymers against biofilms formed by *P. aeruginosa*. We hypothesized that the release of the quorum-sensing inhibitors would trigger the transition of bacteria from the recalcitrant surface-attached biofilm to a suspended planktonic mode of growth, which would render them more susceptible to destruction by *p*-anisaldehyde. Furthermore, we reasoned that the presence of QSIs would inhibit the secretion of QS-mediated secretion of virulence factors. We started, therefore, by testing *p*-anisaldehyde, EGCG, furaneol, and their combinations for their ability to inhibit the formation of biofilms in *P. aeruginosa*. The results of this experiment revealed that *p*-anisaldehyde and EGCG alone had no significant effect on the biofilm formation (Fig. 4.1A). However, the combination of EGCG or furaneol with *p*-anisaldehyde, reduced the amount of biofilm by 43% and 92%, respectively, compared to the non-treated control. Also, there was no significant difference between the levels of biofilms produced in cultures amended by only furaneol or a combination of furaneol and *p*-anisaldehyde. We further confirmed that these compounds do not act synergistically against planktonic cells (data not shown). In agreement with other studies, [16] we found that sub-inhibitory concentrations of furaneol significantly ($P < 0.05$) decreased the swimming, swarming, and twitching motility in *P. aeruginosa* (Fig. 4.1B). At the highest tested concentration, furaneol reduced the flagella-mediated swimming by 54%, swarming motility by 80%,

and the type IV pili-dependent twitching motility by 94%. Additionally, we found that 4 mg mL^{-1} of furaneol reduced the concentration of pyocyanin by approximately six-fold compared to the untreated control (Fig. 4.1C). We also observed a modest effect in the production of exoprotease, which dropped in cultures treated for 24 h with the highest furaneol concentration by 26 Units (Fig. 4.1D).

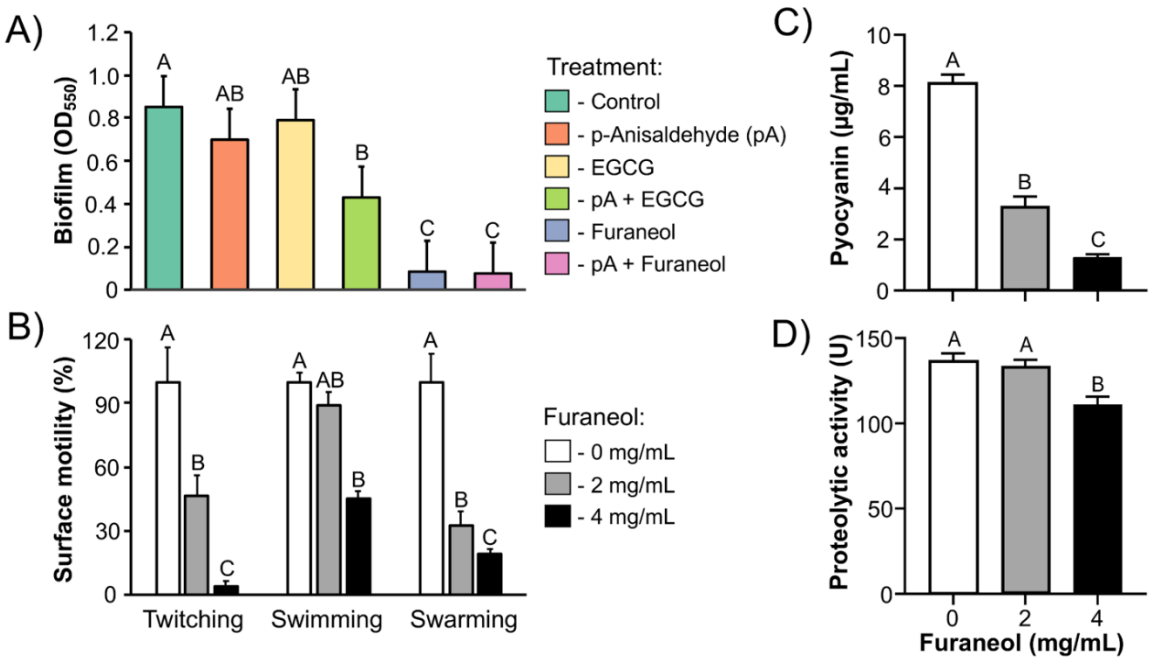

Figure 4.1 The effect of *p*-anisaldehyde (pA), EGCG, furaneol, and their combinations on the formation of static biofilms (A). Also shown is the effect of furaneol on the surface motility (B), accumulation of pyocyanin (C), and exoprotease activity (D) in *P. aeruginosa* PAO1.

The pyocyanin and protease data were analyzed by Tukey's multiple comparisons HSD test ($P < 0.05$), while the surface motility and biofilm data were analyzed by the Kruskal Wallis rank sum test, followed by the Dunn's non-parametric test for multiple comparisons ($P < 0.05$). Treatments that do not share letters are significantly different.

Although quorum sensing inhibitors act to repress the quorum sensing, the exact modulatory effect on the pathogen can be complicated. For example, the application of

sub-MIC concentrations of the antibiotic azithromycin, which acts as a quorum sensing inhibitor in *P. aeruginosa*, resulted in high mortality in mice, which was likely triggered by the bacterial switch from the chronic to acute mode of infection and induction of non-QS-dependent virulence determinants, such as the type III secretion system.[31] Therefore, it is important to combine quorum sensing inhibitors with effective antimicrobials to lessen the chance of the activation of

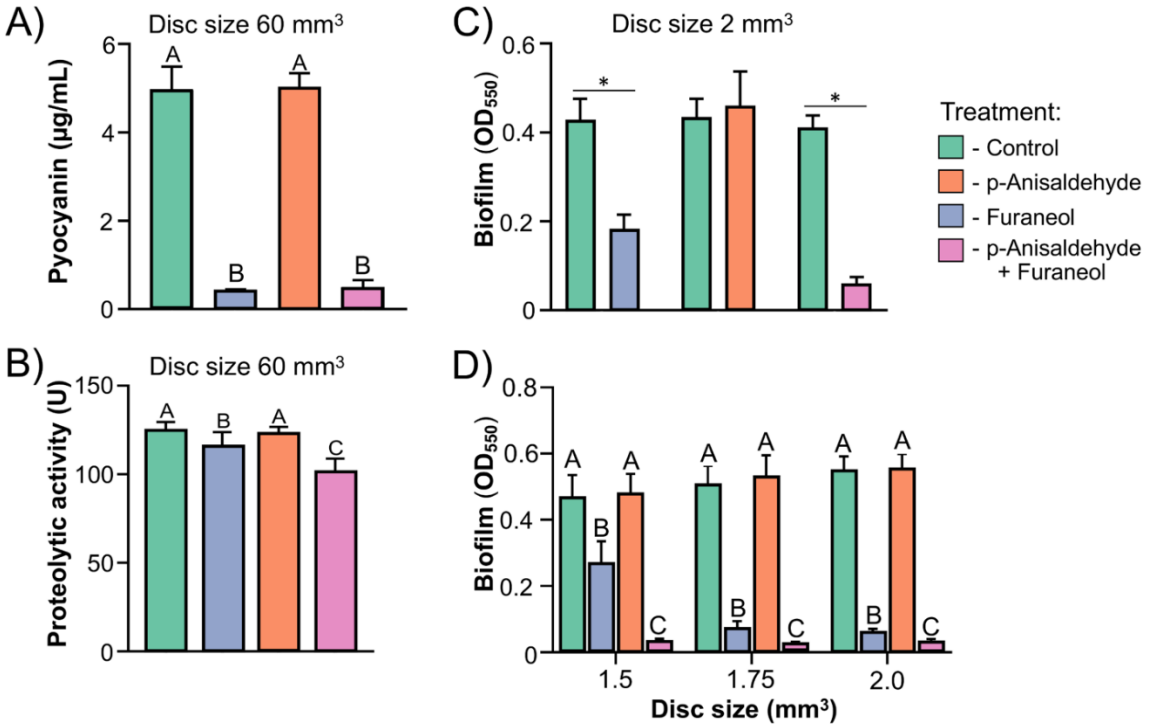

Figure 4.2. The effect of polymeric antimicrobial discs containing *p*-anisaldehyde, furaneol, and the combination of thereof on the production of pyocyanin (A), protease activity (B), and formation of biofilms (C). Panel illustrates the capacity of varying size polymeric discs to eradicate mature biofilms of *P. aeruginosa* (D).

Data represent mean ± standard deviation (SD) of five biological replicates. Bars with different letters or asterisks indicate significant differences as determined by the Tukey's HSD test ($P < 0.05$).

non-quorum sensing-dependent virulence traits and guarantee the complete eradication of the pathogen. We aimed to achieve this goal by generating an antimicrobial polymeric network, which was produced using the thiol-ene photopolymerization in the presence of furaneol and *p*-anisaldehyde, which acted, respectively, as a quorum sensing inhibitor and an antimicrobial agent. The exposure of *P. aeruginosa* PAO1 to polymeric discs containing furaneol or the furaneol/ *p*-anisaldehyde combination strongly repressed the production of pyocyanin (Fig. 4.2A) and reduced the exoprotease activity significantly by 8 and 24 Units, respectively (Fig. 4.2B). We proceeded to measure the ability of the furaneol- and *p*-anisaldehyde-containing polymers to prevent the establishment and eradicate biofilms formed by *P. aeruginosa*. The 24-h exposure to discs containing both compounds effectively prevented bacteria from colonizing the solid surface (Fig. 4.2C) and completely abolished the established biofilms (Fig. 4.2D). This effect was not achieved by treating cultures with the corresponding small molecules.

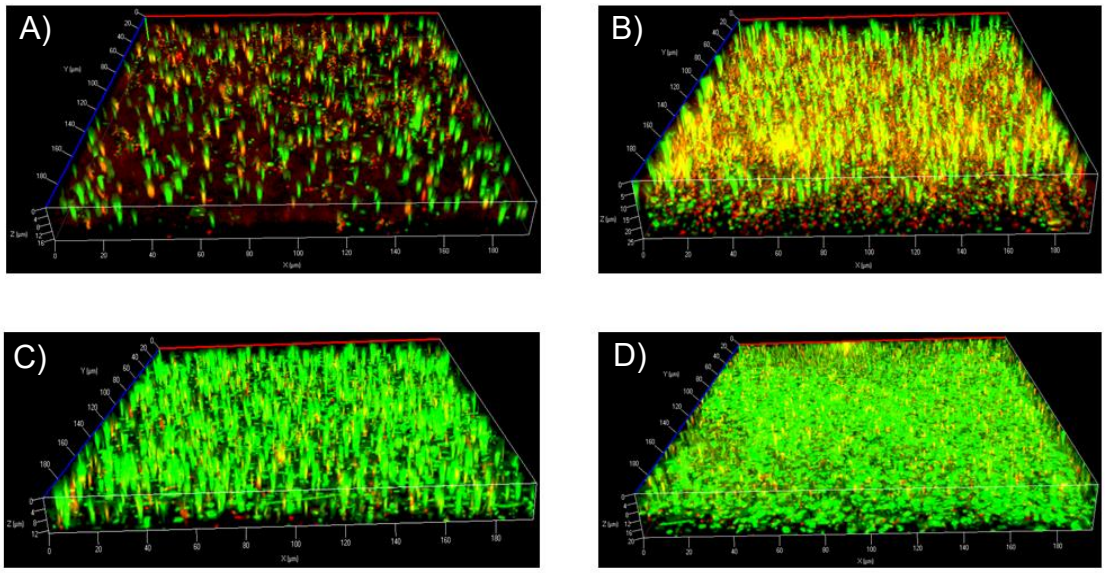

Figure 4.3. Changes in the viability of mature *P. aeruginosa* biofilms after 3 h of exposure to polymeric antimicrobial discs containing a combination of furaneol and *p*-anisaldehyde (A), *p*-anisaldehyde (B), furaneol (C), or no antimicrobials (vehicle control) (D).

Viable cells appear green, while dead cells are stained red. The biofilms were stained using the LIVE/DEAD Bacterial Viability Kit and imaged with a Zeiss LSM microscope at 40x magnification. Three-dimensional images (z-stacks) of adhered biofilms were captured and compiled using the Zen software (Zeiss).

The confocal microscopy revealed that the exposure to the furaneol/*p*-anisaldehyde-containing polymer for only 3 hours significantly impacted the appearance of *P. aeruginosa* biofilms. The LIVE/DEAD staining showed that nearly all the cells in the combination treatment were dead, while considerably higher levels of live bacteria were present in the furaneol and control treatments (Figure 4.3). The presence of both furaneol and *p*-anisaldehyde also changed the appearance of biofilms rendering them less compact and reducing the presence of mushroom-shaped structures. Interestingly, although furaneol and the combination of furaneol with *p*-anisaldehyde performed equally well at

eradicating biofilms (Fig. 4.1A), the polymeric disks containing both compounds outperformed their furaneol-only counterparts (Fig. 4.2D). The effect was also evident during microscopy observations, where biofilms exposed to the furaneol/*p*-anisaldehyde polymer clearly showed a higher proportion of dead cells.

In conclusion, we demonstrated that plant-derived bioactive compounds could be combined to target quorum sensing regulation and biofilms in pathogenic bacteria. In particular, the treatment of *P. aeruginosa* with a mix of furaneol and *p*-anisaldehyde effectively disrupted the secretion of QS-regulated virulence factors and the formation of static biofilms. Both compounds also can be incorporated into antimicrobial thiol-ene polymeric networks, which enables high loading, efficient "encapsulation," solvent-free processing, and sustained release profiles. Our results will facilitate the development of polymeric systems capable of dual phytochemical delivery and controlling microbial growth without promoting antibiotic resistance.

4.5 References

(1) Smith, K. M.; Bu, Y.; Suga, H. Induction and inhibition of *Pseudomonas aeruginosa* quorum sensing by synthetic autoinducer analogs. *Chem. Biol.* **2003**, *10* (1), 81–89.

(2) El-Shaer, S.; Shaaban, M.; Barwa, R.; Hassan, R. Control of quorum sensing and virulence factors of *Pseudomonas aeruginosa* using phenylalanine arginyl b-naphthylamide. *J. Med. Microbiol.* **2016**, *65*, 1194–1204.

(3) Moradali, M. F.; Ghods, S.; Rehm, B. H. A. *Pseudomonas aeruginosa* lifestyle: a paradigm for adaptation, survival, and persistence. *Front. Cell. Infect. Microbiol.* **2017**, *7*, 1–29.

(4) Brackman, G.; Coenye, T. Quorum sensing inhibitors as anti-biofilm agents. *Curr. Pharm. Des.* **2014**, *21* (1), 5–11.

(5) Siryaporn, A.; Kuchma, S. L.; O'Toole, G. A.; Gitai, Z. Surface attachment induces *Pseudomonas aeruginosa* virulence. *Proc. Natl. Acad. Sci.* **2014**, *111* (47), 16860–16865.

(6) Burrows, L. L. *Pseudomonas aeruginosa* twitching motility: type iv pili in action. *Annu. Rev. Microbiol.* **2012**, *66* (1), 493–520.

(7) Daniels, R.; Vanderleyden, J.; Michiels, J. Quorum sensing and swarming migration in bacteria. *FEMS Microbiol. Rev.* **2004**, *28* (3), 261–289.

(8) Asfour, H. Z. Antiquorum sensing natural compounds. *J. Microsc. Ultrastruct.* **2017**, No. 122, 1–12.

(9) Chatterjee, M.; Anju, C. P.; Biswas, L.; Anil Kumar, V.; Gopi Mohan, C.; Biswas, R. Antibiotic resistance in *Pseudomonas aeruginosa* and alternative therapeutic options. *Int. J. Med. Microbiol.* **2016**, *306* (1), 48–58.

(10) Lin, J.; Cheng, J.; Wang, Y.; Shen, X. The Pseudomonas quinolone signal (pqs): not just for quorum sensing anymore. *Front. Cell. Infect. Microbiol.* **2018**, *8* (230), 1–9.

(11) Rutherford, S. T.; Bassler, B. L.; Delany, I.; Rappuoli, R.; Seib, K. L.; Ben-tekaya, H.; Gorvel, J.; Ruhe, C. Bacterial Quorum Sensing : Its role in virulence and possibilities for its control. *Cold Spring Harb Perspect Med* **2014**, *2*, 1–26.

(12) de Kievit, T. R. Quorum sensing in *Pseudomonas Aeruginosa* biofilms. *Environ. Microbiol.* **2009**, *11* (2), 279–288.

(13) LaSarre, B.; Federle, M. J. Exploiting quorum sensing to confuse bacterial

pathogens. *Microbiol. Mol. Biol. Rev.* **2013**, *77* (1), 73–111 DOI: 10.1128/MMBR.00046-12.

(14) Reichelt, J. L.; Borowitzka, M. A. Antimicrobial activity from marine algae: results of a large-scale screening programme. *Hydrobiologia* **1984**, *116–117* (1), 158–168.

(15) Manefield, M.; Rasmussen, T. B.; Henzter, M.; Andersen, J. B.; Steinberg, P.; Kjelleberg, S.; Givskov, M. Halogenated furanones inhibit quorum sensing through accelerated luxr turnover. *Microbiology* **2002**, *148* (4), 1119–1127.

(16) Choi, S.-C.; Zhang, C.; Moon, S.; Oh, Y.-S. Inhibitory effects of 4-hydroxy-2,5-dimethyl-3(2h)-furanone (hdmf) on acyl-homoserine lactone-mediated virulence factor production and biofilm formation in *Pseudomonas aeruginosa* PAO1. *J. Microbiol.* **2014**, *52* (9), 734–742.

(17) Amato, D. V; Amato, D. N.; Blancett, L. T.; Mavrodi, O. V; Martin, W. B.; Swilley, S. N.; Sandoz, M. J.; Shearer, G.; Mavrodi, D. V; Patton, D. L. A bio-based pro-antimicrobial polymer network via degradable acetal linkages. *Acta Biomater.* **2018**, *67*, 196–205.

(18) Amato, D. N.; Amato, D. V.; Mavrodi, O. V.; Braasch, D. A.; Walley, S. E.; Douglas, J. R.; Mavrodi, D. V.; Patton, D. L. Destruction of opportunistic pathogens via polymer nanoparticle-mediated release of plant-based antimicrobial payloads. *Adv. Healthc. Mater.* **2016**, *5* (9), 1094–1103.

(19) King, E. O.; Ward, M. K.; Raney, D. E. Two Simple media for the demonstration of pyocyanin and fluorescin. *J. Lab. Clin. Med.* **1954**, *44* (2), 301–307.

(20) O'Toole, G. A. Microtiter dish biofilm formation assay. *J. Vis. Exp.* **2011**, *47*, 1–2.

(21) Ha, D.-G.; Kuchma, S. L.; O'Toole, G. A. Plate-Based Assay for swarming motility in *Pseudomonas aeruginosa*. In *Pseudomonas methods and protocols*; 2014; pp 67–72.

(22) Filloux, A.; Ramos, J.-L. *Pseudomonas Methods and Protocols*; Filloux, A., Ramos, J.-L., Eds.; Methods in molecular biology; Springer new york: new york, NY, 2014; Vol. 1149.

(23) Turnbull, L.; Whitchurch, C. B. Motility assay: twitching motility. In *Pseudomonas methods and protocols*; Springer New York: New York, NY, 2014; pp 73–86.

(24) Kern, S. E.; Newman, D. K. Measurement of phenazines in bacterial cultures. In *Pseudomonas methods and protocols*; Springer New York: New York, NY, 2014; pp 303–310.

(25) Andrejko, M.; Zdybicka-Barabas, A.; Janczarek, M. Three *Pseudomonas aeruginosa* strains with different protease profiles. *Acta Biochem. Pol.* **2013**, *60*, 83–90.

(26) Schmidtchen, A.; Wolff, H.; Hansson, C. Differential proteinase expression by *Pseudomonas aeruginosa* derived from chronic leg ulcers. *Acta Derm Venereol* **2001**, *81*, 406–409.

(27) Chessa, J.-P.; Petrescu, I.; Bentahir, M.; Van Beeumen, J.; Gerday, C. Purification, physico-chemical characterization and sequence of a heat labile alkaline metalloprotease isolated from a psychrophilic Pseudomonas species. *Biochim. Biophys. Acta - Protein Struct. Mol. Enzymol.* **2000**, *1479* (1–2), 265–274.

(28) Haney, E. F.; Trimble, M. J.; Cheng, J. T.; Vallé, Q.; Hancock, R. E. W. Critical

assessment of methods to quantify biofilm growth and evaluate antibiofilm activity of host defence peptides. *Biomolecules* **2018**, *8* (29), 1–22.

(29) Richter, A. M.; Fazli, M.; Schmid, N.; Shilling, R.; Suppiger, A.; Givskov, M.; Eberl, L.; Tolker-Nielsen, T. Key players and individualists of cyclic-di-gmp signaling in *Burkholderia cenocepacia*. *Front. Microbiol.* **2019**, *9* (3386), 1–15.

(30) Beaudoin, T.; Kennedy, S.; Yau, Y.; Waters, V. Visualizing the effects of sputum on biofilm development using a chambered coverglass model. *J. Vis. Exp.* **2016**, *118*, 1–6.

(31) Skindersoe, M. E.; Alhede, M.; Phipps, R.; Yang, L.; Jensen, P. O.; Rasmussen, T. B.; Bjarnsholt, T.; Tolker-Nielsen, T.; Høiby, N.; Givskov, M. Effects of antibiotics on quorum sensing in *Pseudomonas aeruginosa*. *Antimicrob. Agents Chemother.* **2008**, *52* (10), 3648–3663.

CHAPTER V – CONCLUSIONS

Essential oils (EOs) are extracts of aromatic and medicinal plants that are recognized by the American Food and Drug Administration (FDA) as Generally Recognized as Safe (GRAS) substances and used in alternative medicine, agriculture, food, and cosmetic industries. The EOs contain dozens of chemically-diverse constituents, many of which possess antimicrobial properties and represent an attractive alternative to conventional antibiotics due to the ability to kill microorganisms without promoting resistance.[1,2,3] However, their broader use in the control of microorganisms is restricted by the low solubility, volatility, and lower activity compared to conventional antibiotics. In addition, many details of the mechanism of action and synergistic antimicrobial effects of individual EO constituents remain poorly understood.[4] The overarching aim of my work involved addressing these issues by studying molecular interactions between antimicrobial plant aldehydes and the opportunistic human pathogen *Pseudomonas aeruginosa*.

We tackled the chemical instability of EO-derived phytoaldehydes by incorporating them into thioether acetal polymer networks called PANDAs. We also broadened the antimicrobial activity of PANDAs by synthesizing them with synergistically interacting combinations of plant metabolites. In the first part of my project, we produced a new thiol-ene polymer using the synergistically interacting combination of *p*-bromobenzaldehyde and *p*-anisaldehyde. That approach significantly improved the antimicrobial activity of the polymer material killed and exhibited negligible toxicity against mammalian tissue culture cells. We then probed cellular

effects the *p*-anisaldehyde and demonstrated that the inactivation of the MexAB-OprM multidrug efflux pump sensitizes *P. aeruginosa* to the action of *p*-anisaldehyde.

We built upon these findings by performing a transposon screen of cellular pathways targeted by *p*-anisaldehyde in *P. aeruginosa*. We also demonstrated that the putative efflux pump inhibitor epigallocatechin gallate (EGCG) interacts synergistically with *p*-anisaldehyde and significantly reduces its minimal inhibitory concentration against *P. aeruginosa.* We went further to determine the effects of *p*-anisaldehyde, EGCG, and their combination on the transcriptome of *P. aeruginosa* using RNA-seq. Our results suggested that *p*-anisaldehyde disrupts the envelope of bacterial cells and then accumulates intracellularly, causing their misfolding and aggregation of proteins. In contrast, EGCG likely acts by generating oxidative stress, which contributes to the ability to complement and potentiate the antimicrobial action of *p*-anisaldehyde. The synergistic antimicrobial interaction between the two compounds is further enhanced by the capacity of EGCG to reverse the upregulation of many genes by *p*-anisaldehyde, including those encoding various transporters and key RND efflux pumps. This part of my project highlighted the important microbial genes and associated pathways involved in response to plant-derived phenylpropanoid compounds. Additionally, by studying the interaction of *p*-anisaldehyde and EGCG, we characterized some molecular mechanisms governing the synergistic effects of individual constituents within essential oils.

Finally, we broadened the antimicrobial potential of the thiol-ene polymer platform by incorporating a combination of *p*-anisaldehyde and furaneol, which is a natural plant-derived inhibitor of quorum sensing. The treatment with furaneol/*p*-anisaldehyde-containing polymeric discs strongly repressed the production of pyocyanin,

reduced the exoprotease activity, and effectively eradicated established *P. aeruginosa* biofilms. Our results suggest that furaneol triggers the dispersion of biofilms, which render the pathogen more vulnerable to the antimicrobial action of *p*-anisaldehyde. Our results will facilitate the development of polymeric systems capable of dual phytochemical delivery and controlling microbial growth without promoting antibiotic resistance. Such materials enable the high loading, efficient encapsulation, and sustained release of hydrophobic and volatile phytochemicals and could be used as antimicrobial wound dressings, sprays, surface coatings, and packaging materials.

5.1 References

(1) Cheesman, M. J.; Ilanko, A.; Blonk, B.; Cock, I. E. Developing new antimicrobial therapies: are synergistic combinations of plant extracts/compounds with conventional antibiotics the solution? *Pharmacogn. Rev.* **2017**, *11* (22), 57–72.

(2) Hintz, T.; Matthews, K. K.; Di, R. The use of plant antimicrobial compounds for food preservation. *BioMed Res. Int.* **2015**, *2015*, 1–12.

(3) Langeveld, W. T.; Veldhuizen, E. J. A.; Burt, S. A. Synergy between essential oil components and antibiotics: A Review. *Crit. Rev. Microbiol.* **2014**, *40* (1), 76–94.

(4) Hyldgaard, M.; Mygind, T.; Meyer, R. L. Essential oils in food preservation: mode of action, synergies, and interactions with food matrix components. *Front. Microbiol.* **2012**, *3* (12), 1–12.

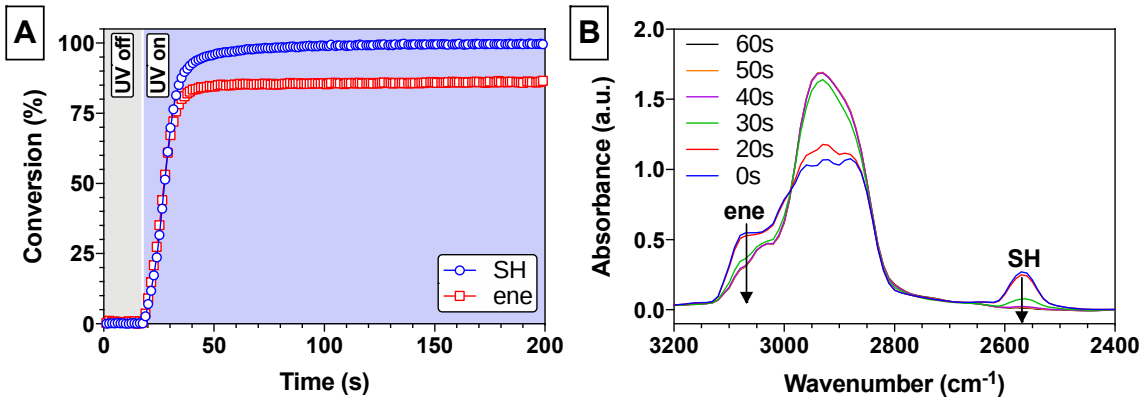

Figure A.1 RT-FTIR polymerization monitoring of pCinA-PETMP resin upon exposure to UV light.

(A) Conversion of both thiol and alkene peaks. (B) Key spectra at various time points illustrating the complete conversion of the SH and incomplete conversion of the alkene.

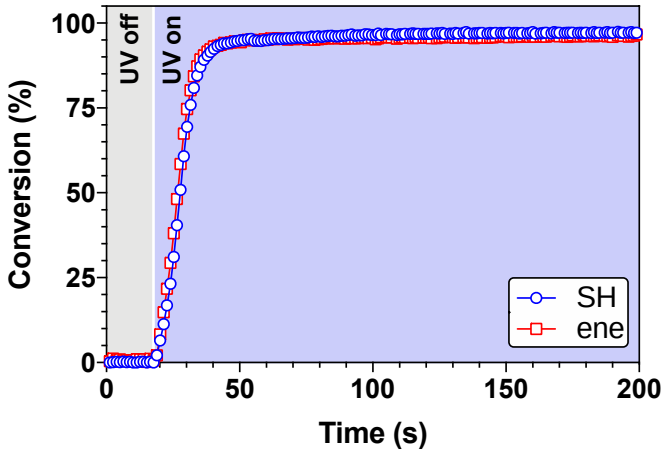

Figure A.2 RT-FTIR polymerization monitoring of 40:60 pBA:pAA – PETMP co-PANDA resin upon exposure to UV light.

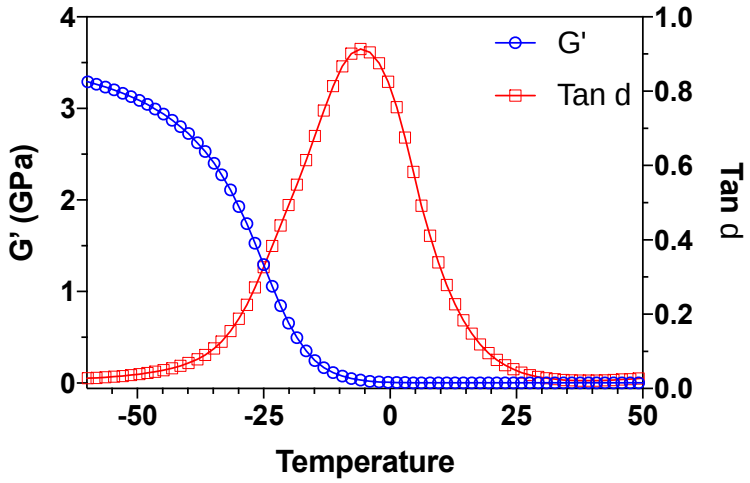

Figure A.3 Dynamic mechanical analysis of 40:60 pBA:pAA co-PANDA disk.

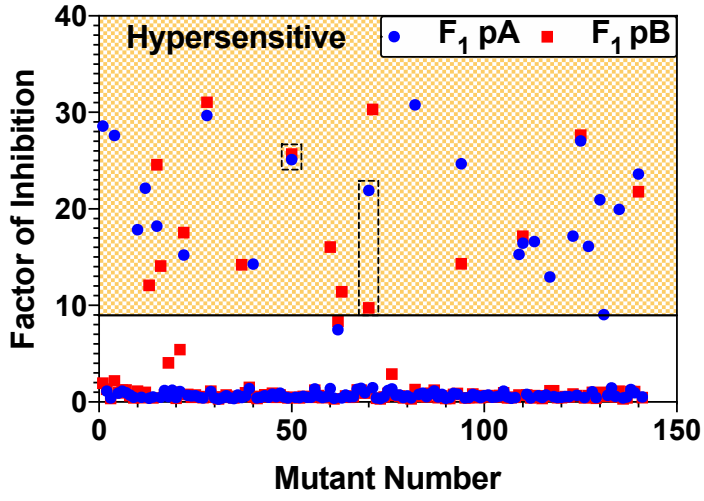

Figure A.4 The results of screening of mutants for hypersensitivity to sub-inhibitory concentrations (0.6 x MIC) of pA and pB.

The shaded part of the graph indicates sensitive mutants (factor of inhibition (F1) values ≥ 9) that were selected for further analysis. The mexA (#50) and oprF (#70) mutants are highlighted with dashed lines.

Table A.1 *Oligonucleotide primers and qPCR probes used in this study.*

Primer or probe	**Sequence**	**Reference**[a]
TET-1FP-3	5’-GCATCTCGGGCACGTTGGGTCCT-3’	Lucigen
TET-1RP-4	5’-CGAGGATGACGATGAGCGCATTGTTAG-3’	Lucigen
rpoD-F	5'-GGGCTGTCTCGAATACGTTGA-3'	Quale et al., 2006
rpoD-R	5'-ACCTGCCGGAGGATATTTCC-3'	Quale et al., 2006
rpoD-P	5'-[FAM]-TGCGGATGATGTCTTCCACCTGTTCC-[TAM]-3’	Quale et al., 2006
mexA-F	5'-AACCCGAACAACGAGCTG-3'	Quale et al., 2006
mexA-R	5'-ATGGCCTTCTGCTTGACG-3'	Quale et al., 2006
mexA-P	5’-[FAM]-CATGTTCGTTCACGCGCAGTTG-[TAM]-3’	Quale et al., 2006
mexC-F	5'-GGAAGAGCGACAGGAGGC-3'	Quale et al., 2006
mexC-R	5'-CTGCACCGTCAGGCCCTC-3'	Quale et al., 2006
mexC-P	5’-[FAM]-CCGAAATGGTGTTGCCGGTG-[TAM]-3’	Quale et al., 2006
mexE-F	5'-TACTGGTCCTGAGCGCCT-3'	Quale et al., 2006
mexE-R	5'-TCAGCGGTTGTTCGATGA-3'	Quale et al., 2006
mexE-P	5’-[FAM]-CGGAAACCACCCAAGGCATG-[TAM]-3’	Quale et al., 2006
mexX-F	5'-GGCTTGGTGGAAGACGTG-3'	Quale et al., 2006
mexX-R	5'-GGCTGATGATCCAGTCGC-3'	Quale et al., 2006
mexX-P	5’-[FAM]-CCGACACCCTGCAGGGCC-[TAM]-3’	Quale et al., 2006

Table A.1 *(Continued)*

Primer or probe	**Sequence**	**Reference**[a]
mexK-R	5'-CAGGCGGTCGGCATAGTC-3'	This study
mexK-P	5’-[FAM]-CAAGGGCTTCGACTACGCGGTG-[BHQ1]-3’	This study
muxB-F	5'-ATGGTGGCGATCCTGCTC-3'	This study
muxB-R	5'-GATGGTCGGGTAGTCCACTTC-3'	This study
muxB-P	5’-[FAM]-GATCGCCTACCGCTTCCTGCCG-[BHQ1]-3’	This study
PA1541-F	5'-TGATCGGCCTGTCCTATTTCTTC-3'	This study
PA1541-R	5'-GTGATCAGGACGATGCCAATG-3'	This study
PA1541-P	5’-[FAM]-CCCTGGCGGTCAAGCGTGTC-[BHQ1]-3’	This study

[a]Oligonucleotide primers and probes targeting *rpoD, mexA, mexC, mexE,* and *mexX* genes were from the study by Quale et al.[42]